KICK-OFF TRAINING

TUM - Garching-bei-München

2018 Jan 8-12

Experiments for wear and underplatform damper mechanics

Stefano Zucca, Daniele Botto

Politecnico di Torino

Agenda

1. **Wear**
   - Mechanism
   - Experimental results
2. **Friction**
   - Basics
   - Experimental results
3. **Test rigs**
   - For wear and friction
   - For blade/damper dynamics

Wear is the result of material removal by physical separation due to microfracture, by chemical dissolution, or by melting at the contact interface.

Wear, when it involves **loss of material**, generally occurs through the **formation of particles**, even if in some situation can result from **atom removal processes (**electrical contact situation that involves sparking or as a result of high temperatures developed during machining.)

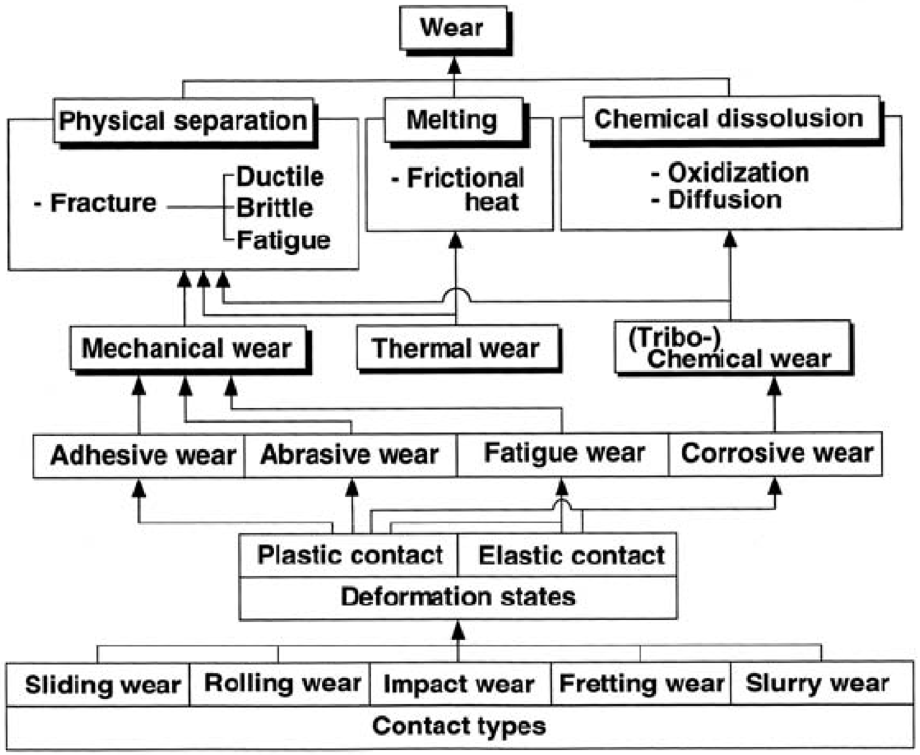

In the literature one can found more than 80 terms describing wear mechanisms!

It is possible to group wear mechanisms into a few generic categories, and in the 1950s wear mechanisms were classified into the following categories:

- adhesion,
- abrasion,
- corrosion,
- surface fatigue,
- and minor categories.

Three representative types of wear volume curves are observed:

Type I Constant wear rate throughout the whole process.

Type II Transition from an initially high wear rate to steady wear at a low rate. This type of wear is quite often observed in metals.

Type III Catastrophic transition from initial wear of low wear rate to wear of a high rate, such as fatigue fracture. This type of wear is often observed in ceramics.

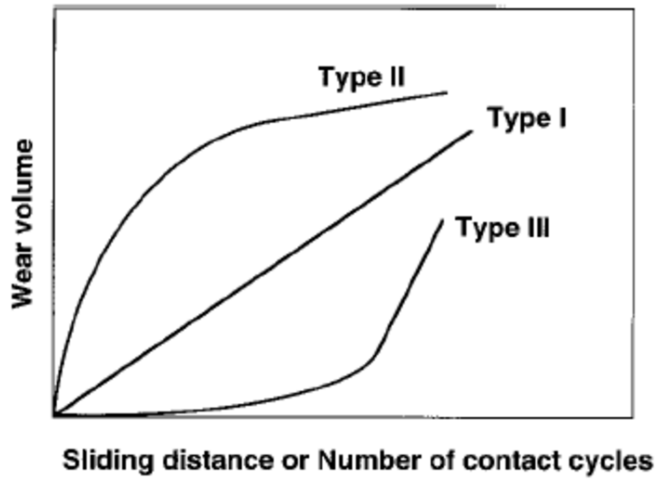

Definition are given for “standard” wear based on “pin on disk” test. In this test a stationary "pin" under an applied normal load is in contact with a rotating disc.

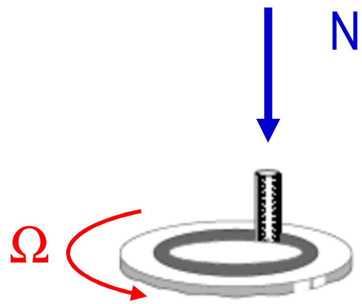

We are more interested in fretting wear where contact surfaces undergo “small” (μm) oscillating displacements.

In general, wear is evaluated by the amount of volume lost and the state of the wear surface. The degree of wear is described by

1. **wear rate**, defined as wear volume per unit distance (the slope of the wear volume curve)
2. **specific wear rate**, defined as wear volume per unit distance and unit load.
3. **wear coefficient**, defined as the product of specific wear rate and the hardness of the wearing material.

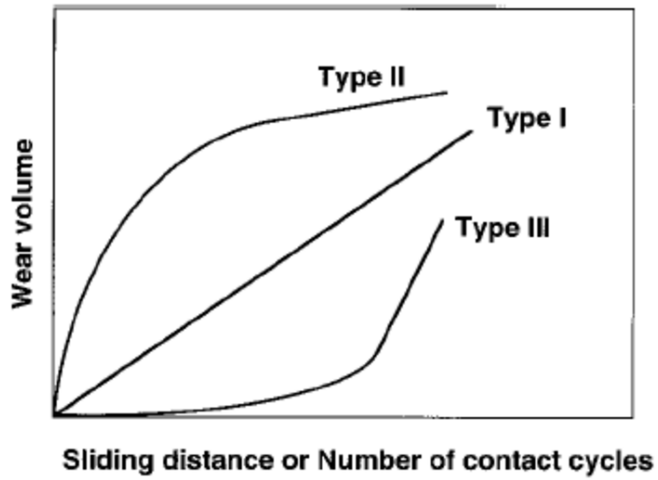

Wear changes drastically even with a relatively small change in a tribosystem, which is composed of dynamic parameters, environmental parameters, and material parameters.

“Wear is not only a material property. It is a system response.”

Area of contact

In engineering, the macro-geometry or contour of the bodies in contact is often used to determine contact area. This is usually done by models, which are based on the elastic, for example, the Hertz contact theory, or plastic deformation. In these approaches, the surfaces are generally assumed to be smooth. Actual surfaces, on the other hand always exhibit some degree of roughness and as a result the actual contact situation is different from that implied by these macro-methods.

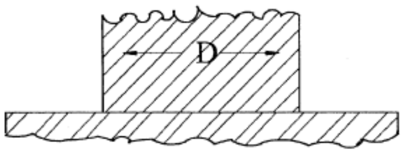

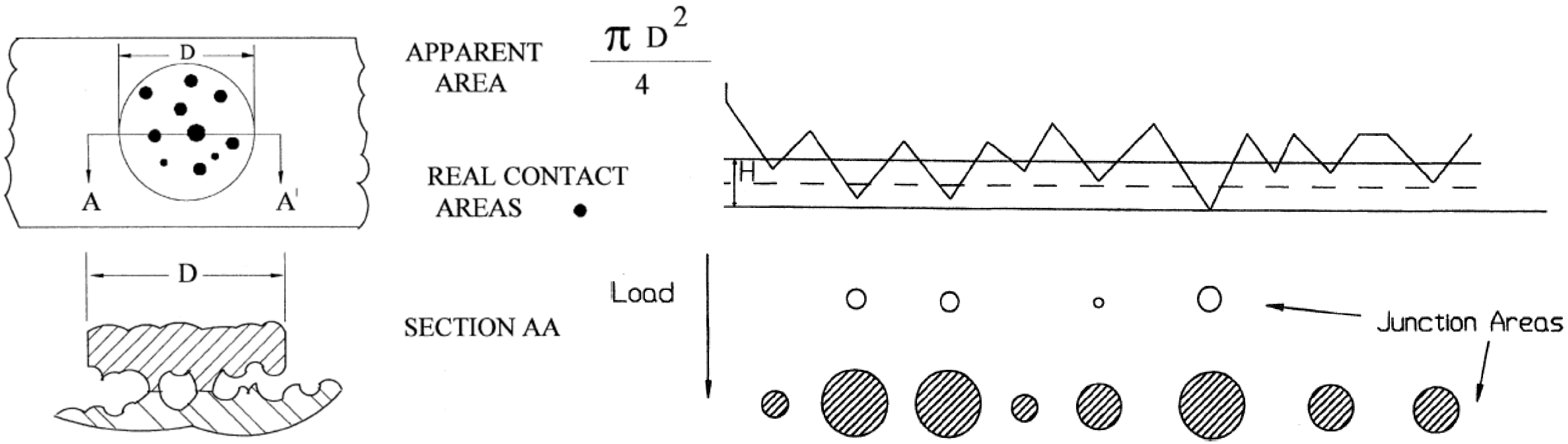

Wear mechanism: adhesive wear

If the contact interface between two surfaces under plastic contact has enough adhesive bonding strength to resist relative sliding, large plastic deformation caused by dislocation is introduced in the contact region under compression and shearing.

As a result of such large deformation in the contact region, a crack is initiated and is propagated in the combined fracture mode of tensile and shearing. When the crack area reaches the contact interface, a wear particle is formed and adhesive transfer is completed.

This type of wear, which occurs when there is enough adhesive bonding at the contact interface, is called adhesive wear.

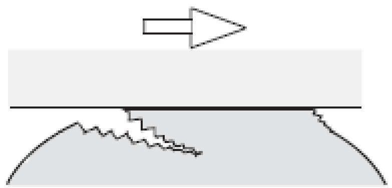

(a)Adhesive wear

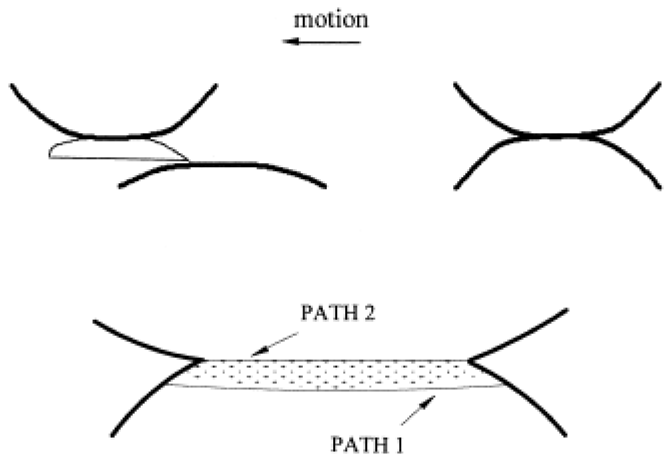

If it is assumed that the real contact is composed of

- **n contact points** of equal size and
- a new contact point is formed after the disappearance of the former one

the total number of contacts n stays constant during sliding. By supposing a circular contact area of **radius a**, the possible volume of wear particles generated after **sliding the distance of 2a** is assumed as the half **sphere volume** described by **$2\pi a^3/3$**.
The possible wear volume V for n contact points after sliding the distance L is given by

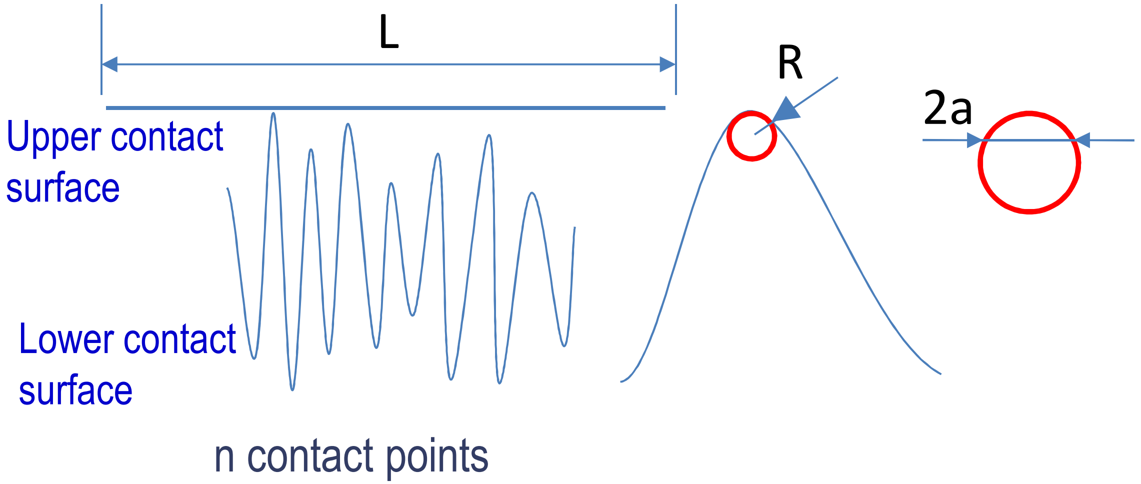

$$V_{sc} = \frac{2}{3}\pi a^3 \quad \text{Volume for single contact}$$

$$V = n \cdot V_{sc} \frac{L}{2a} = n \cdot \frac{2}{3}\pi a^3 \frac{L}{2a}$$

$$n\pi a^2 = \frac{N}{H}$$

Since the normal contact pressure with plastic deformation is almost equal to the hardness value H of the wearing material, the total real contact area for n contact points $n\pi a^2$ is

If the probability K that the rupture of any given junction will result in adhesive wear is introduced, the number of junctions producing adhesive wear in a unit sliding distance is

$$m = K^*n,$$

and then the wear volume V under normal load N after sliding distance L becomes

$$\boxed{V = K_{ad}\frac{NL}{H}}$$

The adhesive wear volume is

1. proportional to the normal load, N
2. proportional to the sliding distance, L
3. inversely proportional to the hardness of the wearing material, H.

Abrasive wear is wear caused by hard particles and protuberances. When two surfaces are involved, the wear situation is generally referred to as abrasion.
A distinction is usually made between two types of abrasion, two-body and three-body abrasion, because of significant differences in the wear behavior associated with these two situations.

Two-body abrasion is when the wear is caused by protuberances on or hard particles fixed to a surface.

Three-body abrasion is when the particles are not attached but between the surfaces.

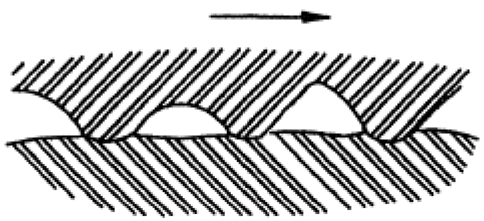

Two–Body Abrasion

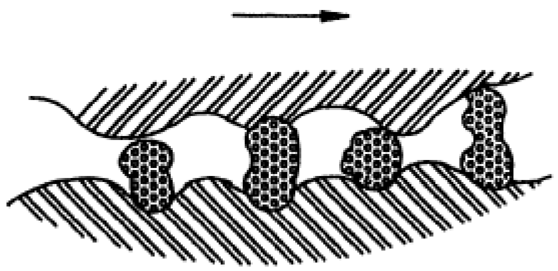

Three–Body Abrasion

Three bodies

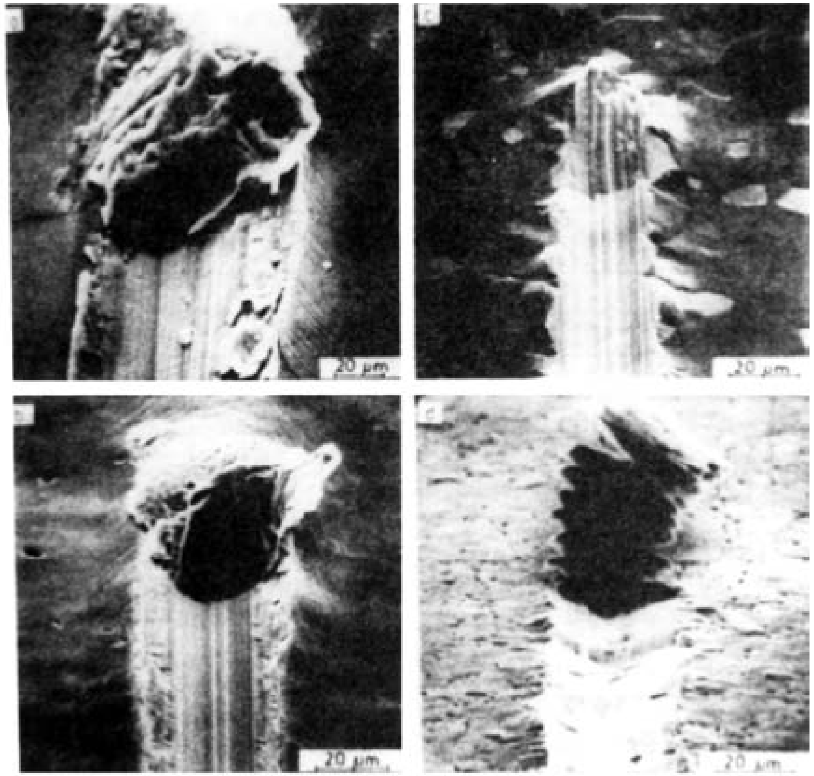

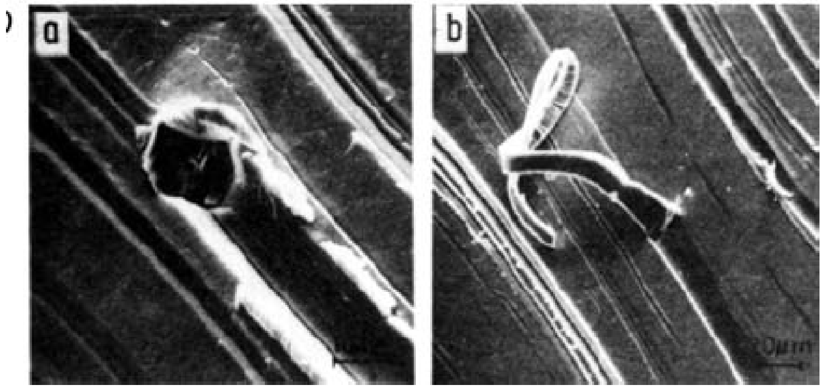

Two bodies

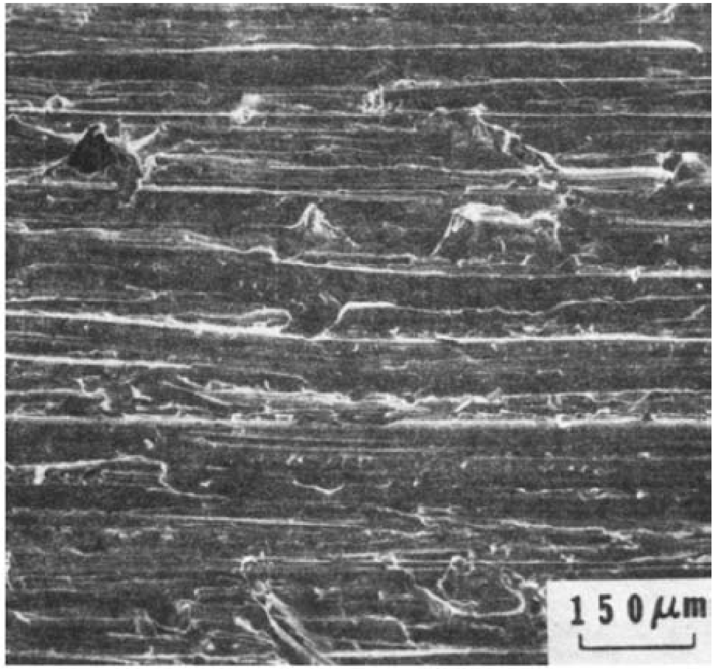

Dependency on third body size

The precise reasons for the dependency on size is not known, but there appears to be a very definite relationship that applies to many situations. it has been suggested that in certain cases the larger particles may just be sharper.

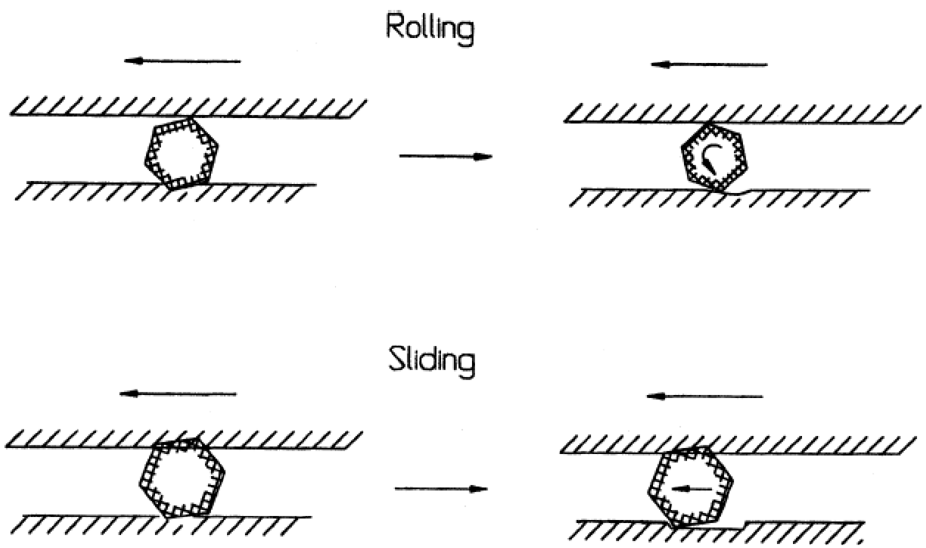

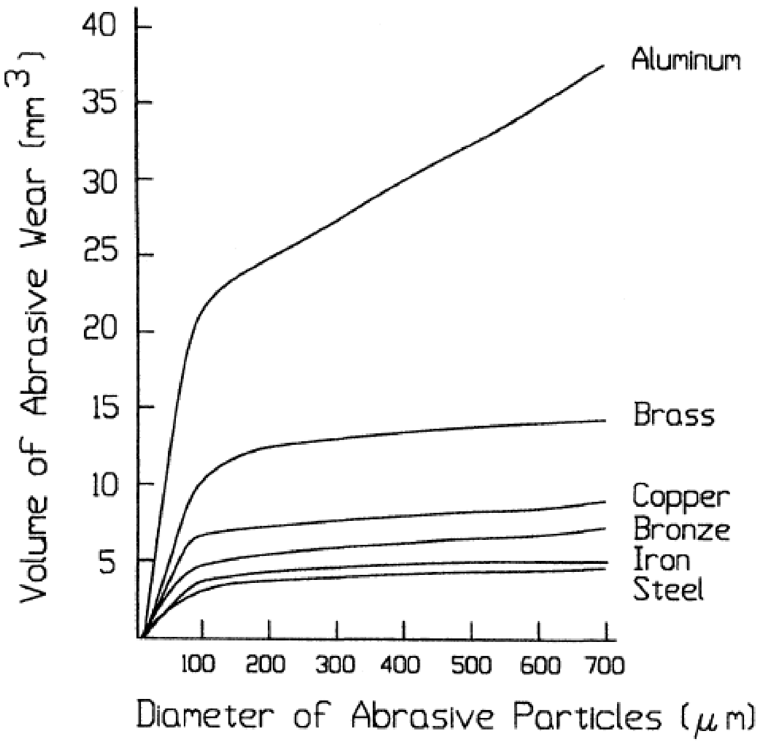

If the contact interface between two surfaces has interlocking of an inclined or curved contact, ploughing takes place in sliding.

As a result of ploughing, a certain volume of surface material is removed and an abrasive groove is formed on the weaker surface.

This type of wear is called abrasive wear.

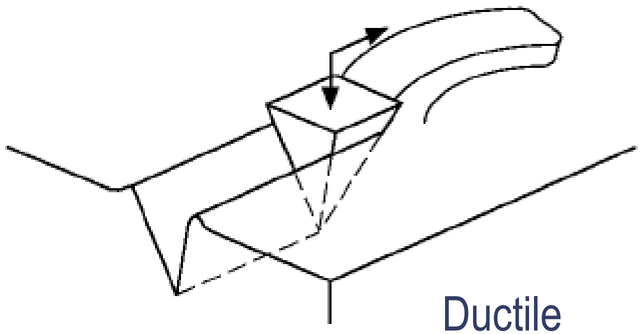

Ductile

(a)

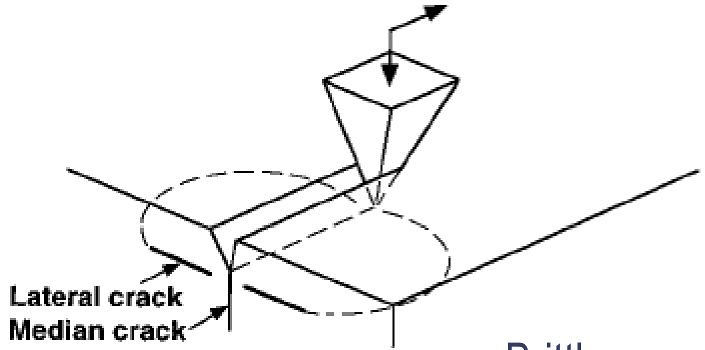

Brittle

(b)

Ductile Material

Estimation of wear volume We assume a simplified contact model in which the abrasive has a conical shape with an angle θ ,and the indentation depth of the abrasive is d

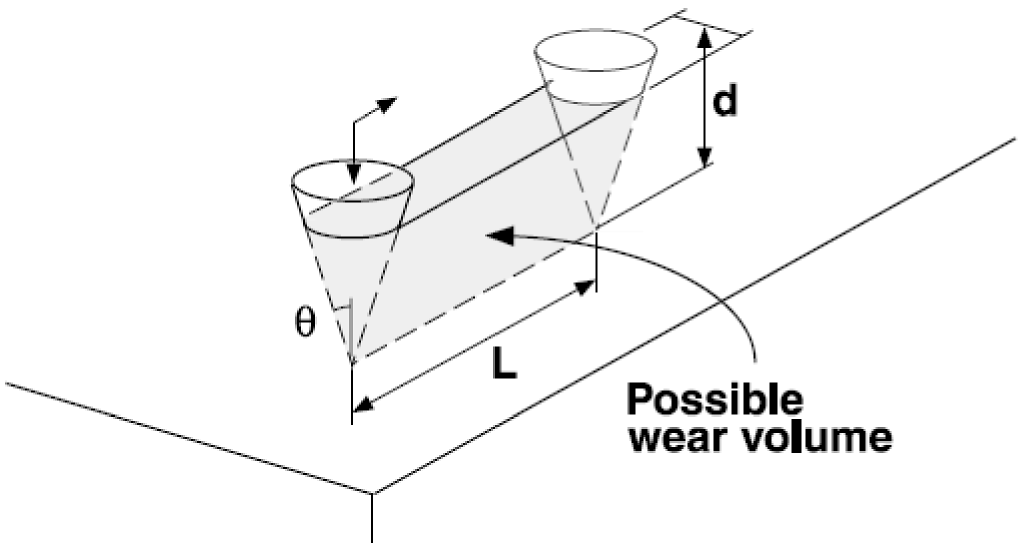

The wear volume V, which is ploughed by harder asperities after sliding a distance of L, is given by

$$V = d^2 \tan\vartheta \cdot L$$

Ductile Material

The normal contact pressure under plastic contact can be assumed to be equal to the hardness value H of the wearing material, then the real contact area is expressed by

$$\frac{1}{2}\pi(d\tan\vartheta)^2 = \frac{N}{H} \longleftarrow V = d^2 \tan\vartheta \cdot L$$

Therefore the possible wear volume V under normal load N and after sliding distance L is given by

$$V = \frac{2}{\pi\tan\vartheta}\frac{NL}{H}$$

The abrasive wear volume is

1. proportional to the normal load N and the sliding distance L
2. inversely proportional to the hardness H of the wearing material.

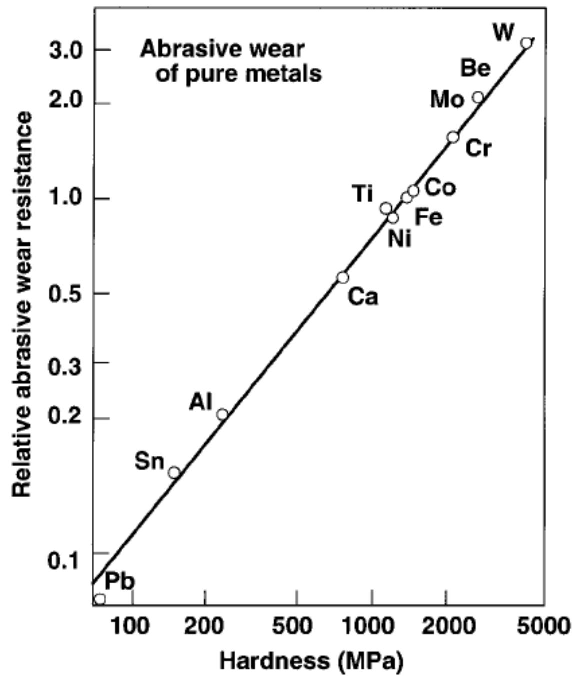

Wear mechanism: abrasive wear

Ductile Material

There are three modes of wedge forming and ploughing in abrasive grooving

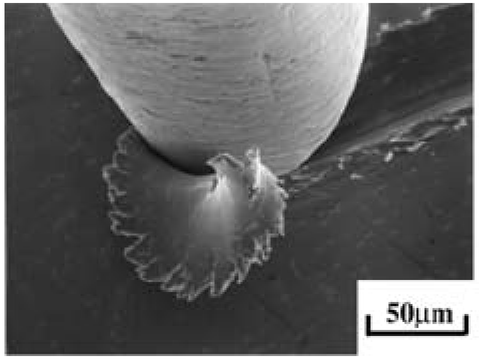

Cutting mode

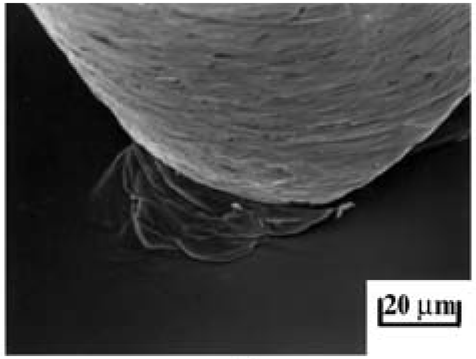

Wedge-forming mode

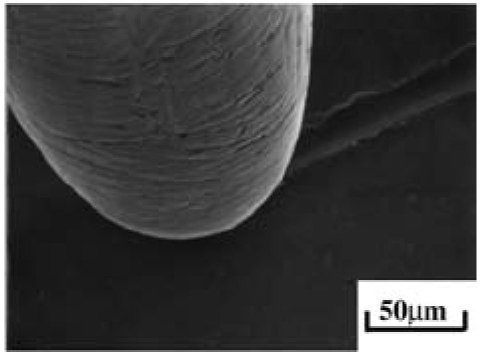

Ploughing mode

Cutting Long and curled ribbon-like wear particles are formed. Low friction assists in this wear mode.

Wedge-forming Wedge-like wear particle is formed at the tip of the grooving asperity and stays there working as a kind of built-up wedge to continue grooving. Sliding takes place at the bottom of the wedge where adhesive transfer of a thin layer from the underlying counterface continues to grow the wedge slowly. This wear mode appears as a combined effect of adhesion at an inclined or curved contact interface and shear fracture at the bottom of the wedge. High friction or strong adhesion assists in this wear mode.

Ploughing A wear particle is not generated by a single pass of sliding and only a shallow groove is formed. Repeated sliding and accumulation of plastic flow at the surface is necessary for the generation of wear particles.

Degree of wear

In all these three abrasive wear modes, grooves are formed as the result of wear particle generation. Plastic flow of material forms **ridges** on both sides of a **groove**. If we introduce the groove volume ΔV_g per unit sliding distance and the ridge volume ΔV_r per unit sliding distance (both observed above the initial surface level) on both sides of the groove, the difference (ΔV_g—ΔV_r) gives the wear volume at one groove in one pass of sliding. With these descriptions, the concept of degree of wear β at one groove is introduced

$$\beta = \frac{\Delta V_g - \Delta V_r}{\Delta V_g}$$

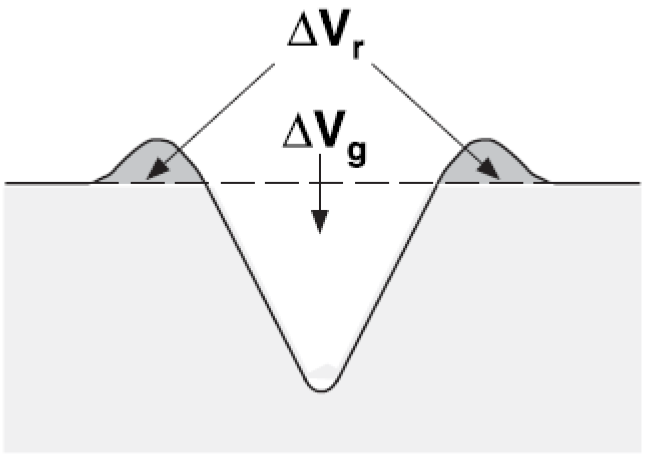

- β = 1 corresponds to the state of ideal material removal without forming ridges

- β = 0 means the ideal ploughing with no material removal.

Brittle Material

In the case of brittle material a wear particle is generated due to mainly brittle fractures caused by initiation and propagation of cracks. Therefore, wear rate of the brittle material is strongly dependent on fracture toughness.

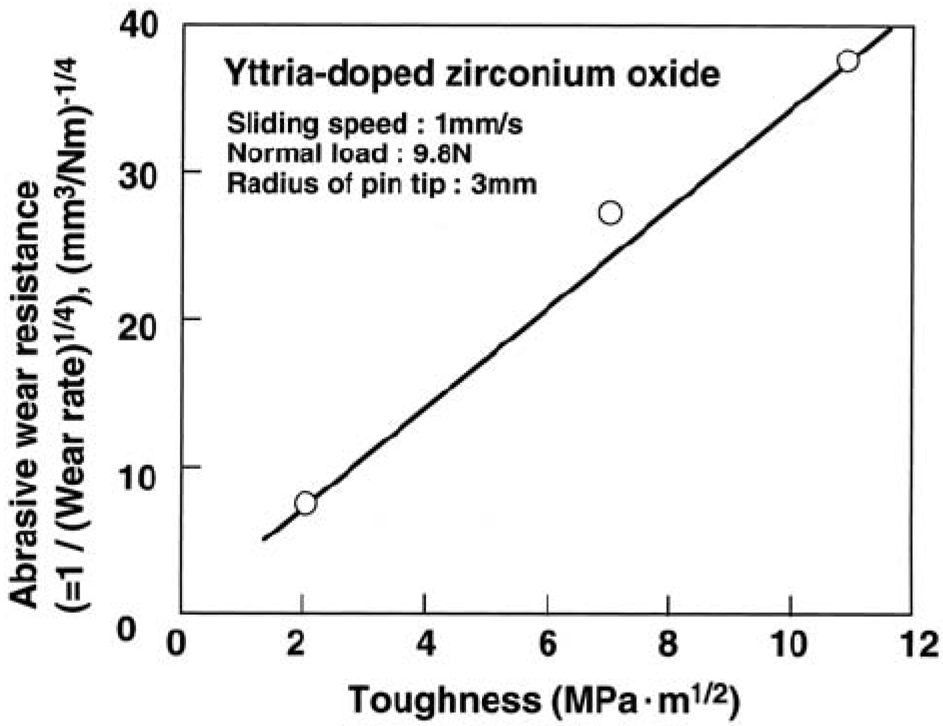

Crack (Evans and Marshall, 1981) length c is defined by the function of normal load N, fracture toughness Kc, hardness H, and Young's modulus E

$$c = \alpha_1 \frac{N^{5/8}}{K_c^{1/2} H^{1/8}} \left(\frac{E}{H}\right)^{3/5}$$

The depth b of lateral fracture is estimated by the radius of plastic contact zone, and is given by

$$b = \alpha_2 \left(\frac{E}{H}\right)^{2/5} \left(\frac{N}{H}\right)^{1/2}$$

α_1 and α_2 being material constant

wear particle generated by lateral crack propagation which reaches to the surface.

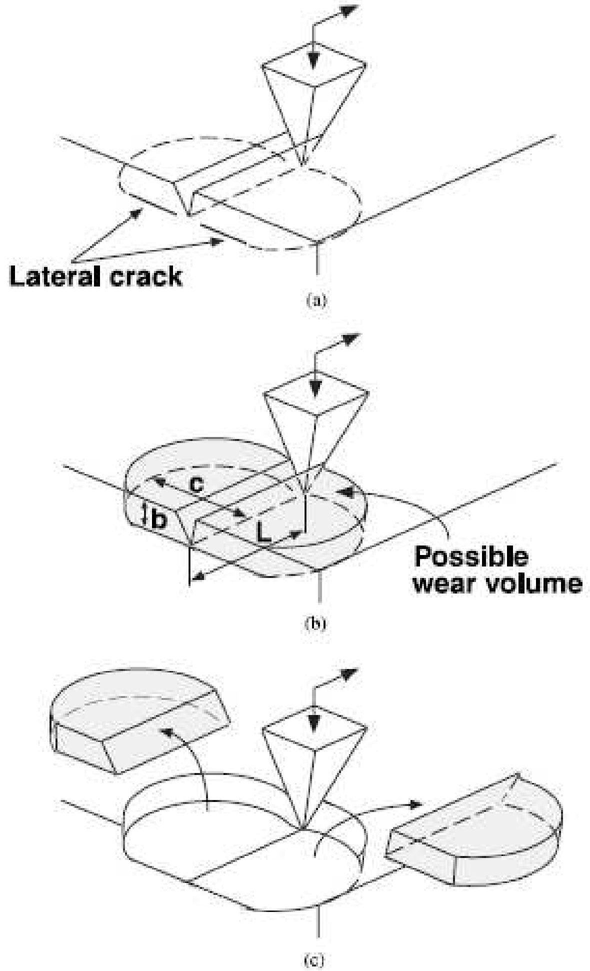

Wear volume V in scratching of the brittle material with a hard asperity is given by the following equation

$$V = 2c \cdot b \cdot L = \alpha_3 \frac{N^{9/8}}{K_c^{1/2} H^{5/8}} \left(\frac{E}{H} \right) L$$

L is the sliding distance and α_3 is a material-dependent constant

It is clear that abrasive wear rate depends strongly on both hardness and toughness.

There is strong evidence to suggest that the elastic modulus (E) can also have an important influence on wear behavior. In particular the ratio of hardness and elastic modulus H/E, has been shown by a number of authors to be a more suitable parameter for predicting wear resistance than is hardness alone.

Test rigs overview and details of a wear test at high temperature (1000°C)

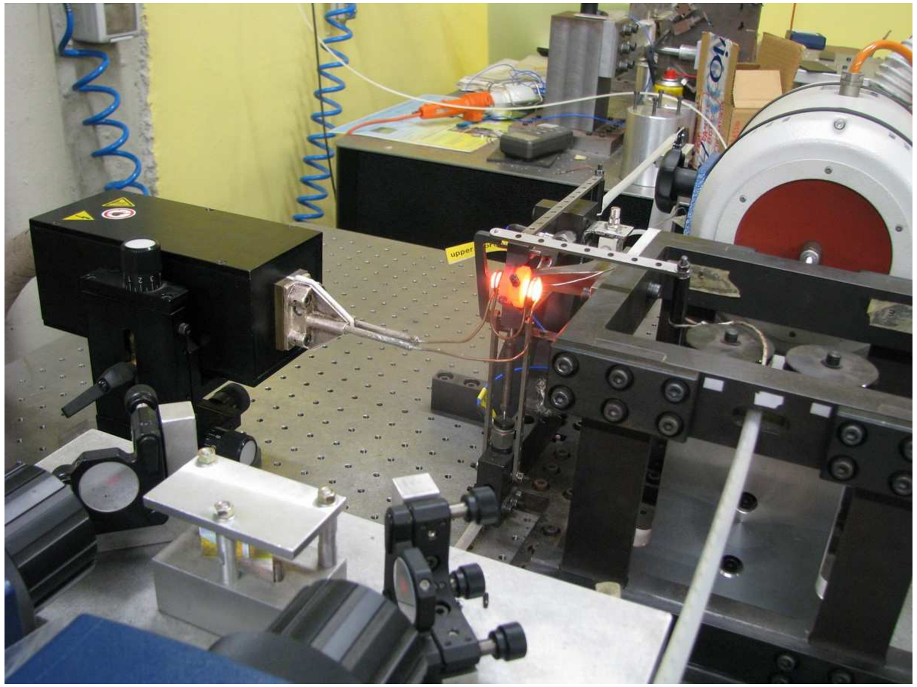

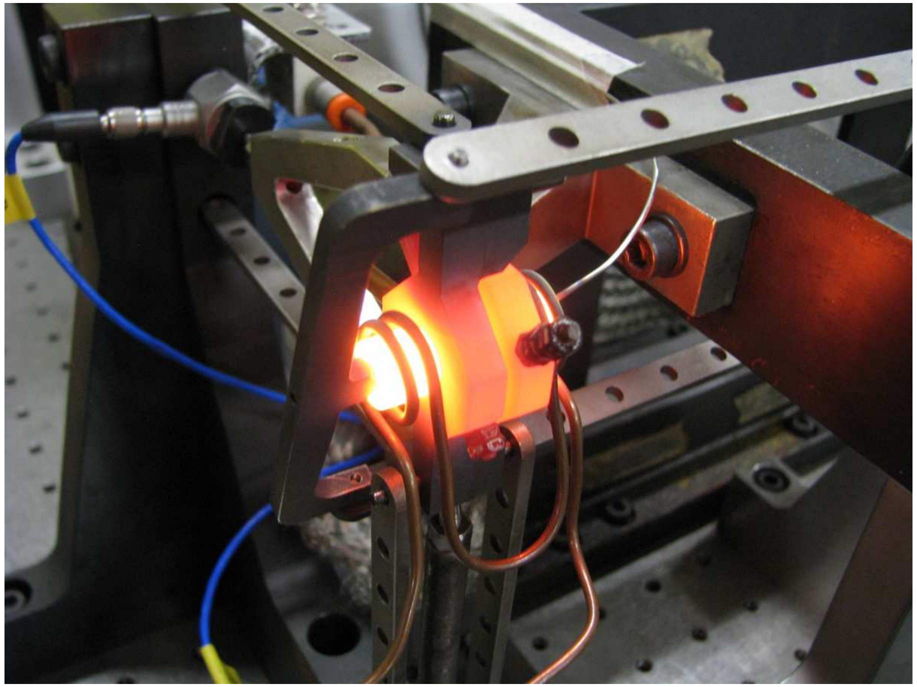

Flat/Flat specimens

Spherical/Flat specimens

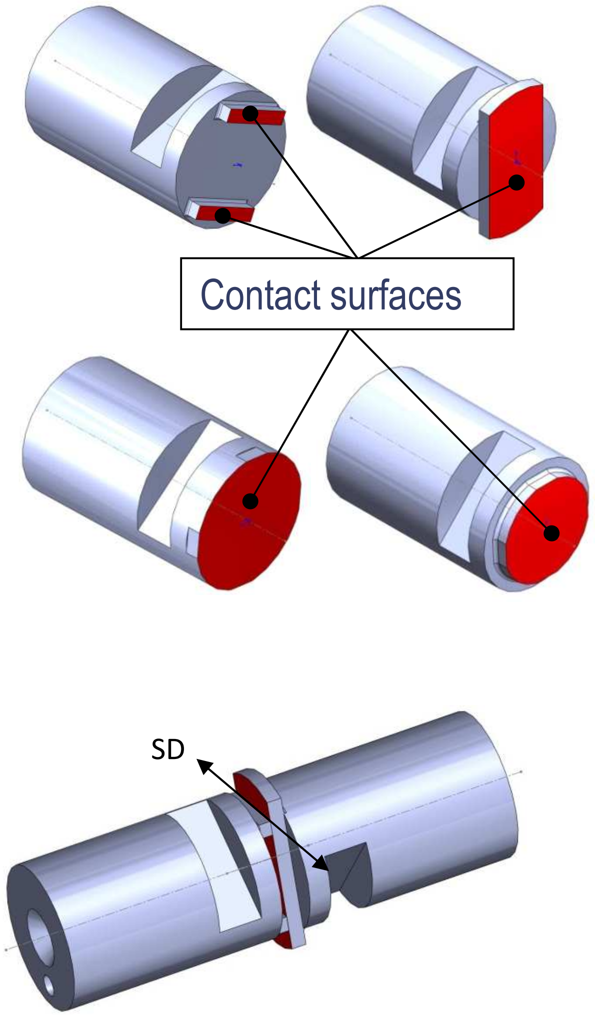
Contact surfaces
SD

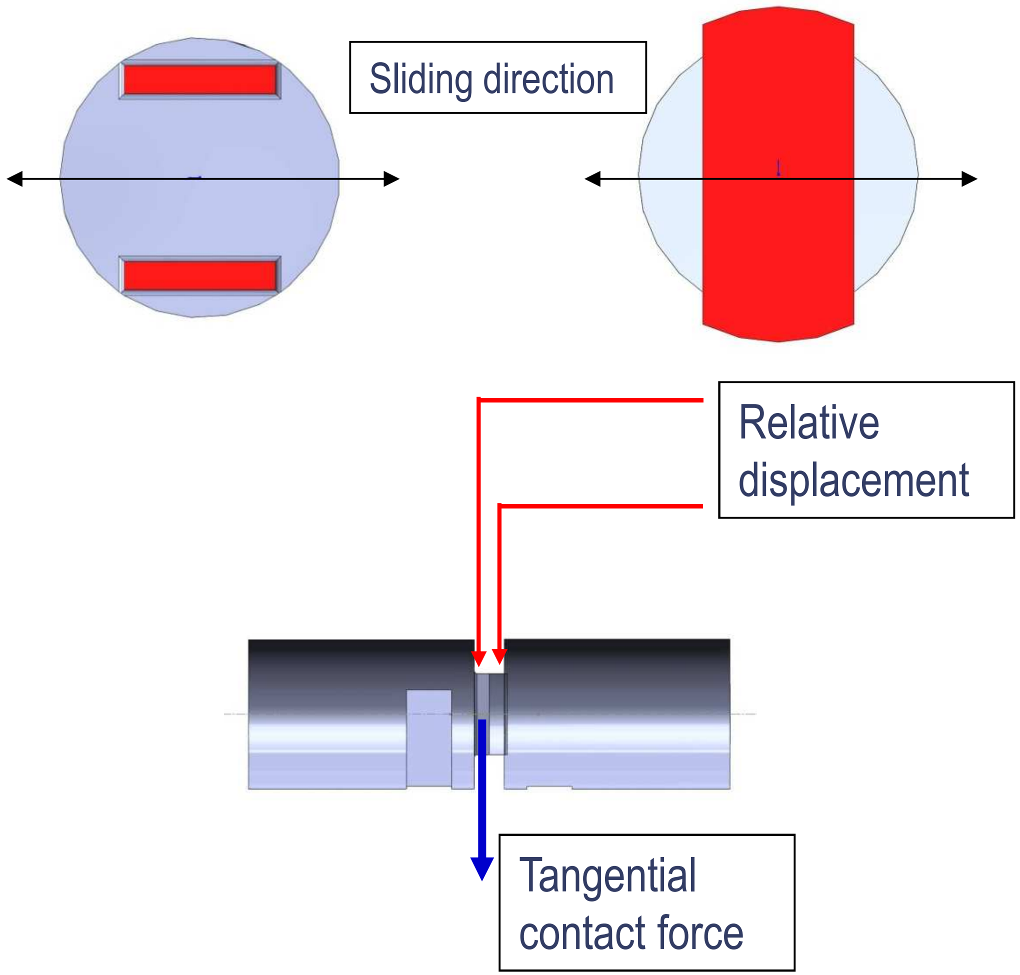
Sliding direction
Relative displacement
Tangential contact force

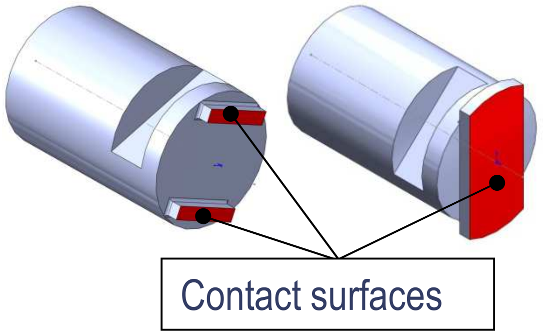

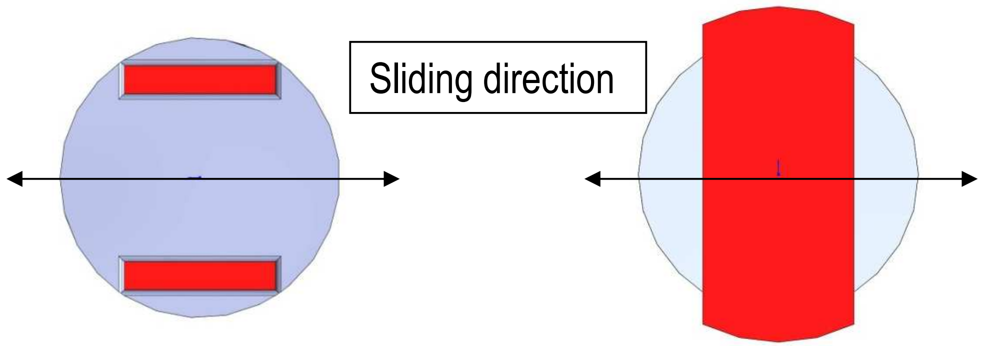

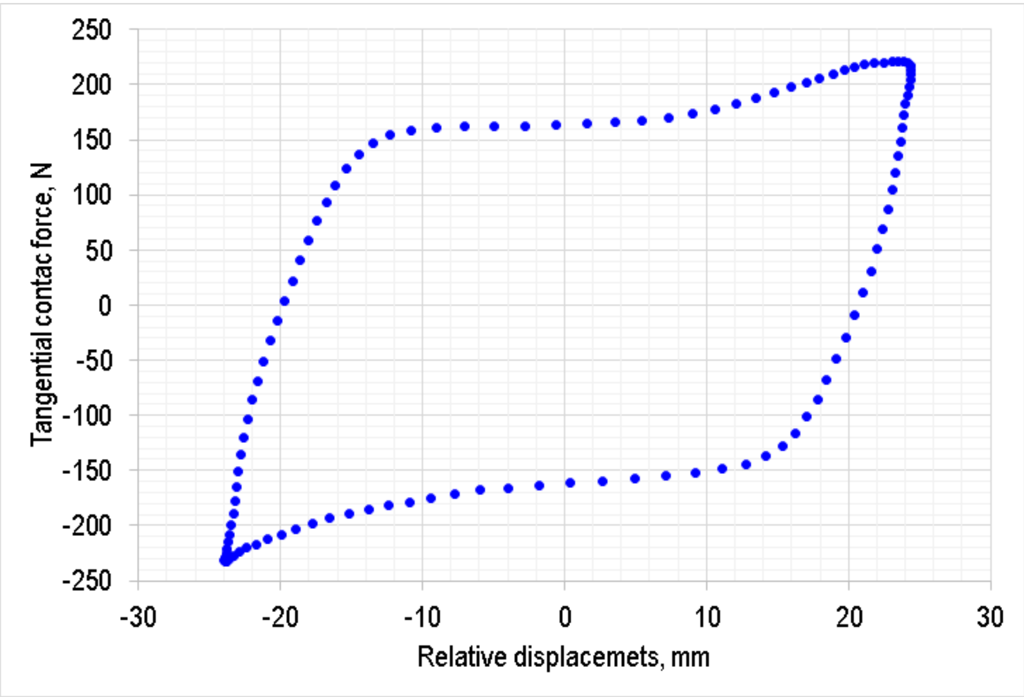

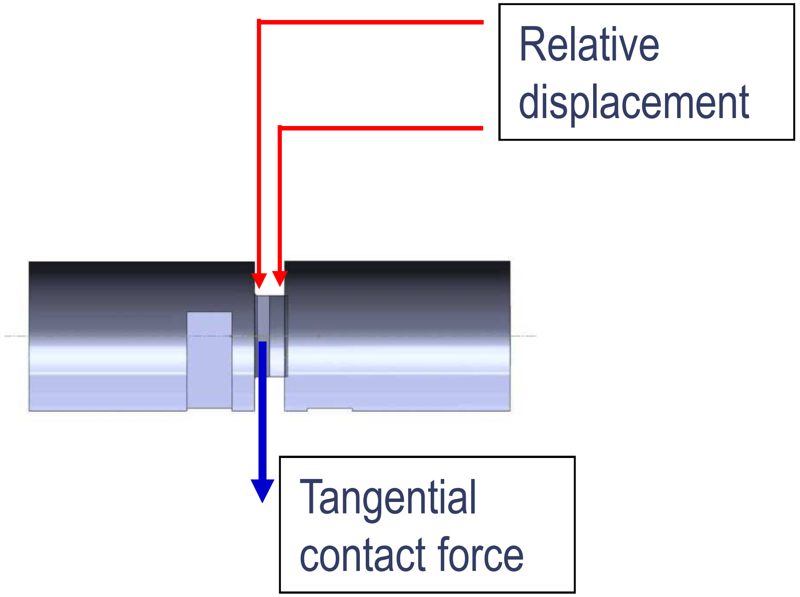

Hysteresis loop
Tangential force against relative displacement

Experimental results: wear

New

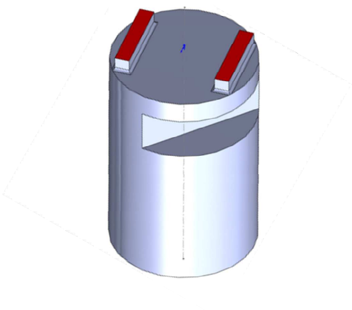

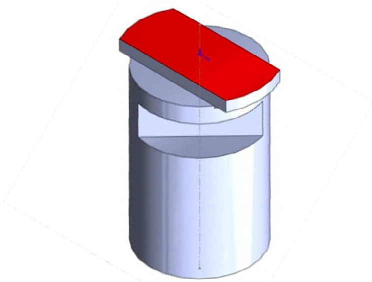

New

5M Wear cycles

New

10M Wear cycles

New

15M Wear cycles

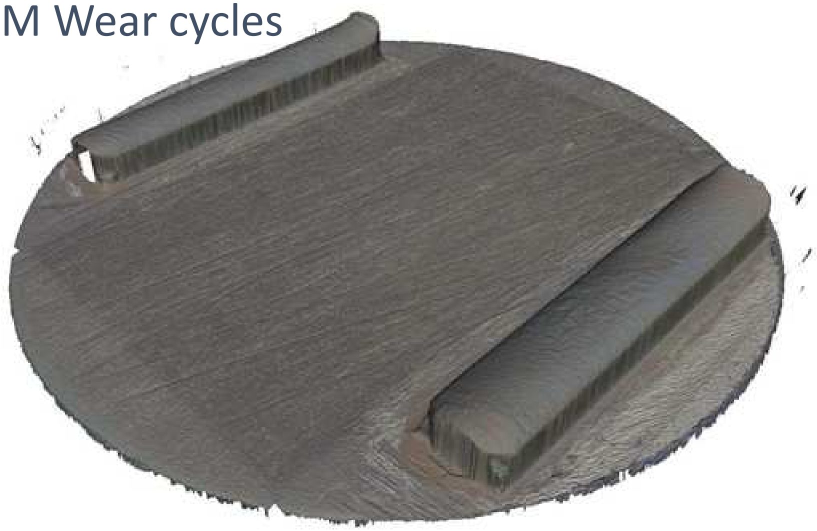

The most commonly used techniques to evaluate wear are
1. weighing and
2. measurement of changes in dimensions.

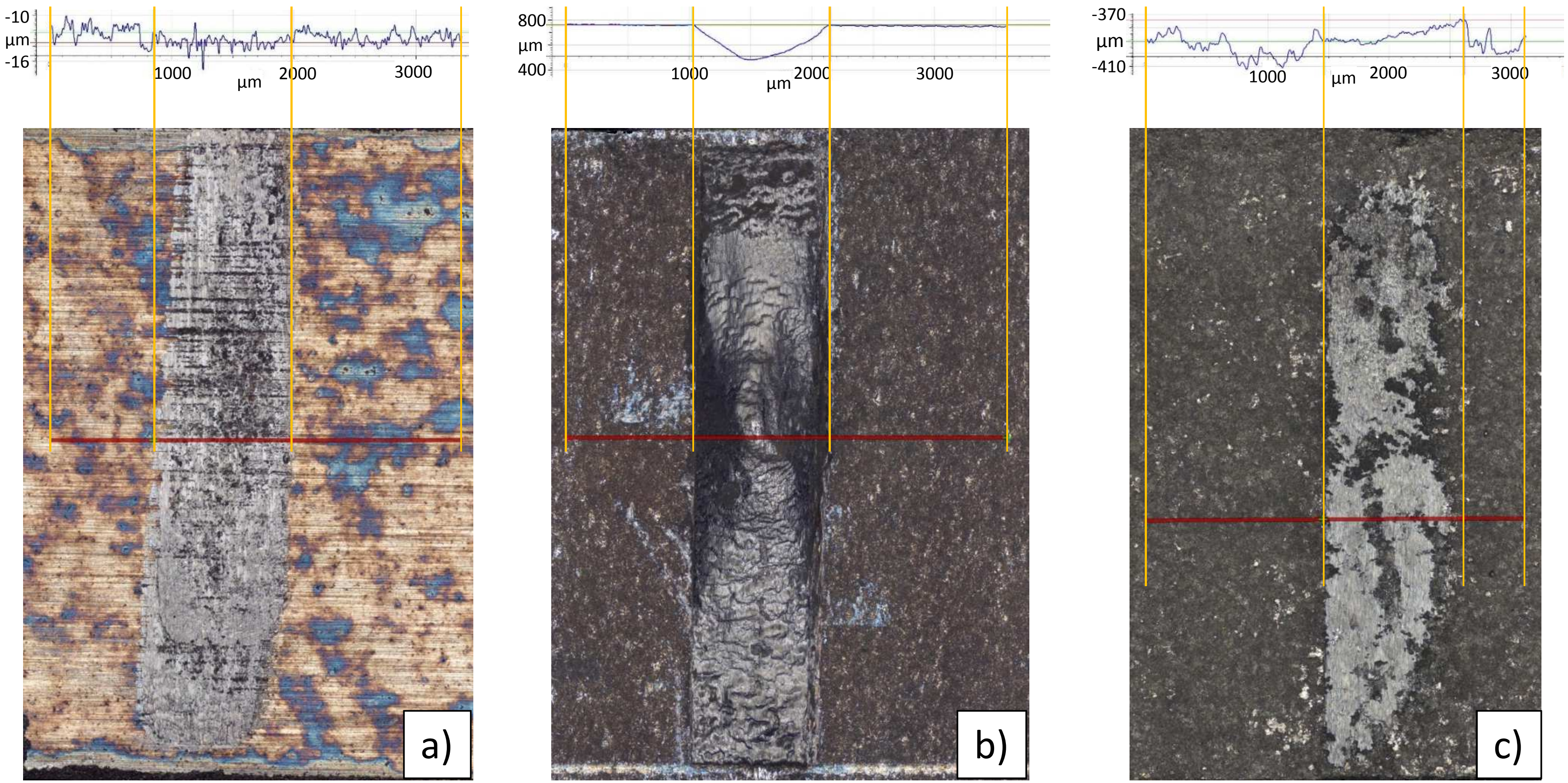

Measurement may often be difficult if the worn volumes are small.

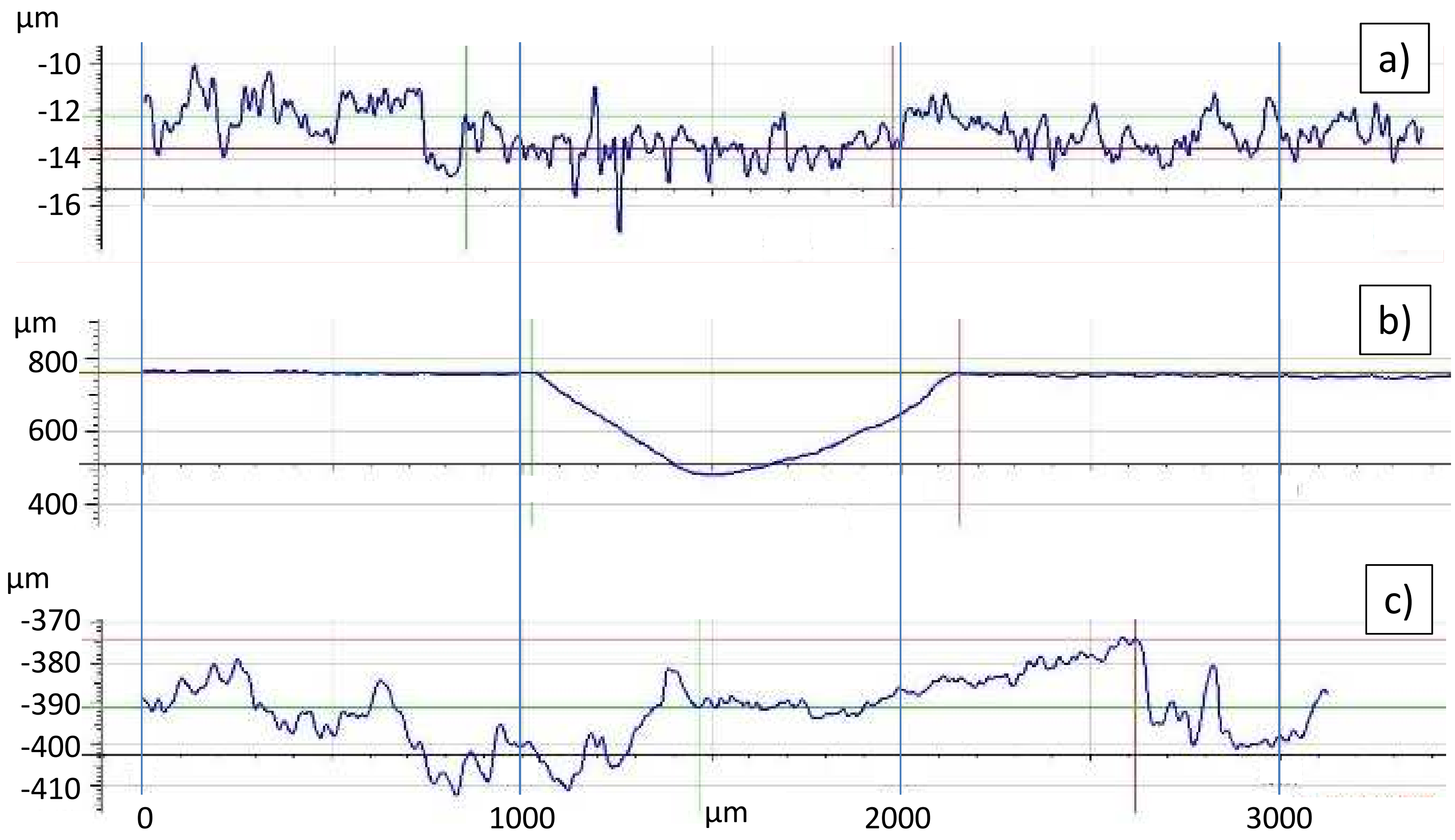

Measurement may often be difficult if the worn volumes are small.

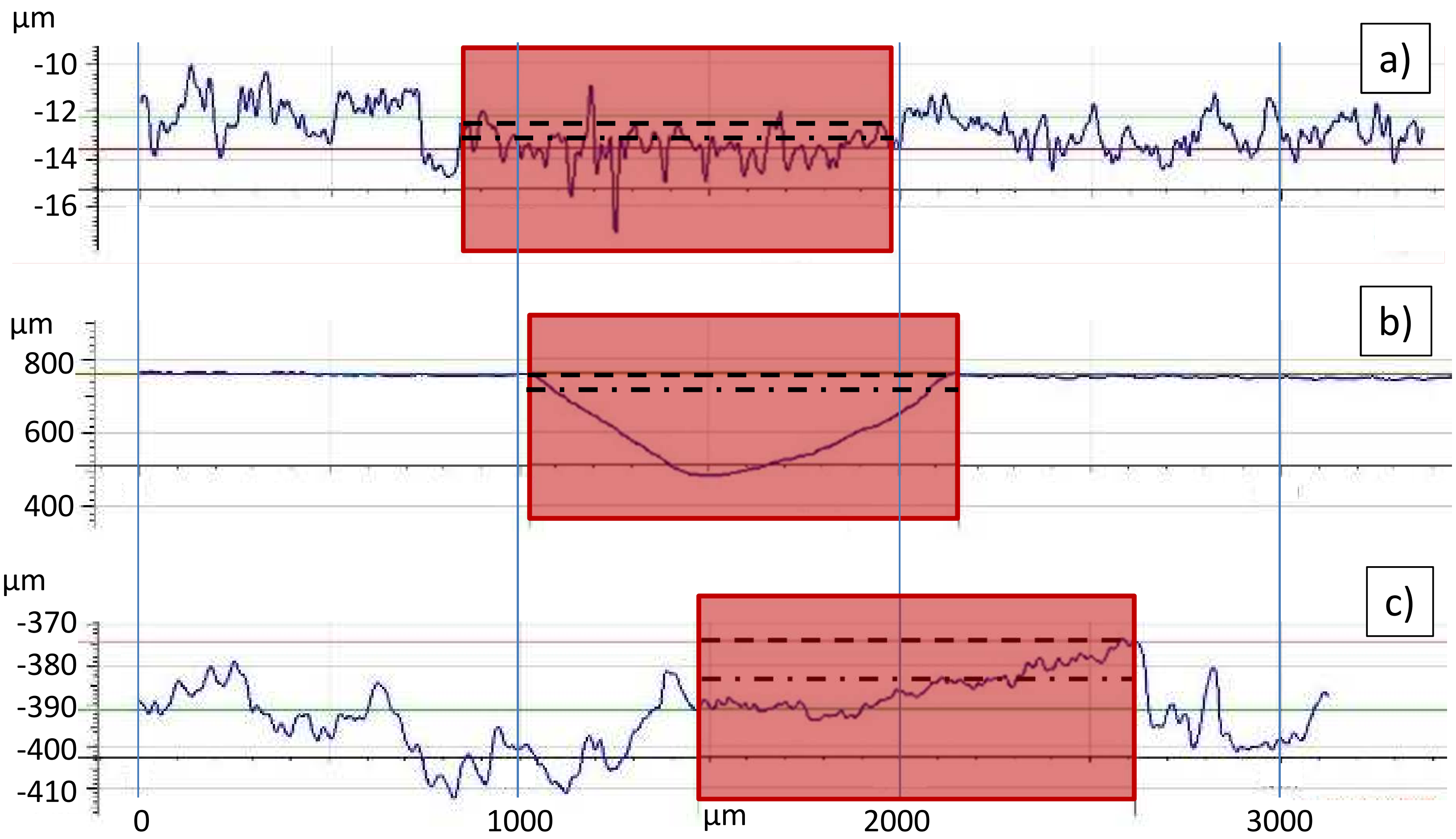

Direct topography comparison

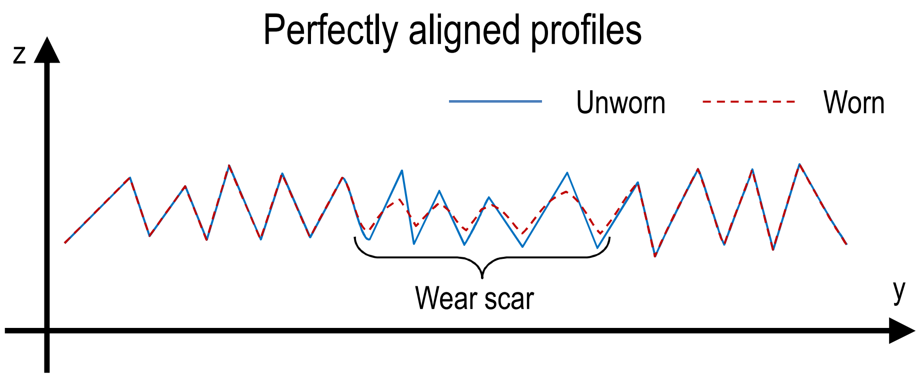

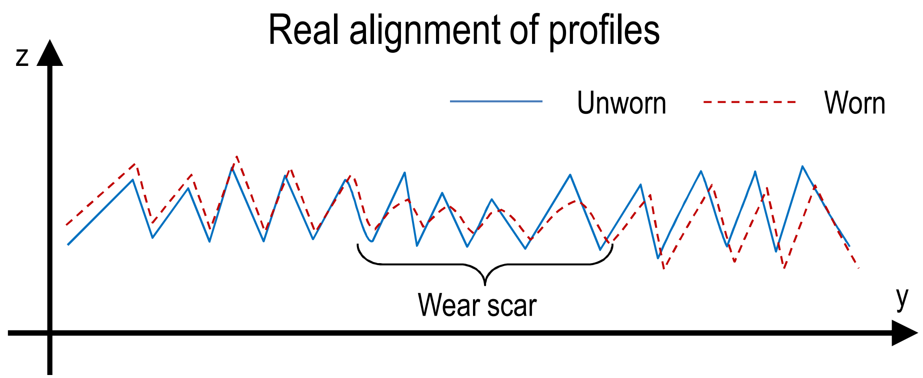

Indirect topography comparison A reference surface defined on the unworn surface is used to evaluate the volume loss.

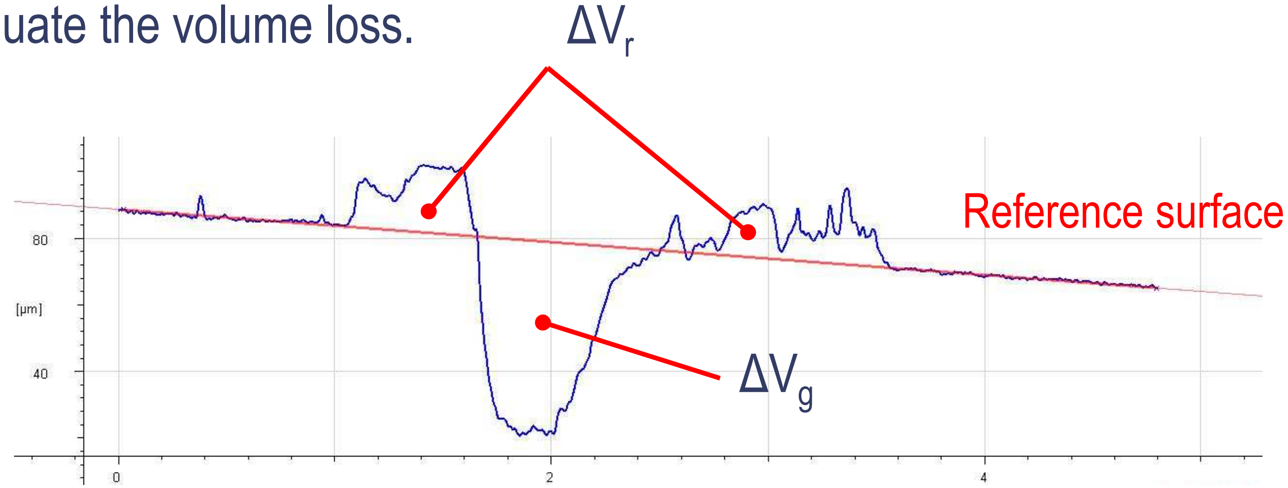

Indirect topography comparison

Correction to take into account surface roughness

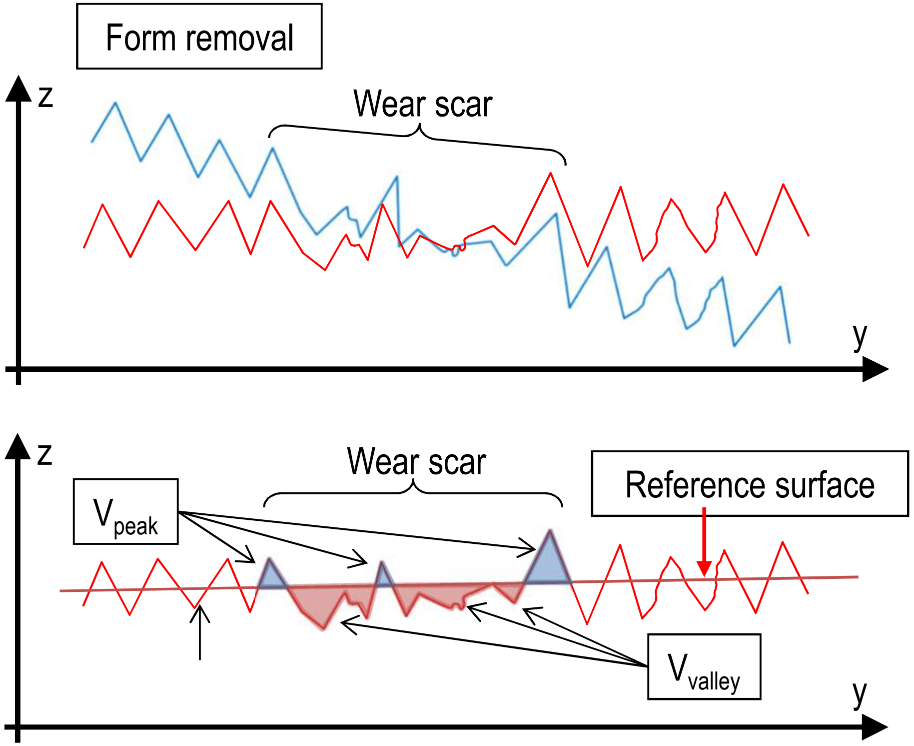

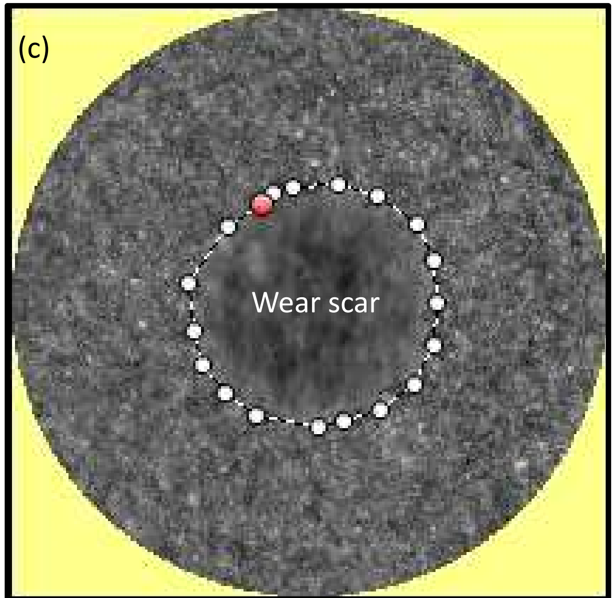

	Hole	Peak
Surface (mm²)	10.4	3.14
Volume (mm³)	0.0867	0.0143

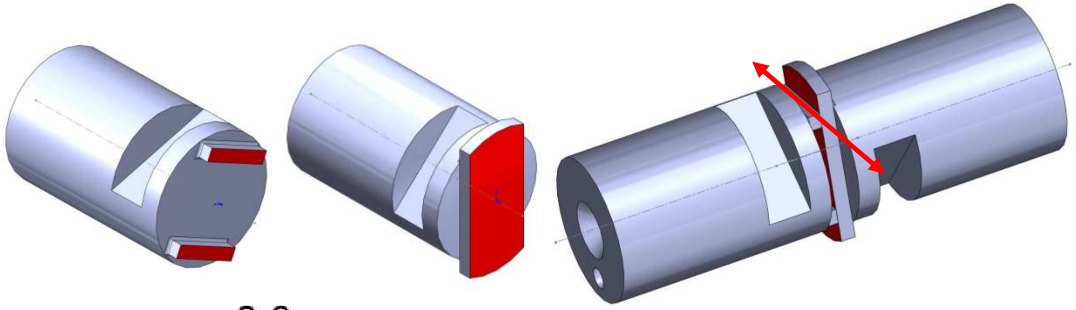

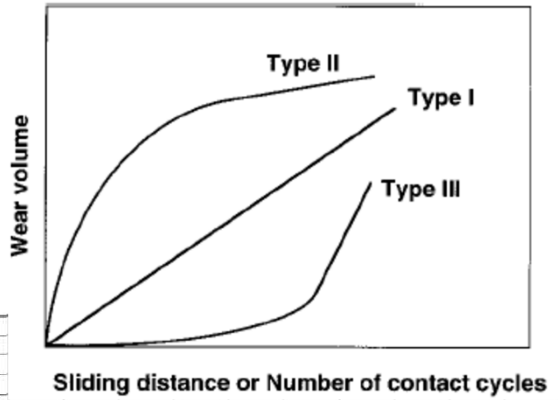
Type II
Type I
Type III
Wear volume
Sliding distance or Number of contact cycles

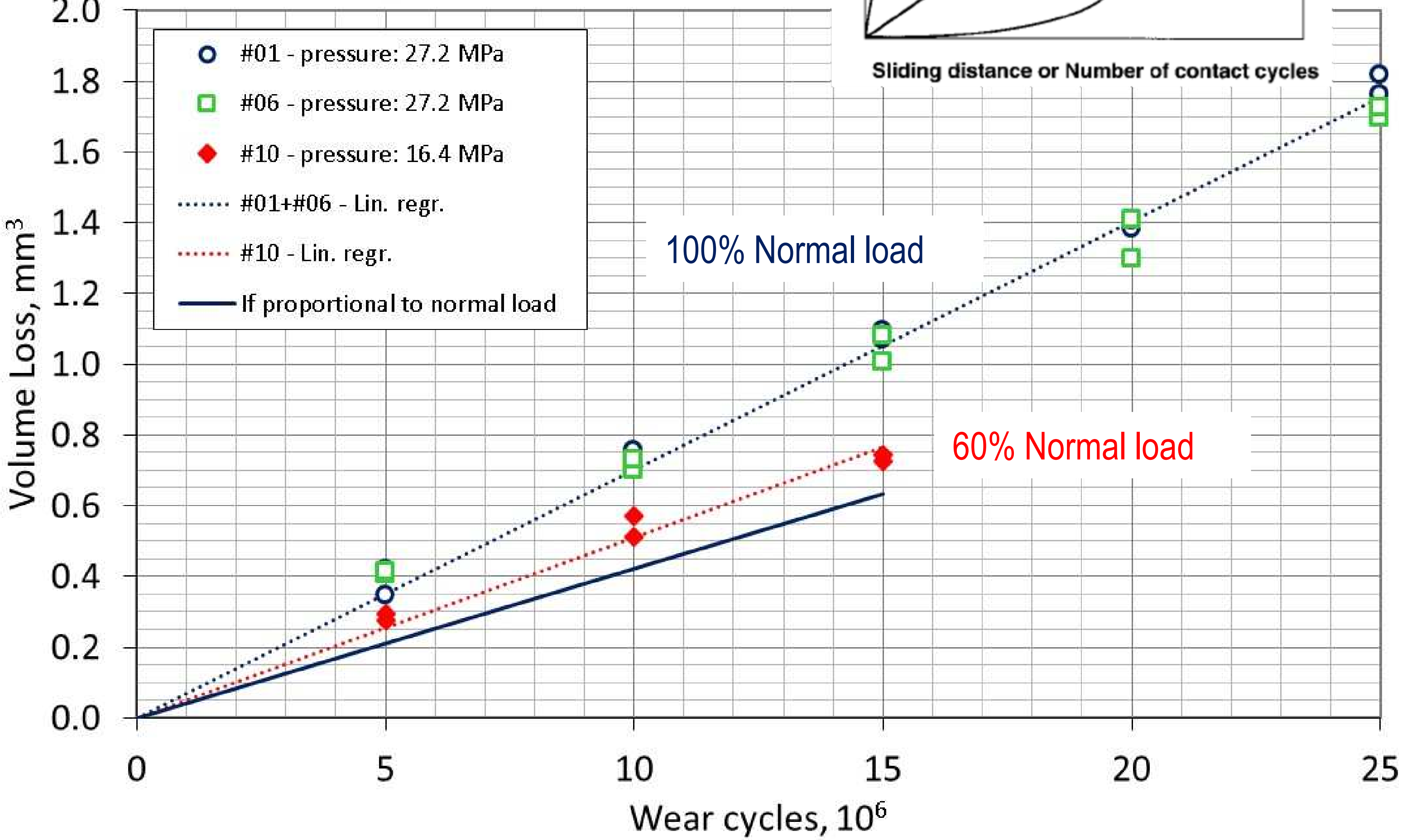
#01 - pressure: 27.2 MPa
#06 - pressure: 27.2 MPa
#10 - pressure: 16.4 MPa
#01+#06 - Lin. regr.
#10 - Lin. regr.
If proportional to normal load
100% Normal load
60% Normal load
Volume Loss, mm3
Wear cycles, 10^6
2.0
1.8
1.6
1.4
1.2
1.0
0.8
0.6
0.4
0.2
0.0
0
5
10
15
20
25

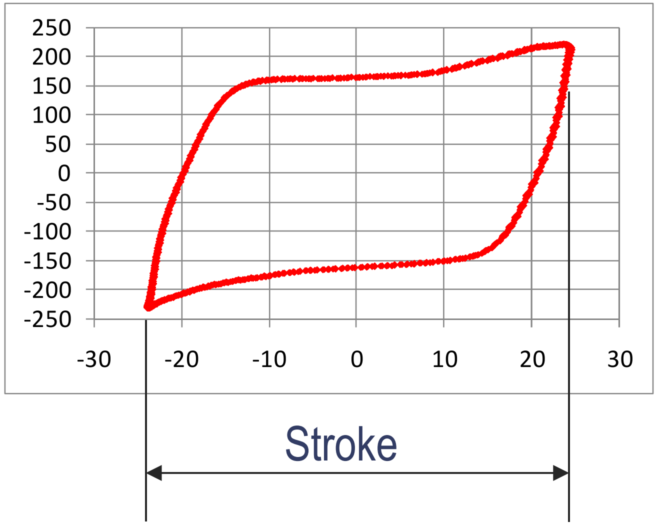

$$V_{volume\,loss} = \frac{K_{ad}}{3}\frac{NL}{H}$$

$$V_{volume\,loss} = \frac{2}{\pi \tan\vartheta}\frac{NL}{H}$$

N: normal load

L: sliding distance

$T \le \mu \cdot N$

Hysteresis loop

Le area within the hysteresis loop is the energy injected into the contact

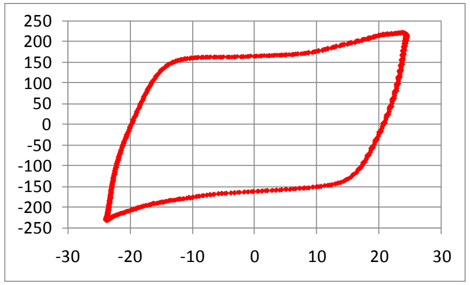
250
200
150
100
50
0
-50
-100
-150
-200
-250
-30
-20
-10
0
10
20
30

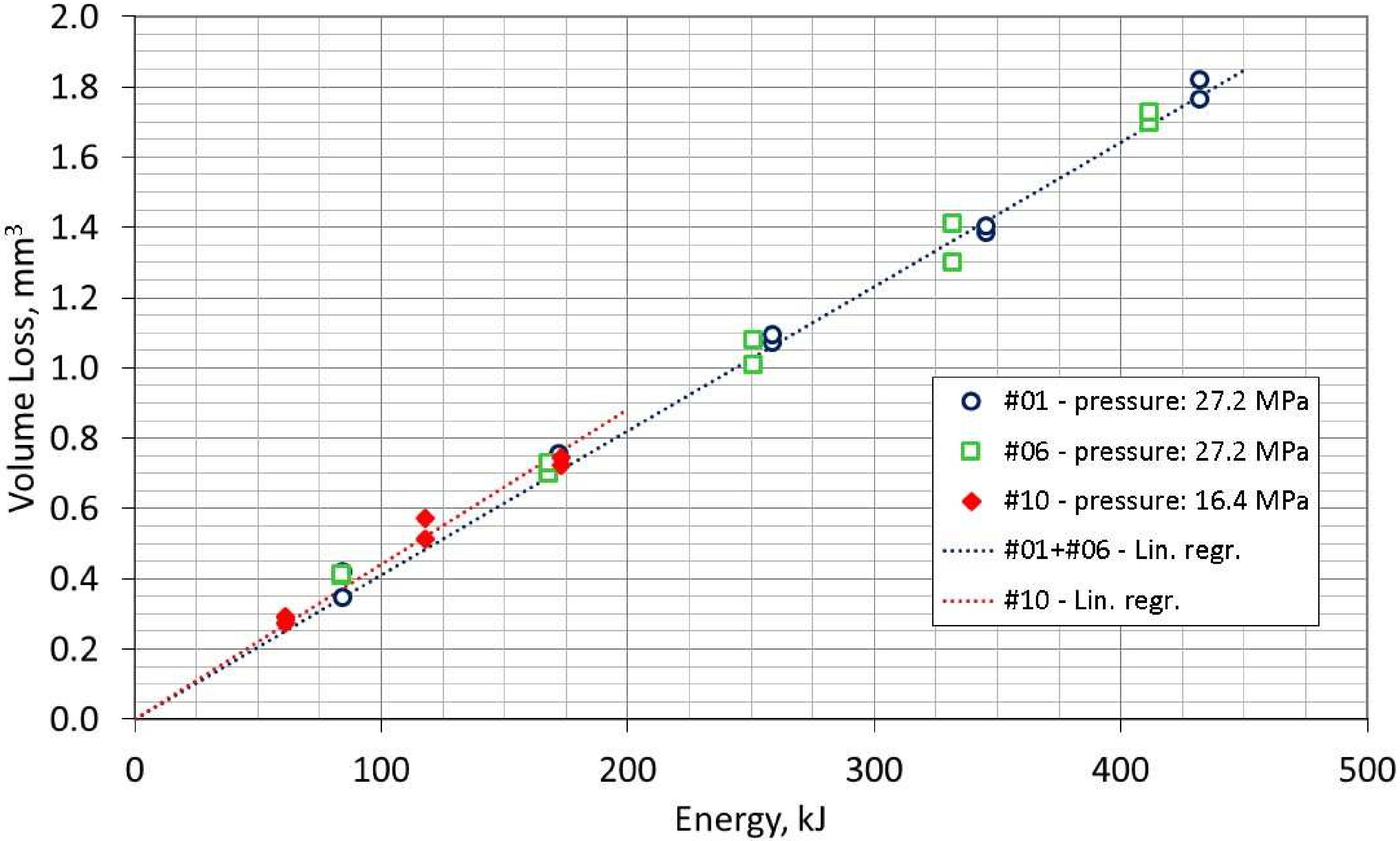
Volume Loss, mm^3
Energy, kJ
2.0
1.8
1.6
1.4
1.2
1.0
0.8
0.6
0.4
0.2
0.0
0
100
200
300
400
500
#01 - pressure: 27.2 MPa
#06 - pressure: 27.2 MPa
#10 - pressure: 16.4 MPa
#01+#06 - Lin. regr.
#10 - Lin. regr.

New

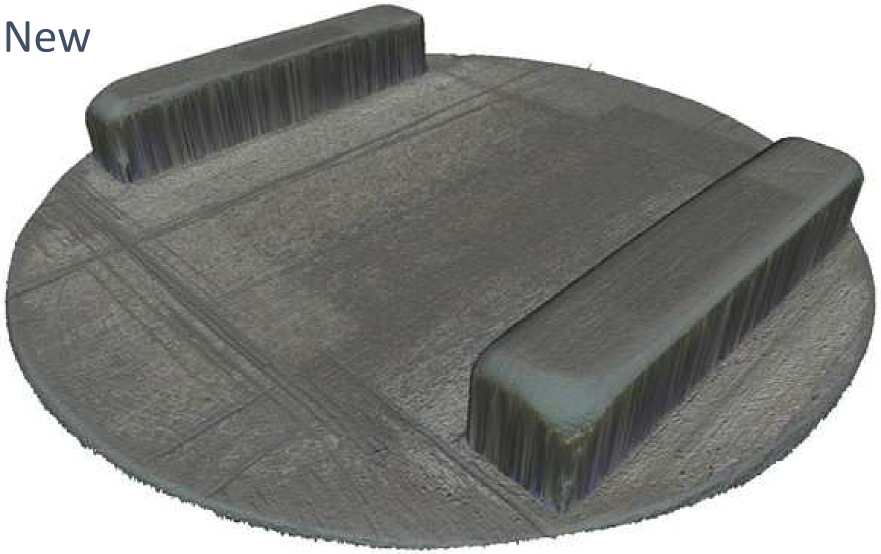

New

5M Wear cycles

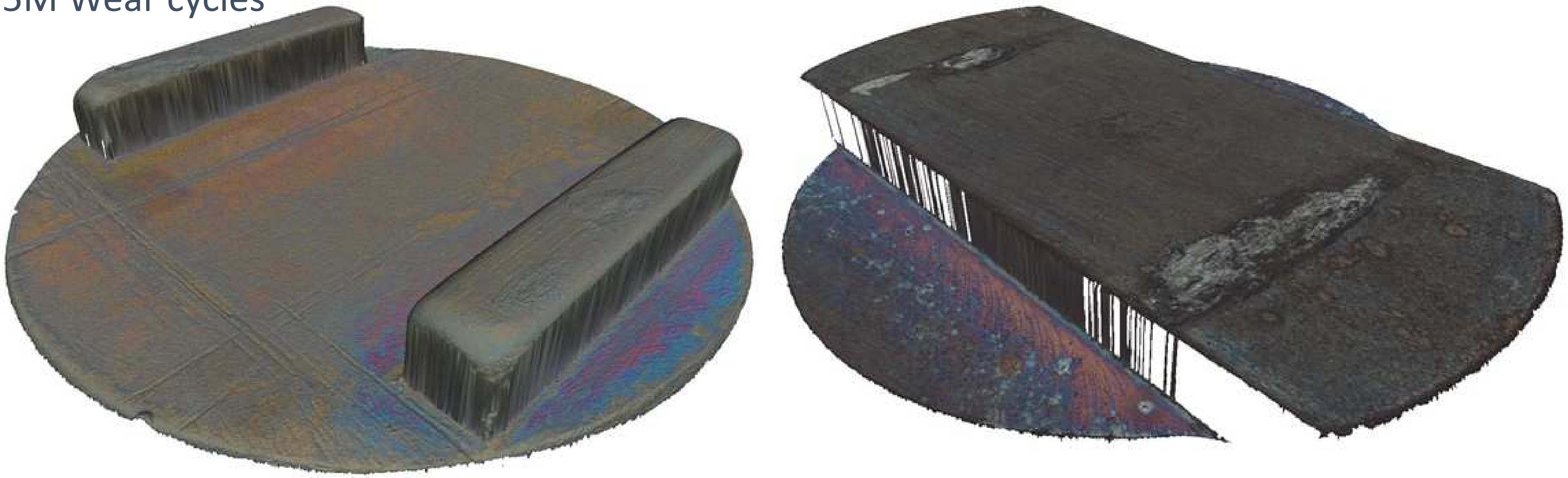

New

10M Wear cycles

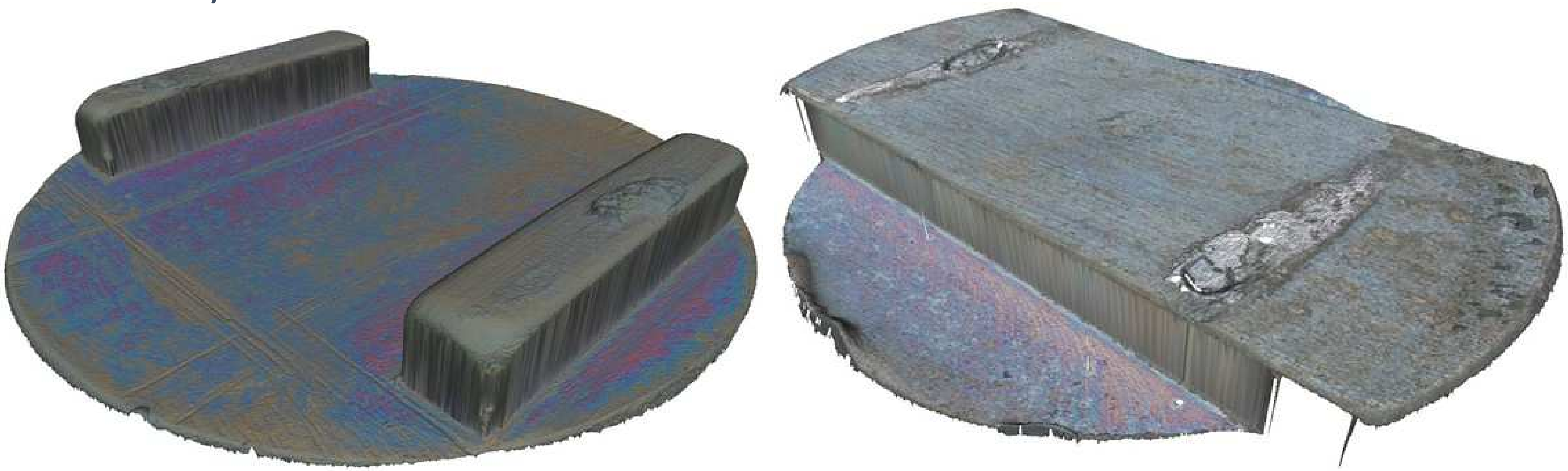

New

15M Wear cycles

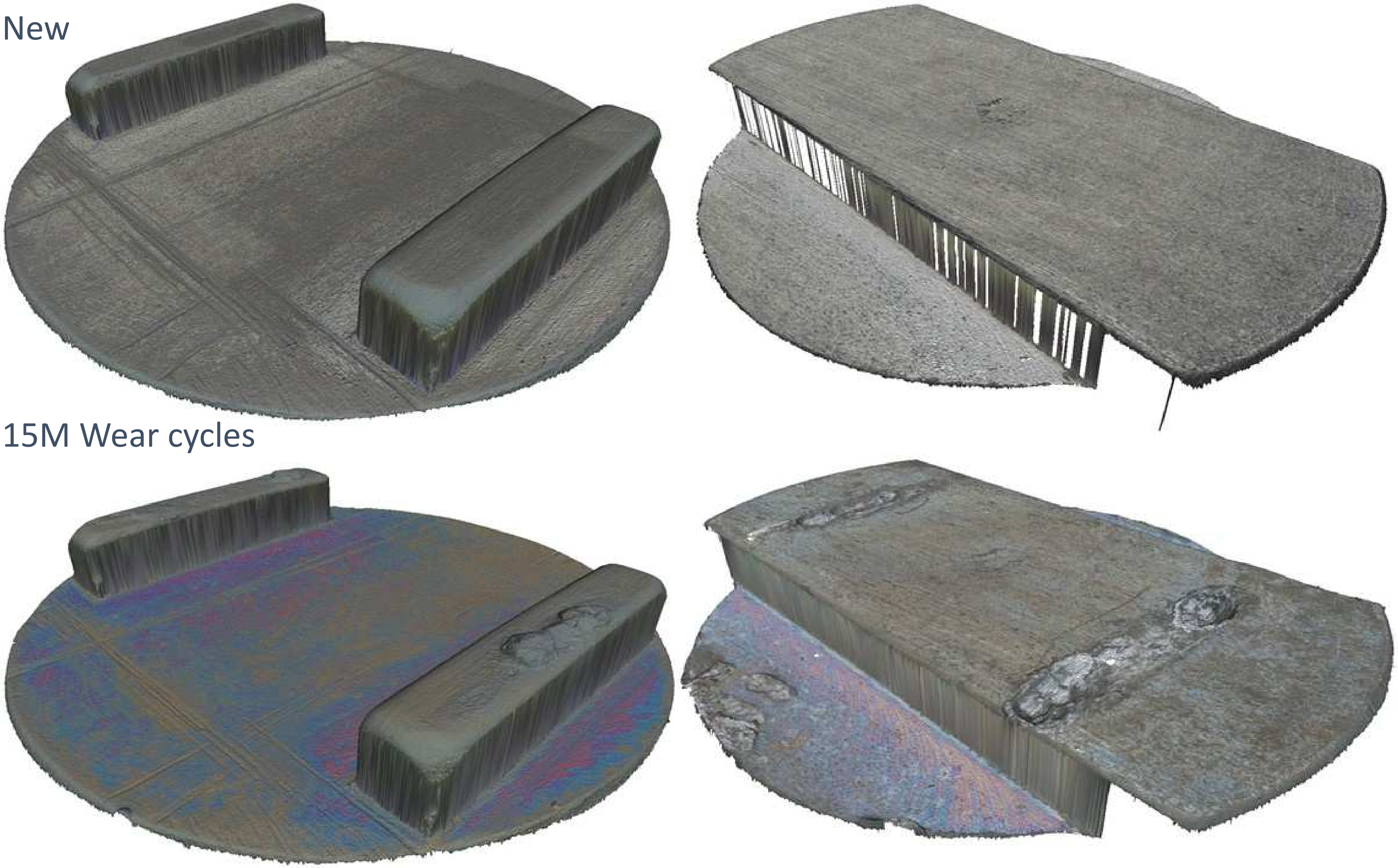

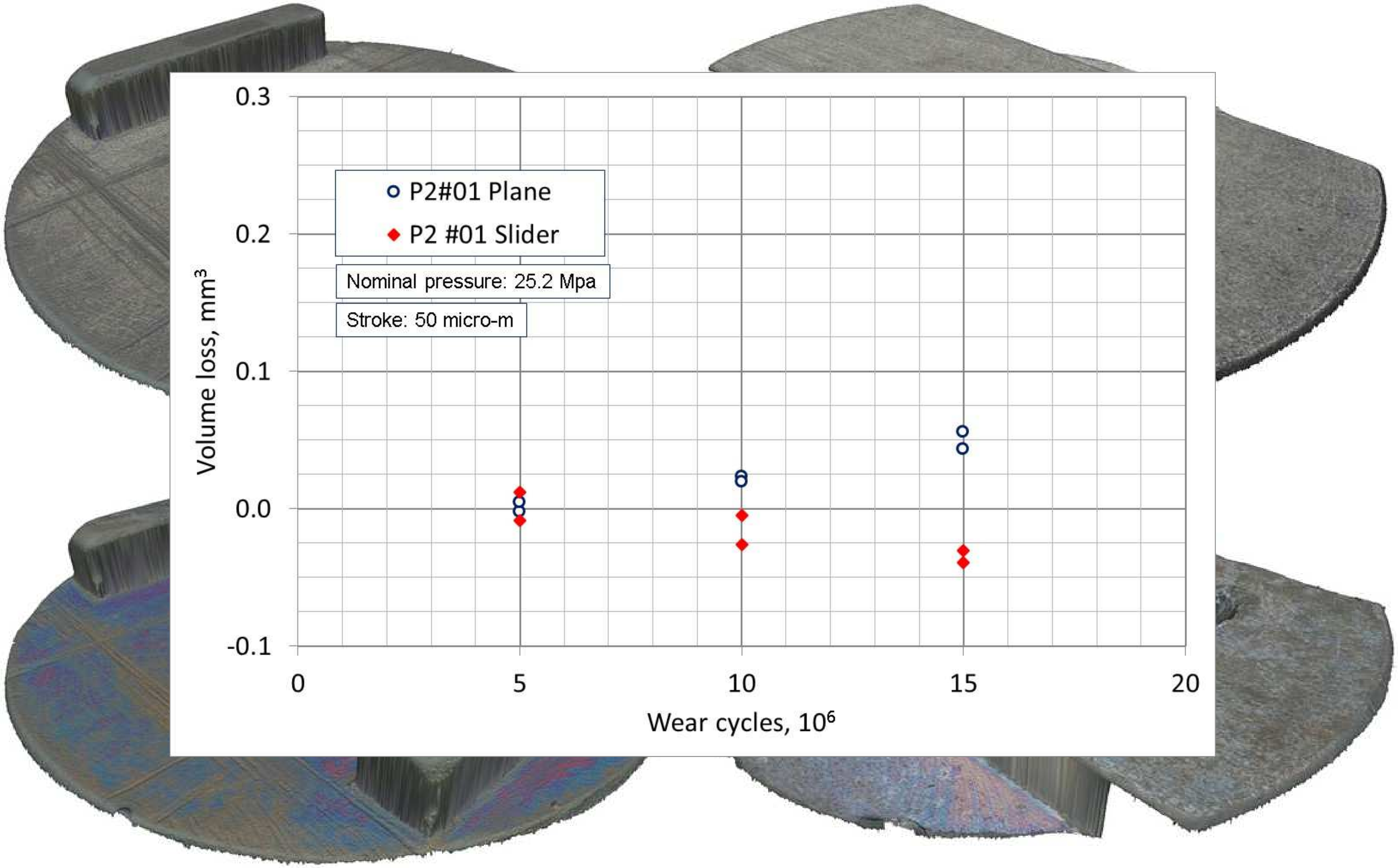

P2#01 Plane
P2 #01 Slider
Nominal pressure: 25.2 Mpa
Stroke: 50 micro-m
Volume loss, mm³
0.3
0.2
0.1
0.0
-0.1
0
5
10
15
20
Wear cycles, 10⁶

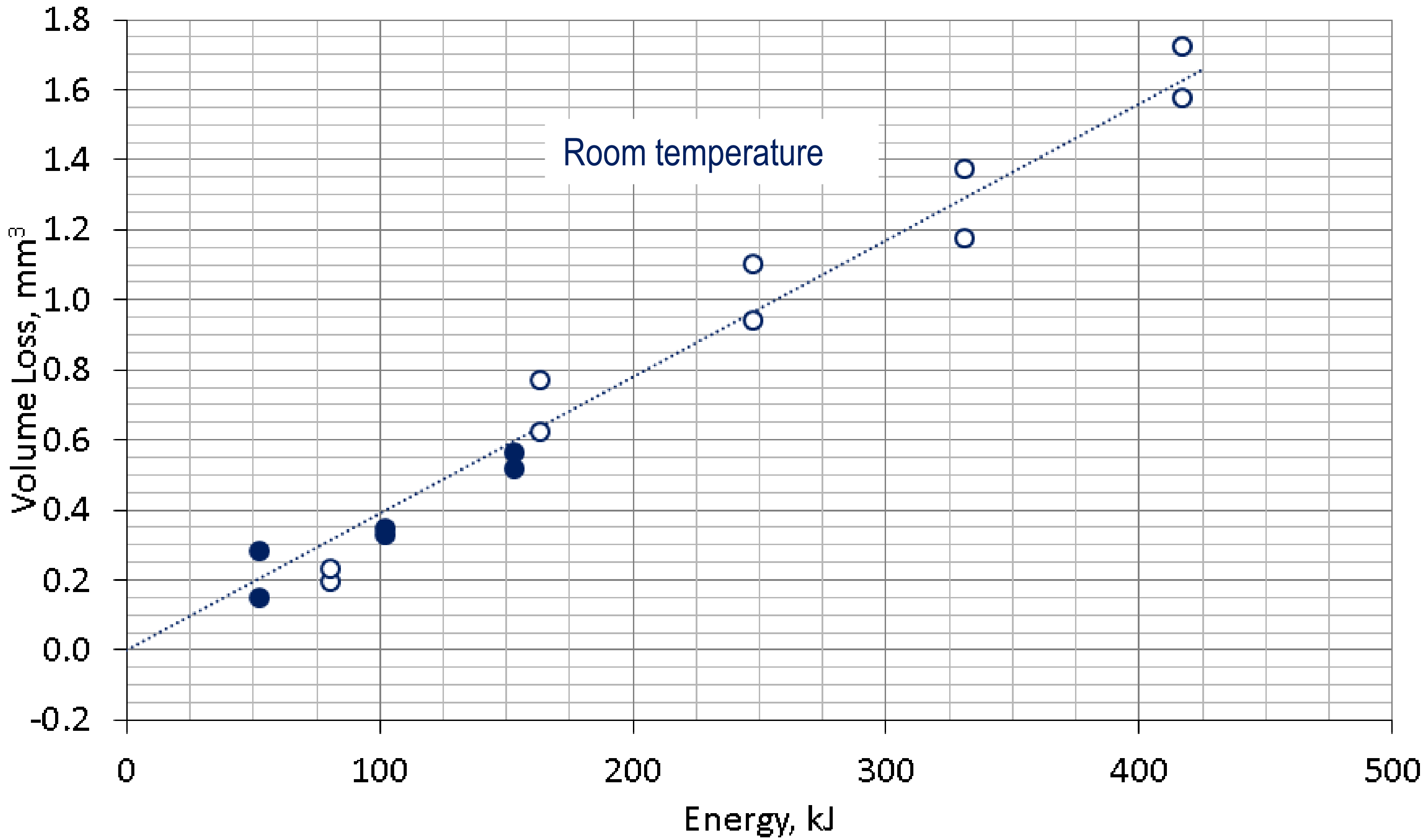
Room temperature
Volume Loss, mm³
Energy, kJ
1.8
1.6
1.4
1.2
1.0
0.8
0.6
0.4
0.2
0.0
-0.2
0
100
200
300
400
500

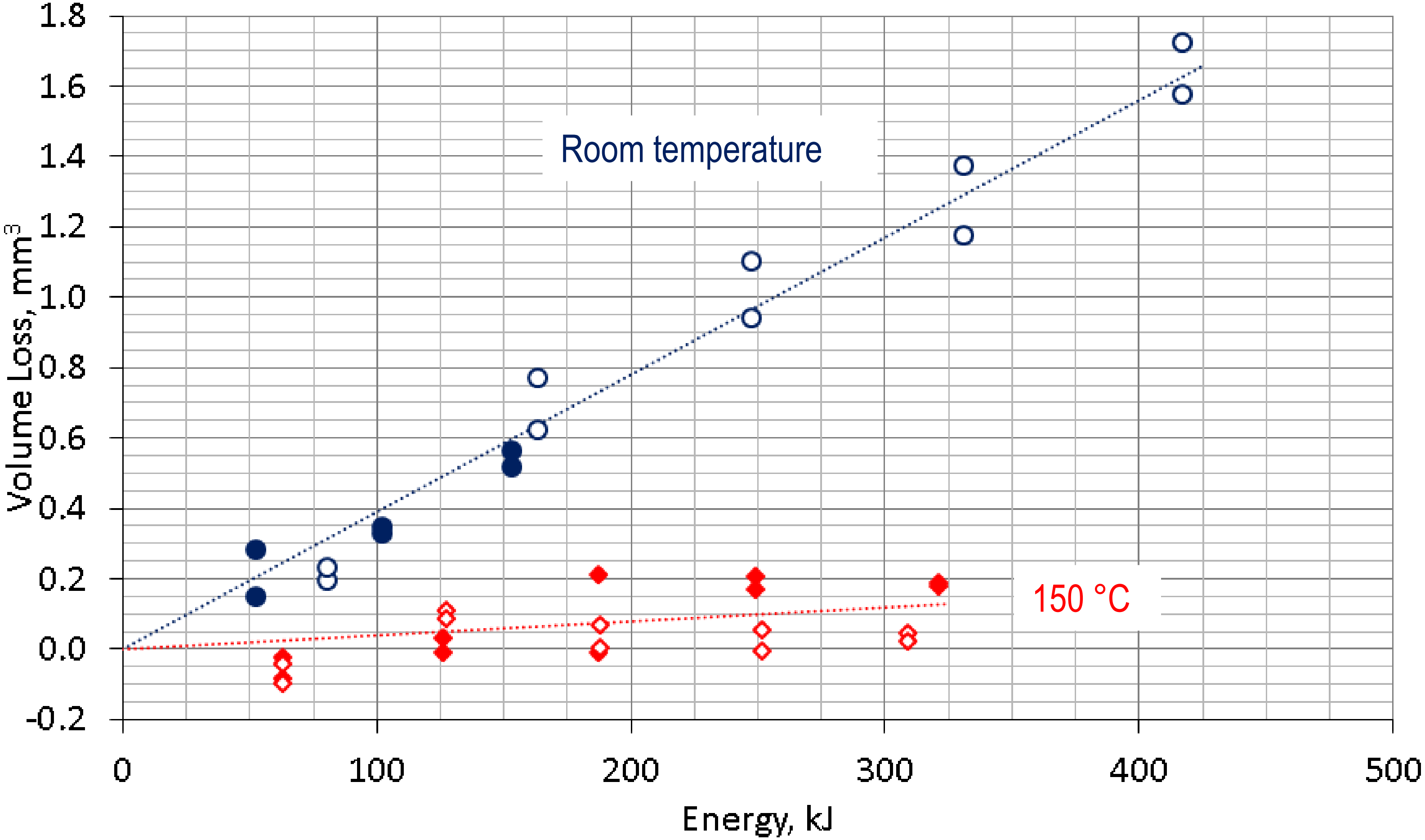
Room temperature
150 °C
Volume Loss, mm3
Energy, kJ
1.8
1.6
1.4
1.2
1.0
0.8
0.6
0.4
0.2
0.0
-0.2
0
100
200
300
400
500

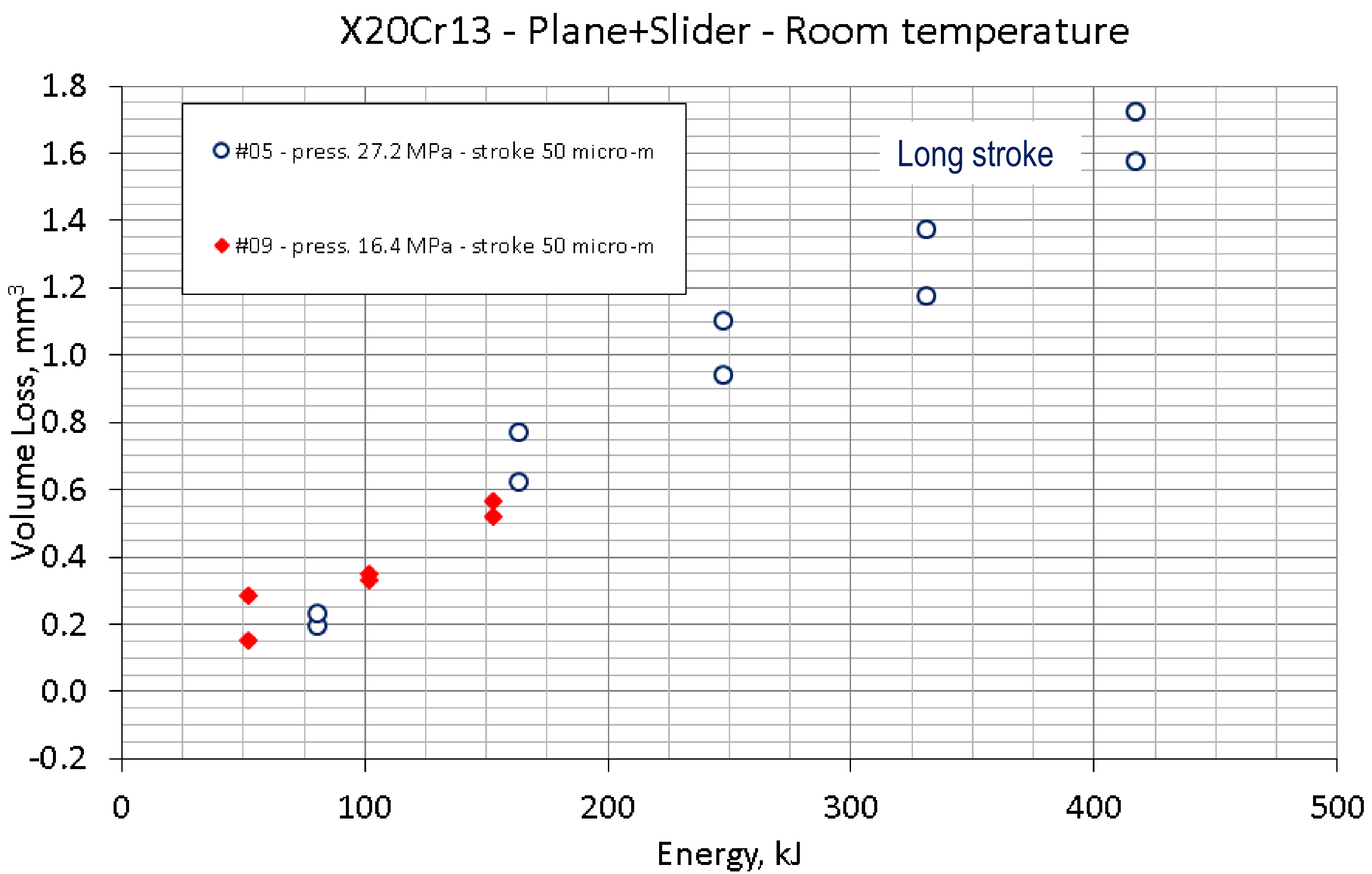
X20Cr13 - Plane+Slider - Room temperature
#05 - press. 27.2 MPa - stroke 50 micro-m
#09 - press. 16.4 MPa - stroke 50 micro-m
Long stroke
Volume Loss, mm3
Energy, kJ
1.8
1.6
1.4
1.2
1.0
0.8
0.6
0.4
0.2
0.0
-0.2
0
100
200
300
400
500

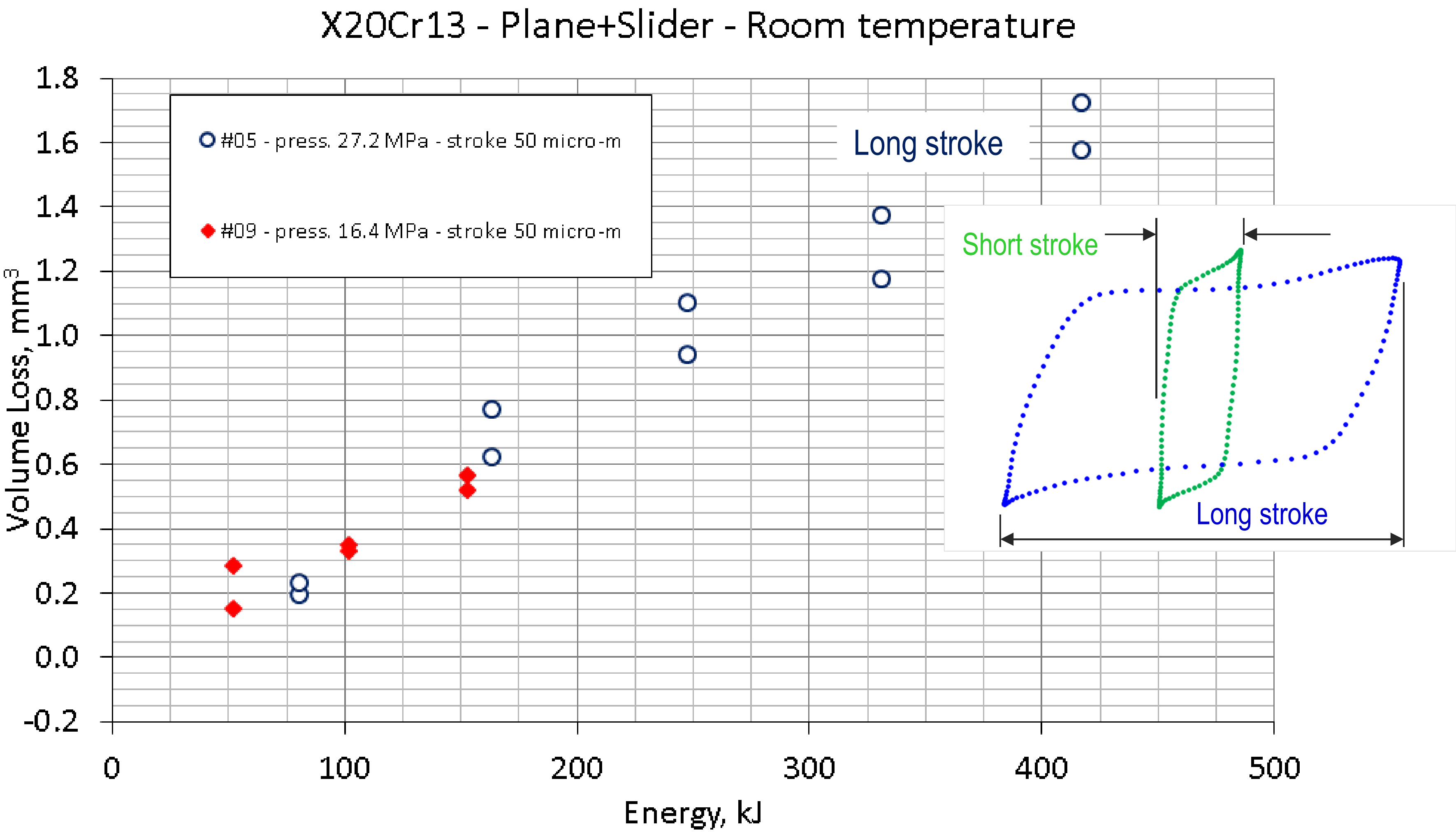

X20Cr13 - Plane+Slider - Room temperature
#05 - press. 27.2 MPa - stroke 50 micro-m
#09 - press. 16.4 MPa - stroke 50 micro-m
Long stroke
Short stroke
Long stroke
Volume Loss, mm3
Energy, kJ
1.8
1.6
1.4
1.2
1.0
0.8
0.6
0.4
0.2
0.0
-0.2
0
100
200
300
400
500

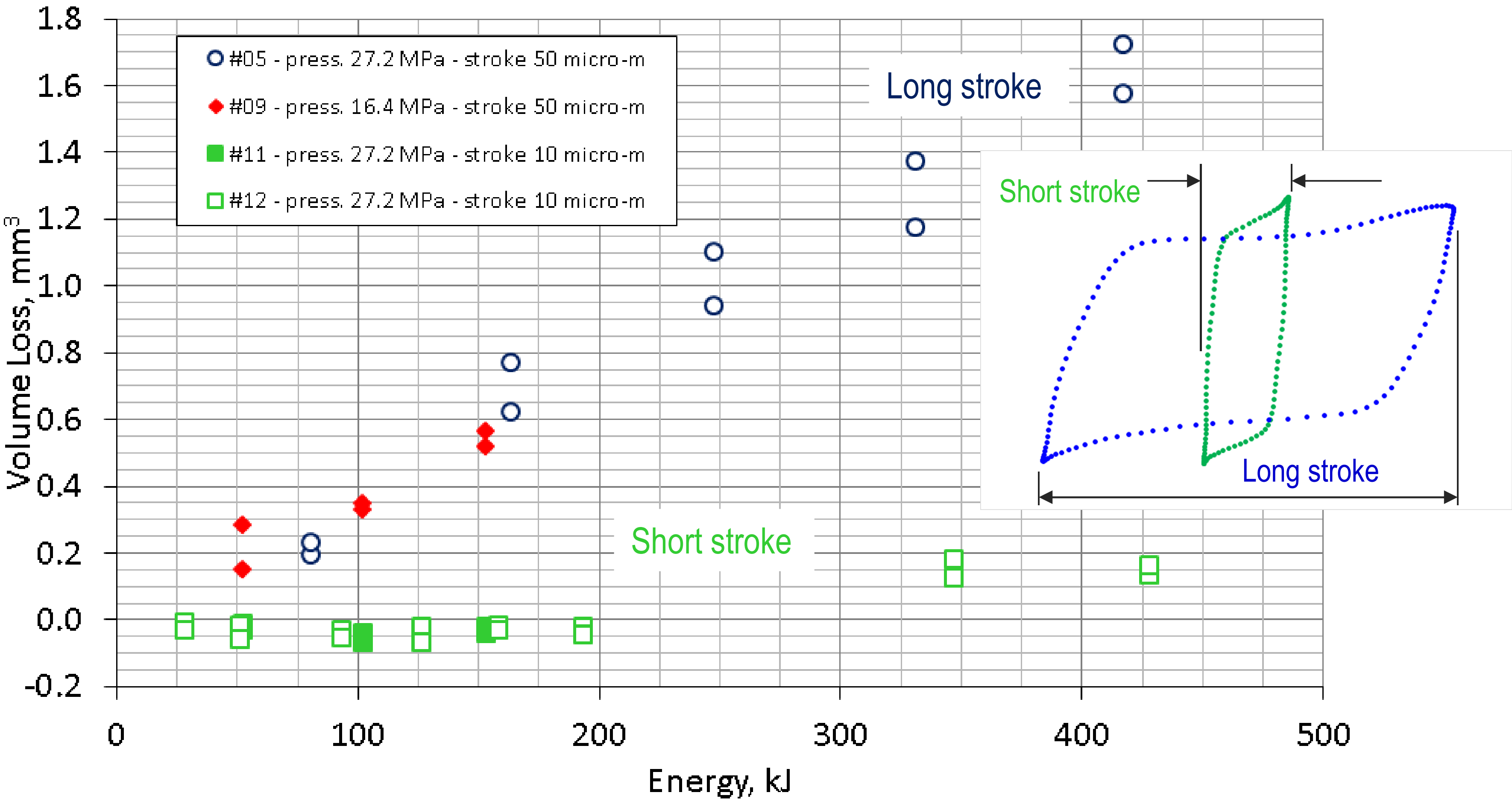

#05 - press. 27.2 MPa - stroke 50 micro-m
#09 - press. 16.4 MPa - stroke 50 micro-m
#11 - press. 27.2 MPa - stroke 10 micro-m
#12 - press. 27.2 MPa - stroke 10 micro-m
Long stroke
Short stroke
Short stroke
Long stroke
Volume Loss, mm3
Energy, kJ
1.8
1.6
1.4
1.2
1.0
0.8
0.6
0.4
0.2
0.0
-0.2
0
100
200
300
400
500

Friction is the resistance to motion which is experienced when one body moves tangentially over another with which it is in contact. Thus friction is not only a material properties but

it is a system response in the form of a reaction force

In the earlier days, friction was thought to be due to the "interlocking of asperities"- Asperities are the very small (usually microscopic) bumps or protuberances on most surfaces, which constitute the "roughness" of surfaces. Actually, asperities "interfere" with each other's passage rather than interlock.

There were some objections to the "interlocking" theory over 100 years ago, but the most serious doubts about the interlocking concept came with the experiments of W.B. Hardy (1923), where interlocking or interference could clearly not explain experimental results of friction.

Adhesion, cohesion, atomic attraction, molecular attraction, and similar terms were used then to explain friction, and Bowden and Tabor (1950) pursued the idea of adhesion as the source of friction. They showed that friction force was proportional to the real area of contact between two surfaces.

Bowden and Tabor (1950) explained that when two asperities are forced into contact they will weld together due to the adhesion between the two materials. When one of the solids is moved in a tangential direction relative to the other the micro-welded junctions will break but their shear strength causes a resistance to motion. During sliding, new micro-welded junctions are formed and broken continuously.

Models of friction (Greenwood,1955) were developed, usually around the assumption that friction force is the product of contact area of shear and the shear strength of the material in the asperities

$$\mu \propto A_s \tau / A_N \sigma_Y$$

τ : shear strength of the bond between asperities,
σ_Y : yield strength,
A_s: cross-sectional area of shear,
A_N: area carrying the normal load.

But $A_s \sim A_N$ and τ/σ_Y is constant then

the major problem with this model is that μ of all materials would be about the same!

The adhesion model of friction was, however, criticized on the basis of several objections, such as:

- the agreement between the theoretically calculated and the experimentally obtained values of the coefficient of friction is not particularly good,
- the model does not take into account the surface roughness effect on friction,
- there is a lack of evidence that the junctions produced will be of necessary strength, and
- when the normal force pressing the surfaces together is removed the adhesion cannot be detected.

Bowden and Tabor (1964) also included the ploughing effect in their concept of friction. When a hard asperity or a hard particle penetrates into a softer material and ploughs out a groove by plastic flow in the softer material this action creates a resistance to motion

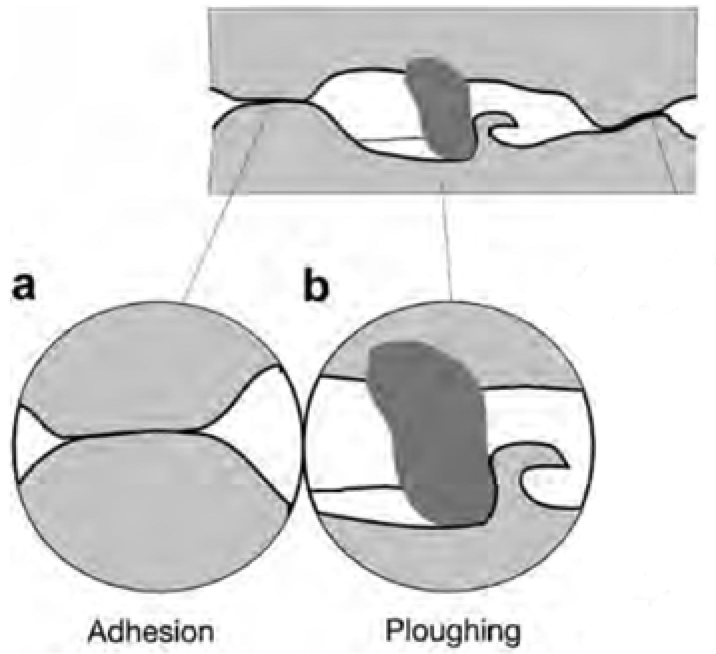

A new concept of friction, called the genesis of friction, was presented by **Suh** and **Sin** (1981). They focused on microscale friction mechanisms and showed that the mechanical properties affect the frictional behaviour to a greater extent than chemical properties.

The effect of friction can be divided into three basic mechanisms

1. asperity deformation
2. adhesion
3. particle ploughing,

The adhesion mechanism in many practical cases may not be the most dominant of the three.

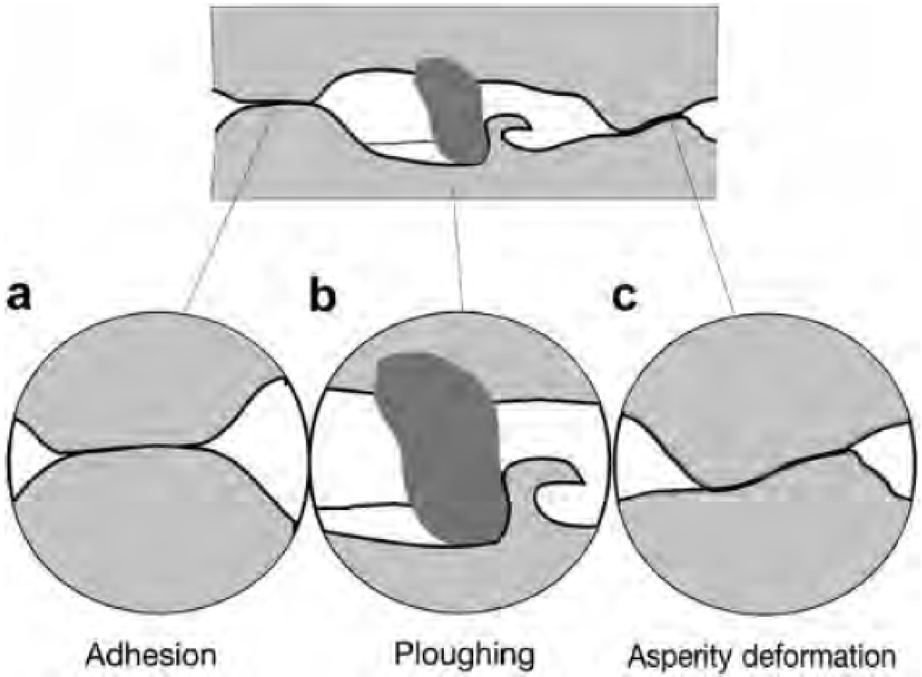

Friction: the genesis of friction by Suh and Sin 5/10

1. Friction due to asperity deformation, μ_d = 0÷0.43 . It appears that asperity deformation is responsible for the static coefficient of friction. Once the original asperities have been deformed, asperity interlocking cannot take place. This component can contribute to steady-state friction if new asperities are continuously generated as a result of the wear process.
2. Friction due to adhesion, μ_a = 0÷0.4. The low value is for a well-lubricated surface. The high value is for identical metals sliding against each other without any surface contamination or oxide layers.
3. Friction due to ploughing, μ_p = 0÷0.4. The low value is obtained either when wear particles are totally absent from the interface or when a soft surface is slid against a hard surface with a mirror finish. The high value is associated with two identical metals sliding against each other with deep penetration by wear particles.

Suh and Sin claim that the ploughing component of the surfaces by wear particles is the most important in most sliding situations.

Others studies show that there is no clear relationship between the coefficient of friction and the theoretical shear strength.

Suh and Sin identified five different friction stages that occurred in steel contacts before steady-state friction

1. Initially, the friction force is largely a result of ploughing of the surface by asperities. Adhesion does not play any significant role due to surface contamination. Asperity deformation takes place and affects the static coefficient of friction and the surface is easily polished. Consequently, the coefficient of friction in the initial stage is largely independent of material combinations, surface conditions and environmental conditions.

2. The polishing wear process at stage 1 has removed surface contamination and elements of bare surface will appear, resulting in a slow increase in the coefficient of friction due to increased adhesion.

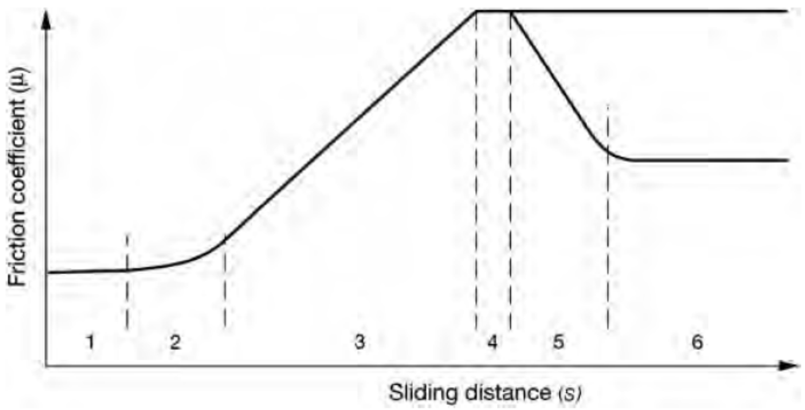

Suh and Sin identified five different friction stages that occurred in steel contacts before steady-state friction

3. The coefficient of friction increases due to a rapid increase in the number of wear particles entrapped between the sliding surfaces as a consequence of higher wear rates. The deformation of asperities continues and the adhesion effect increases due to larger clean interfacial areas. Some of the wear particles are trapped between the surfaces, causing ploughing. If the wear particles are entrapped between metals of equal hardness they will penetrate into both surfaces, preventing any slippage between the particle and the surface and resulting in maximum ploughing friction.

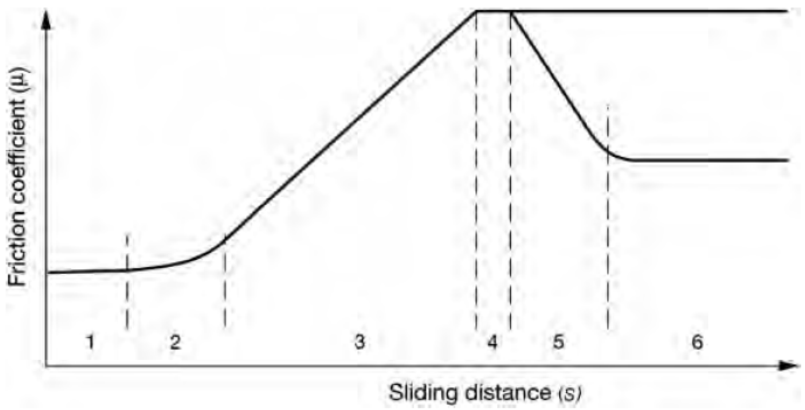

Suh and Sin identified five different friction stages that occurred in steel contacts before steady-state friction

4. The number of wear particles entrapped between the surfaces remains constant because the number of entrapped particles entering is the same as the number leaving the interface. The adhesion contribution also remains constant and the asperity deformation continues to contribute, since the wear by delamination creates new rough surfaces with asperities. Stage 4 represents the steady-state friction when two identical materials slide against each other or when the mechanisms of stage 5 are not significant.

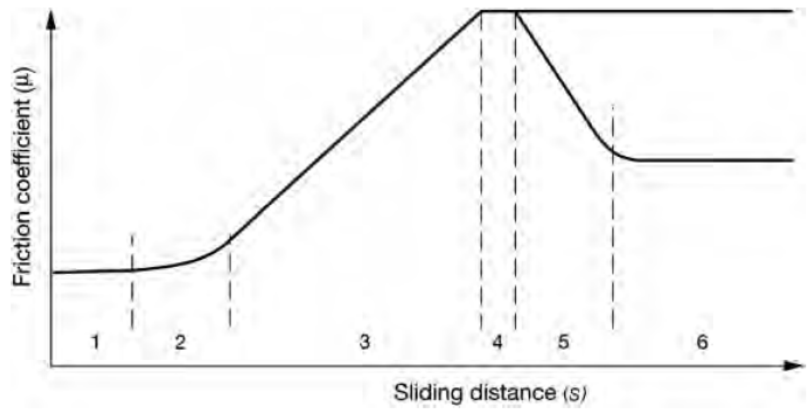

Suh and Sin identified five different friction stages that occurred in steel contacts before steady-state friction

5. In some cases, such as when a very hard stationary slider is slid against a soft specimen, the asperities of the hard surface are gradually removed, creating a mirror-like smooth surface. The frictional force decreases, due to the decrease in asperity deformation and ploughing, because wear particles cannot anchor so easily to a polished surface.

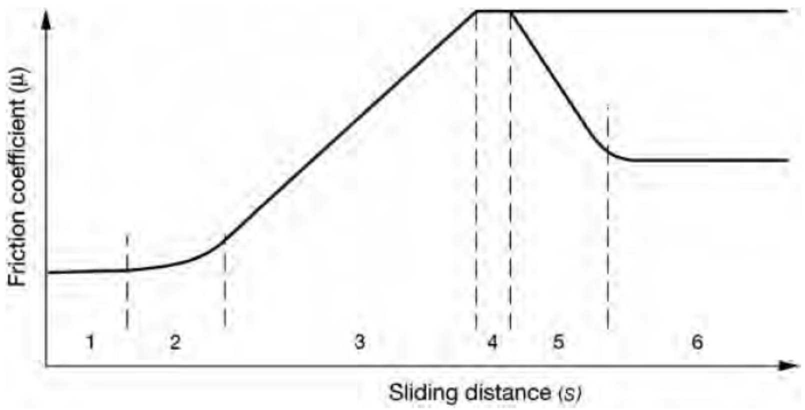

6. The coefficient of friction slowly levels off and reaches a steady-state value as the hard surface becomes mirror smooth to a maximum extent and the softer surface also acquires a mirror finish.

Friction is the resistance to motion which is experienced when one body moves tangentially over another with which it is in contact. Thus friction is not a material property; it is a system response in the form of a reaction force.

The coefficient of friction, m, is the (maximum) tangential frictional force T divided by the normal load N on the contact

$$\mu = \frac{T}{N}$$

Basically friction can be divided in three components, an adhesion force, T_a, due to adhesion between the two surfaces, a deformation force, T_d, due to deformation of the surfaces, and ploughing force T_p

$$T = T_a + T_d + T_p$$

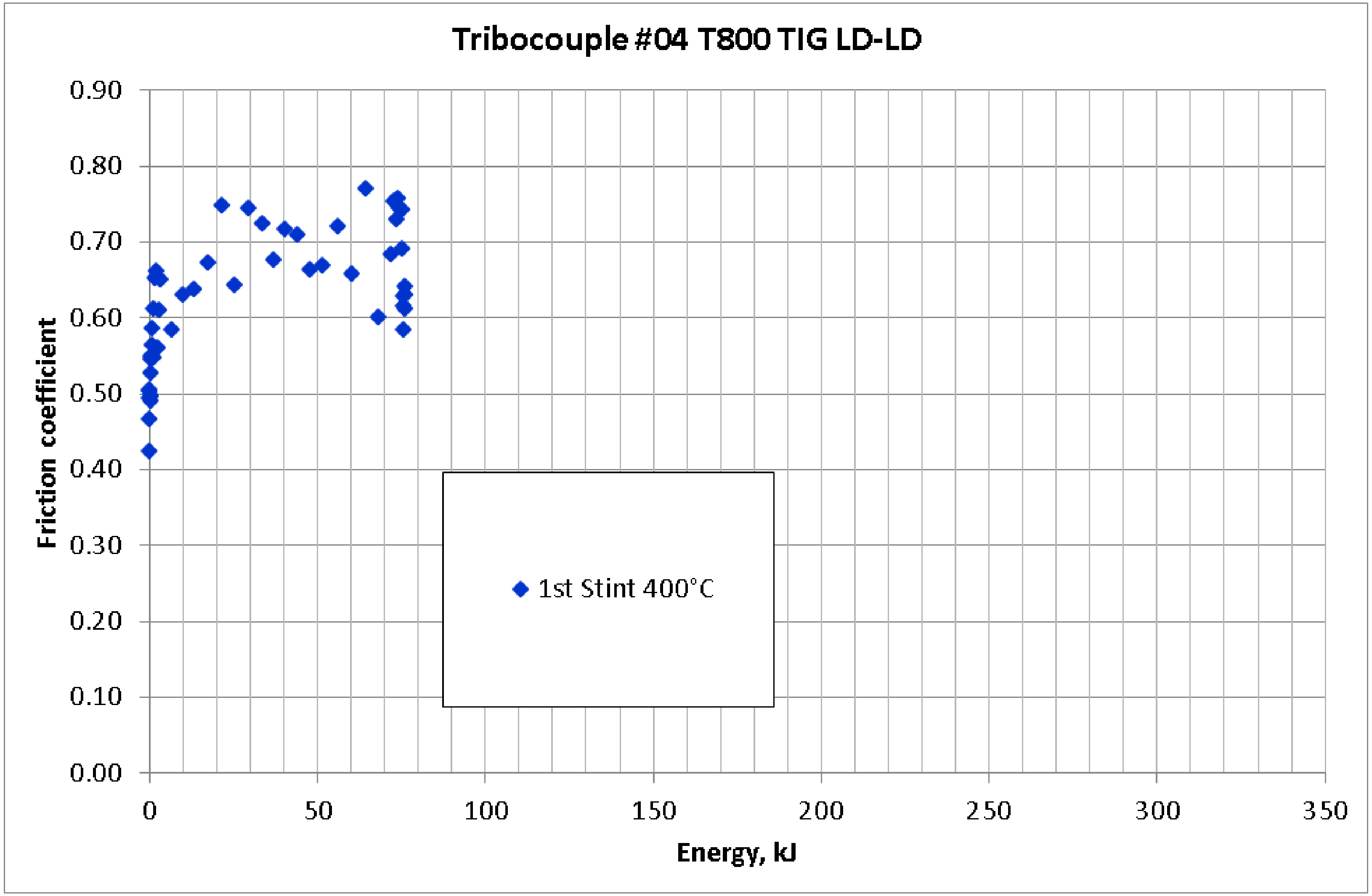
Tribocouple #04 T800 TIG LD-LD
Friction coefficient
0.90
0.80
0.70
0.60
0.50
0.40
0.30
0.20
0.10
0.00
0
50
100
150
200
250
300
350
Energy, kJ
1st Stint 400°C

Experimental results: friction coefficient

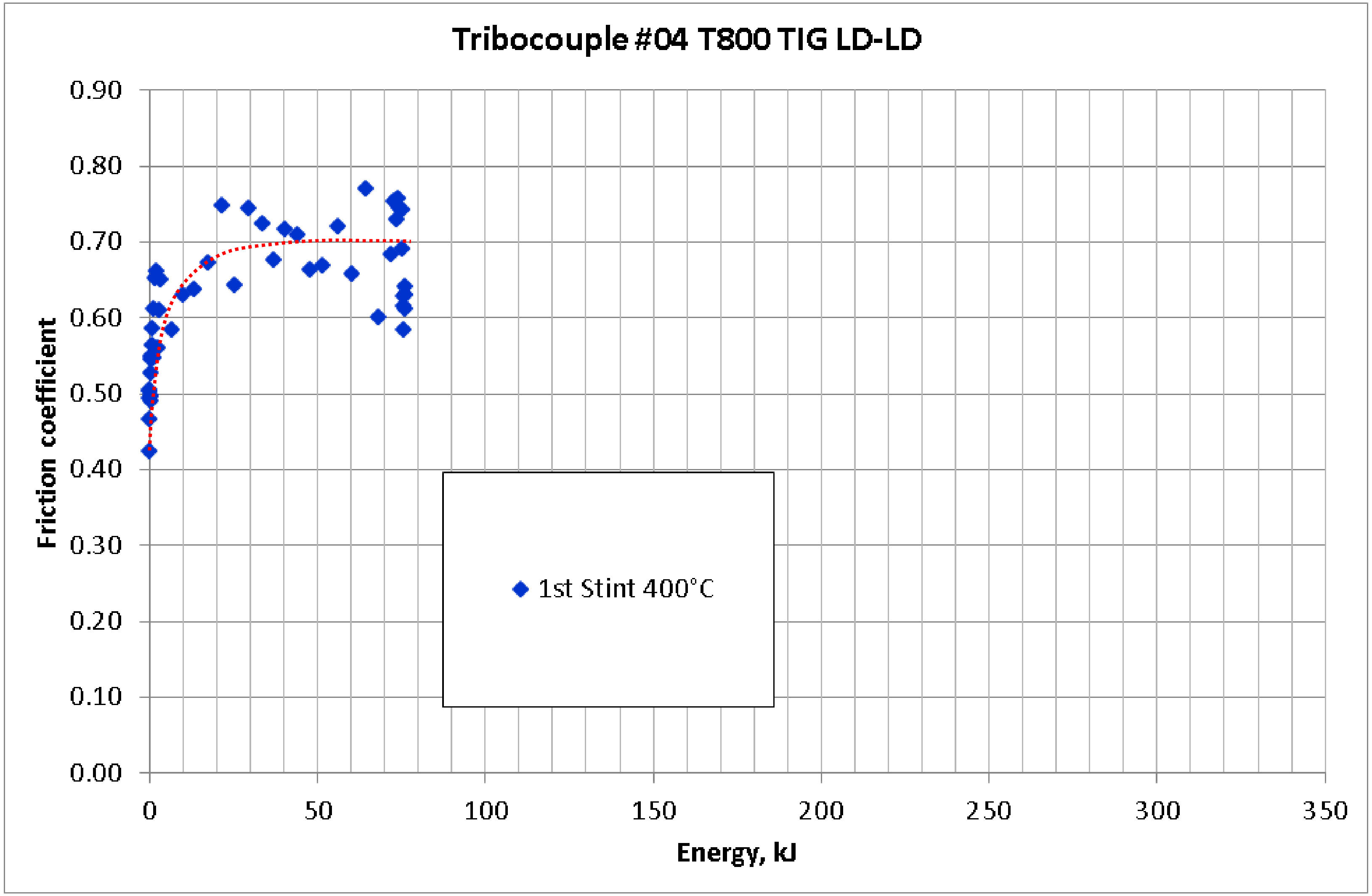

Experimental results: friction coefficient

After a running-in period the experiment was stopped and the wear particles were removed

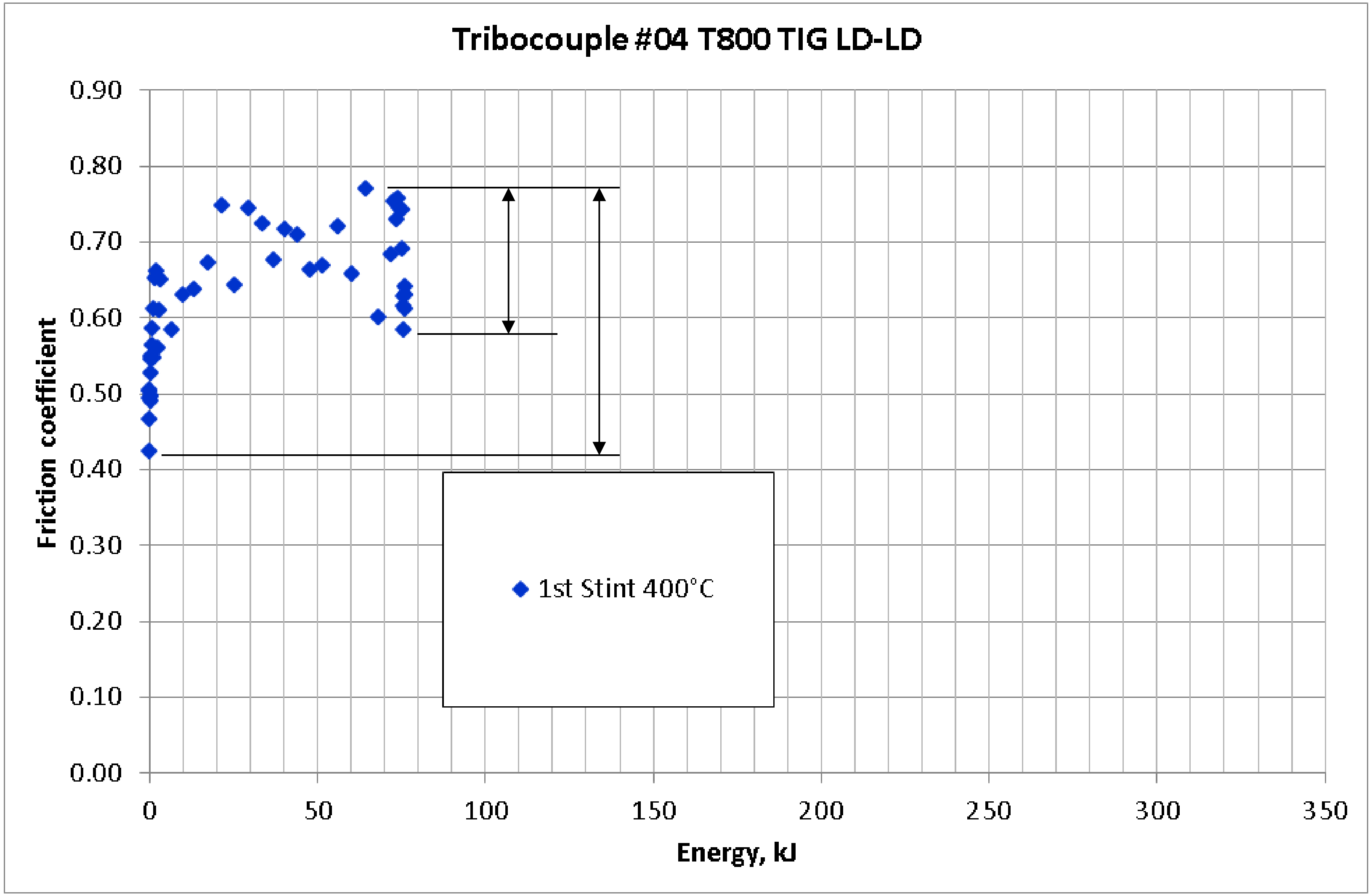

Experimental results: friction coefficient

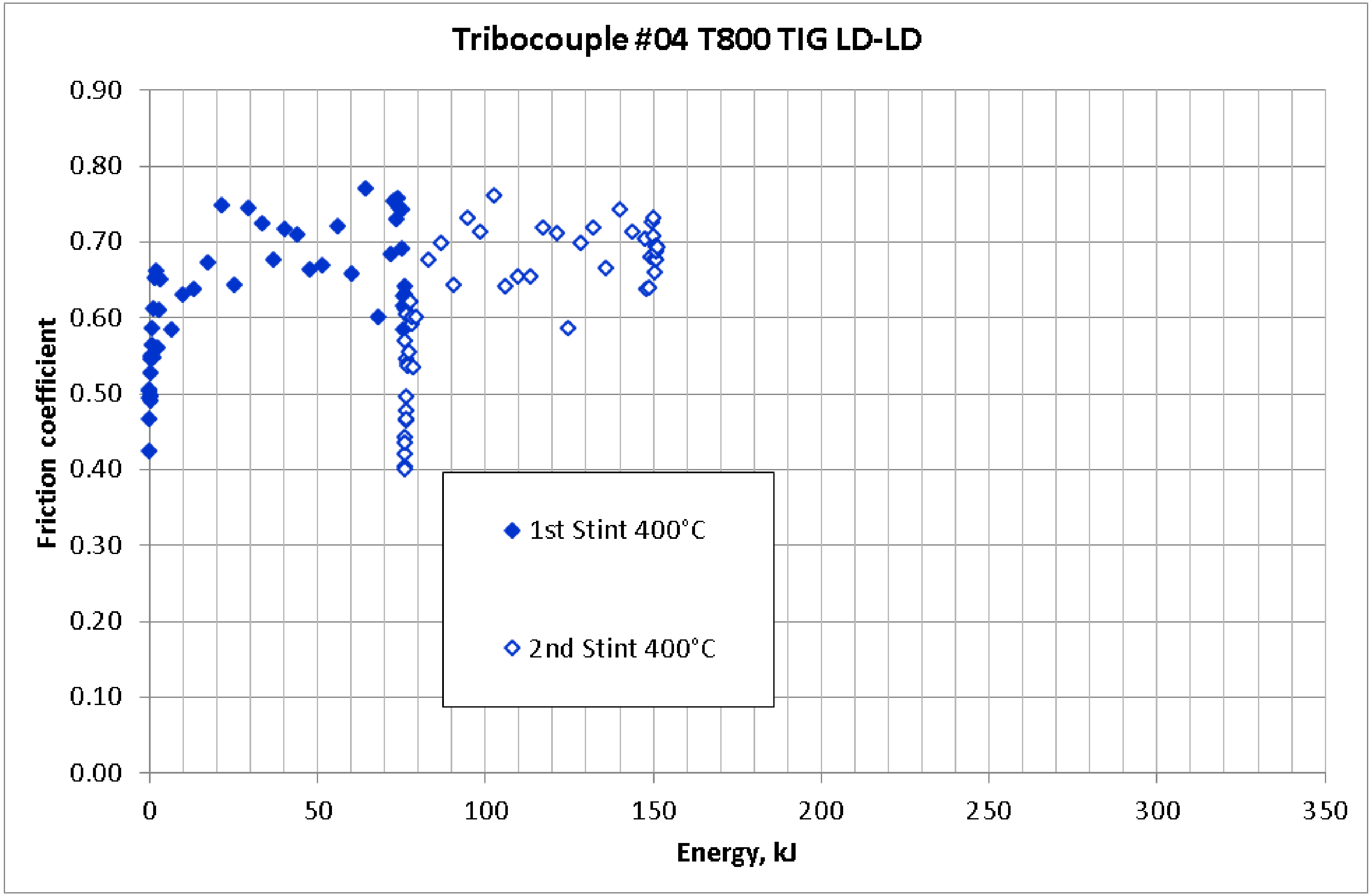

Experimental results: friction coefficient

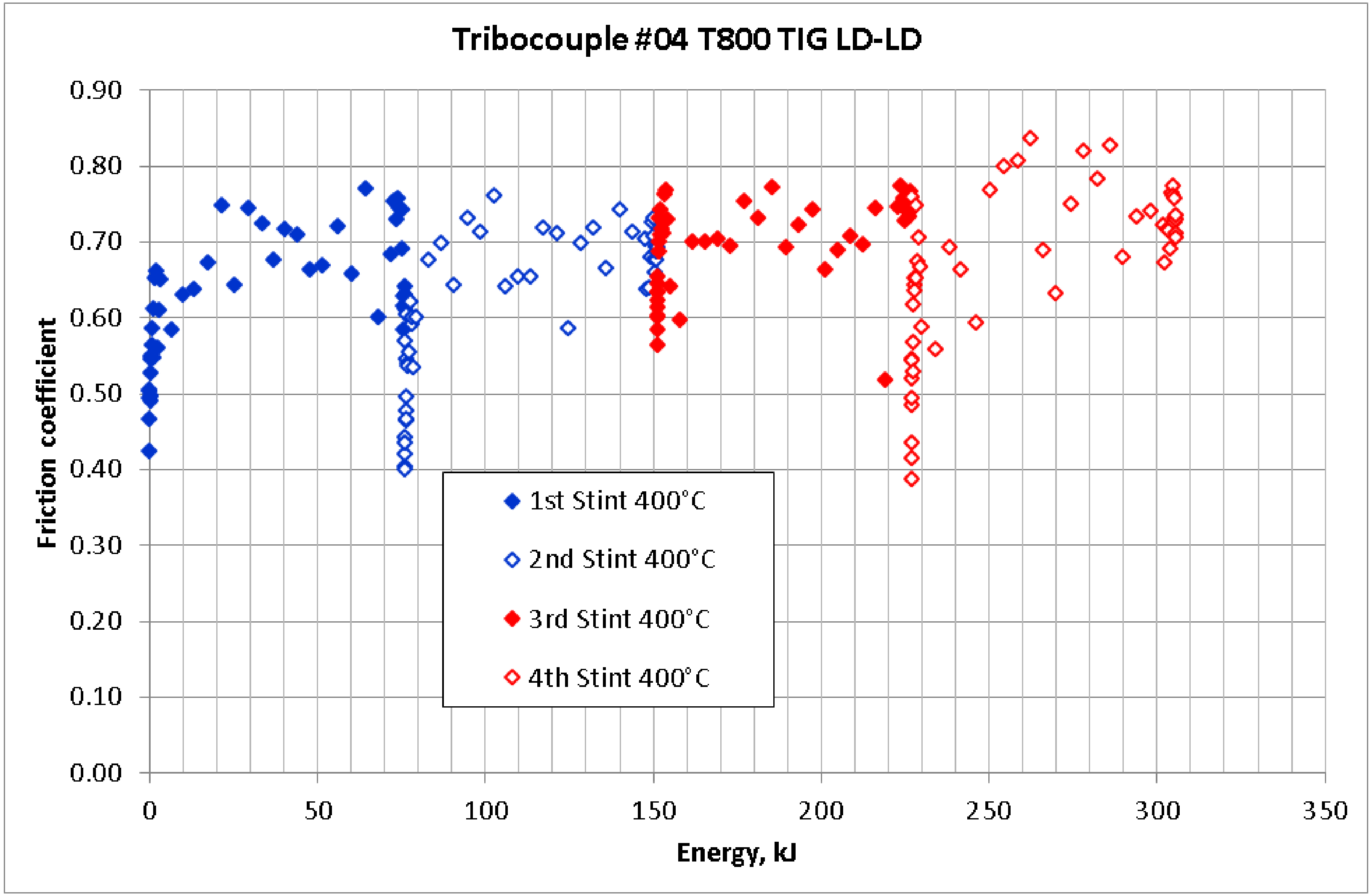

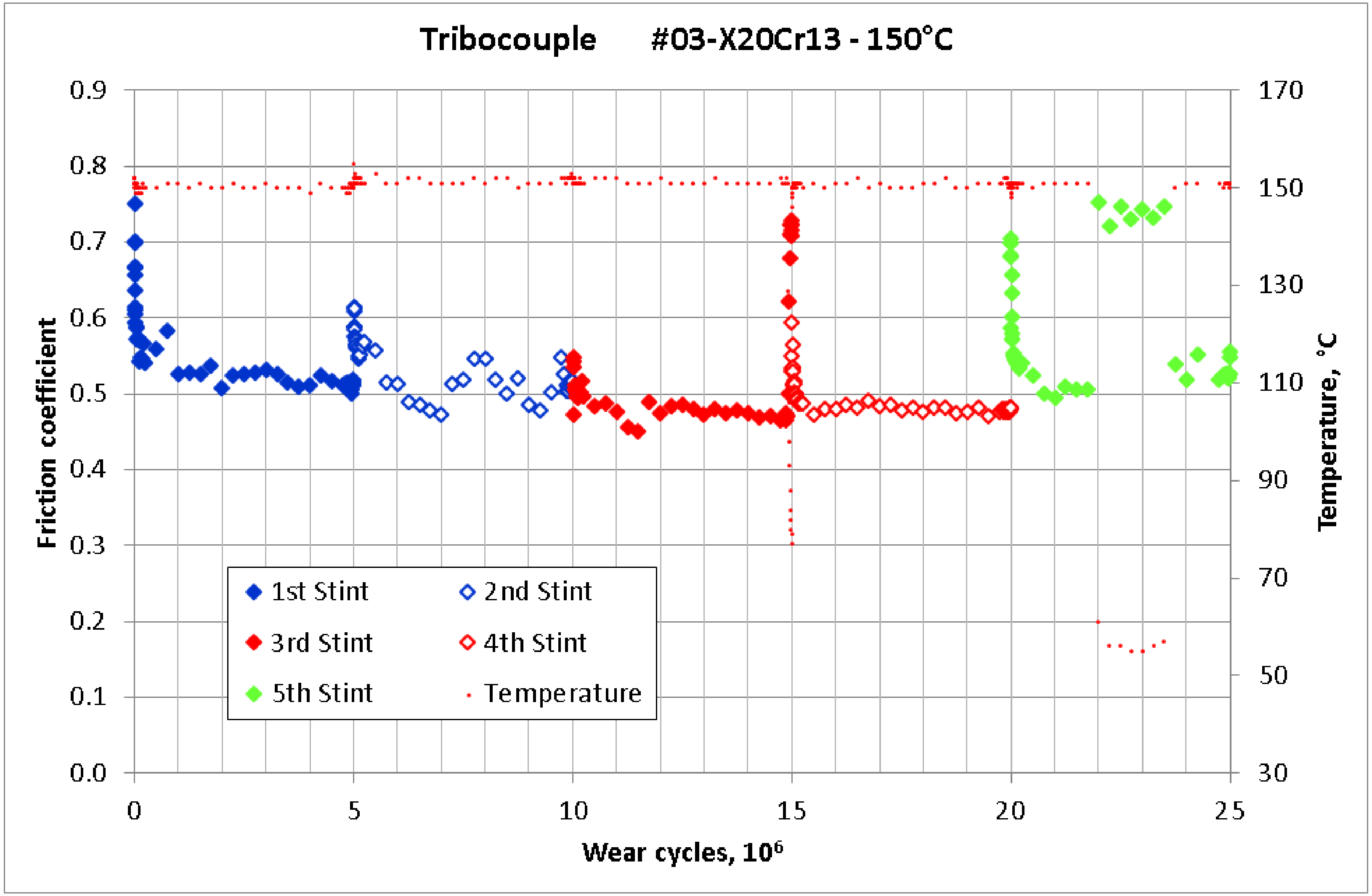

Tribocouple #03-X20Cr13 - 150°C
Friction coefficient
0.9
0.8
0.7
0.6
0.5
0.4
0.3
0.2
0.1
0.0
Temperature, °C
170
150
130
110
90
70
50
30
0
5
10
15
20
25
Wear cycles, 10⁶
1st Stint
2nd Stint
3rd Stint
4th Stint
5th Stint
Temperature

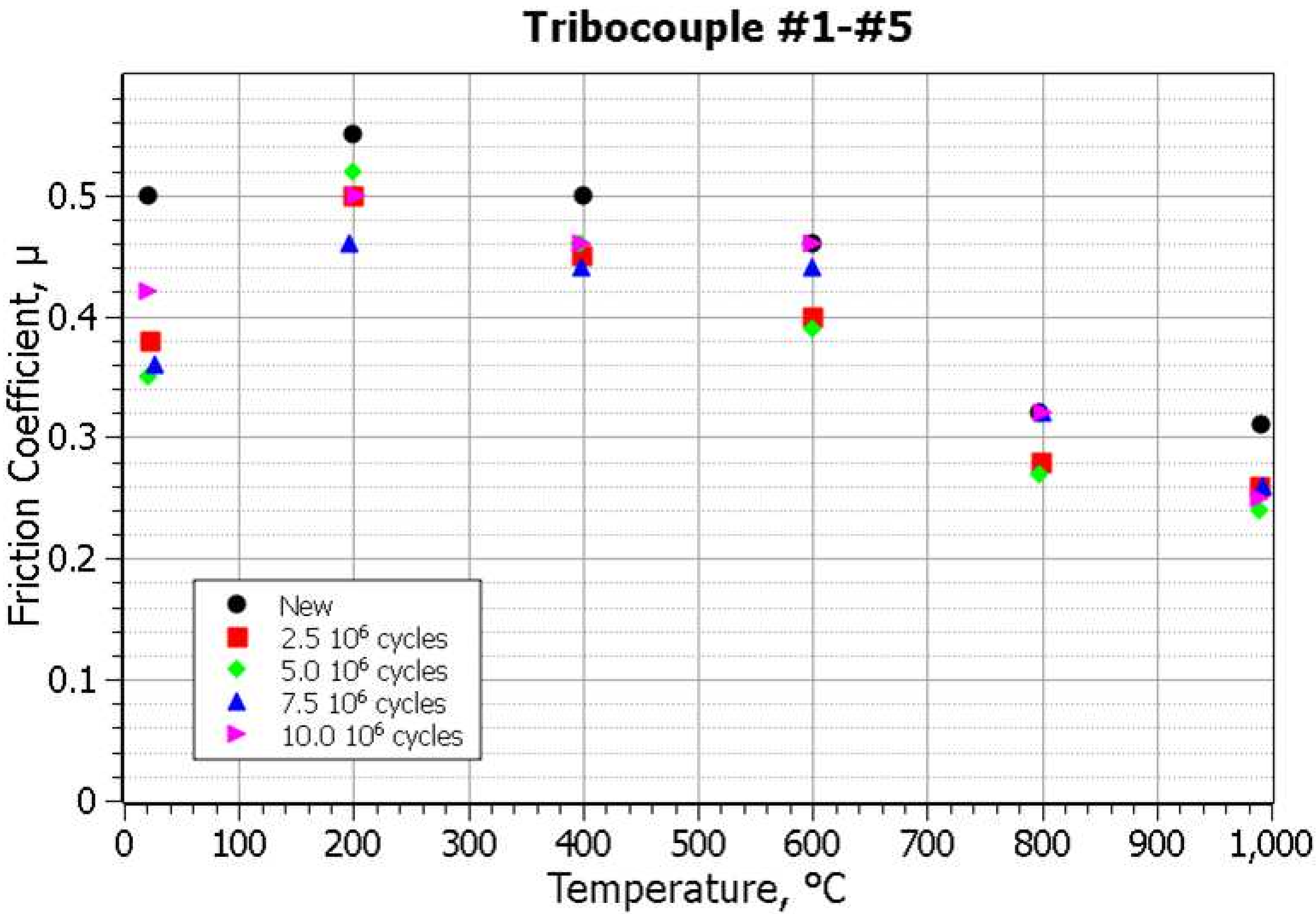

Tribocouple #1-#5
Friction Coefficient, μ
0
0.1
0.2
0.3
0.4
0.5
0
100
200
300
400
500
600
700
800
900
1,000
Temperature, °C
New
2.5 10⁶ cycles
5.0 10⁶ cycles
7.5 10⁶ cycles
10.0 10⁶ cycles

Scheme

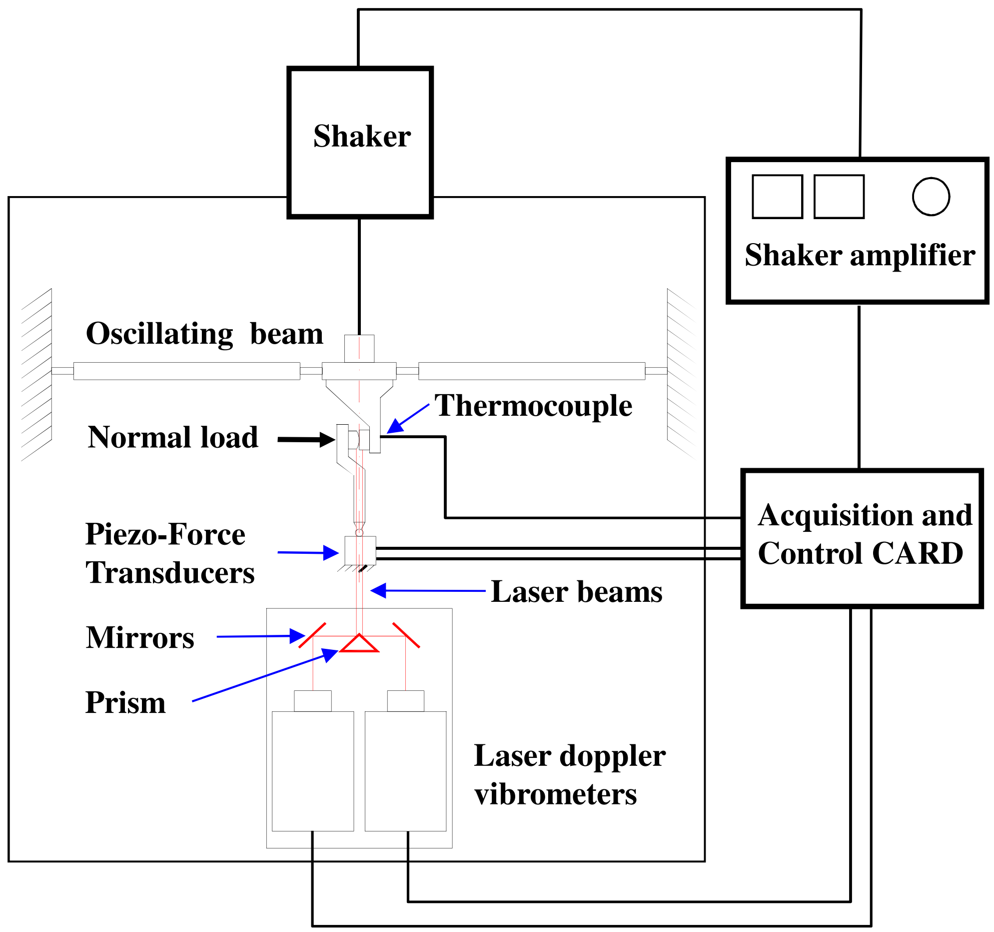

Shaker
Shaker amplifier
Oscillating beam
Thermocouple
Normal load
Piezo-Force Transducers
Acquisition and Control CARD
Laser beams
Mirrors
Prism
Laser doppler vibrometers

Scheme

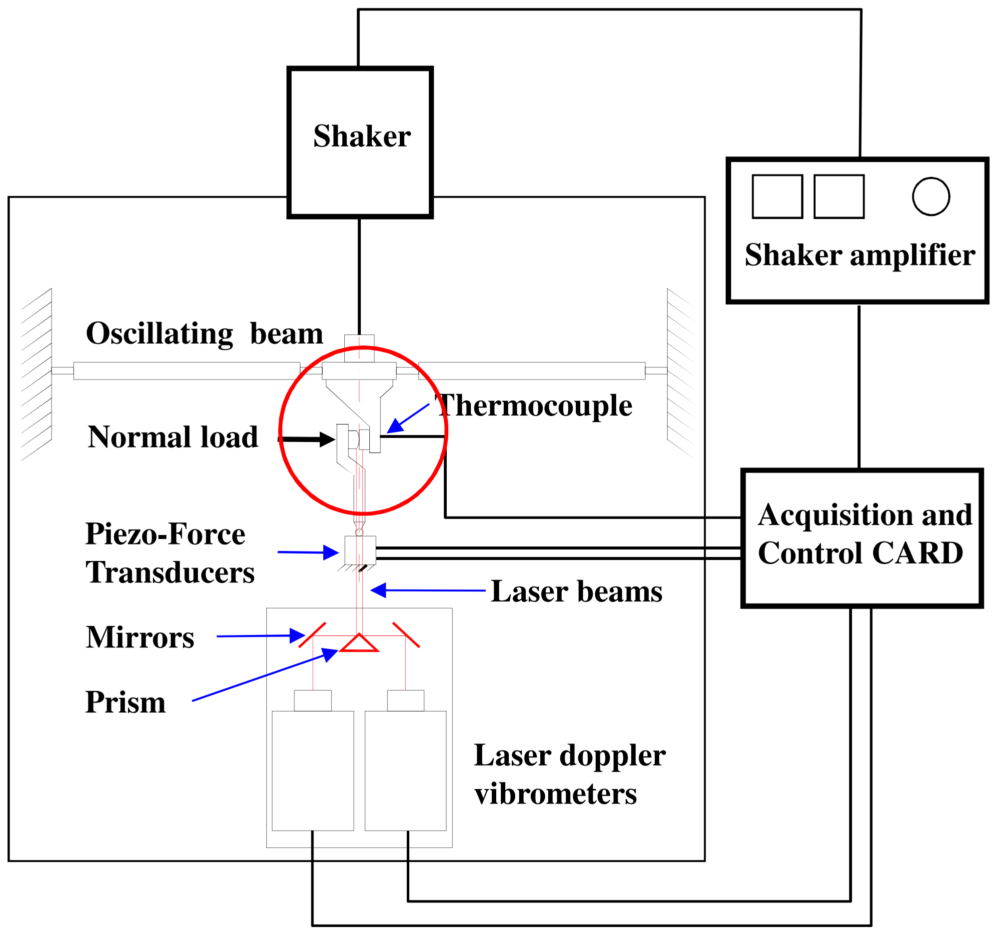

Shaker
Shaker amplifier
Oscillating beam
Thermocouple
Normal load
Acquisition and Control CARD
Piezo-Force Transducers
Laser beams
Mirrors
Prism
Laser doppler vibrometers

Scheme

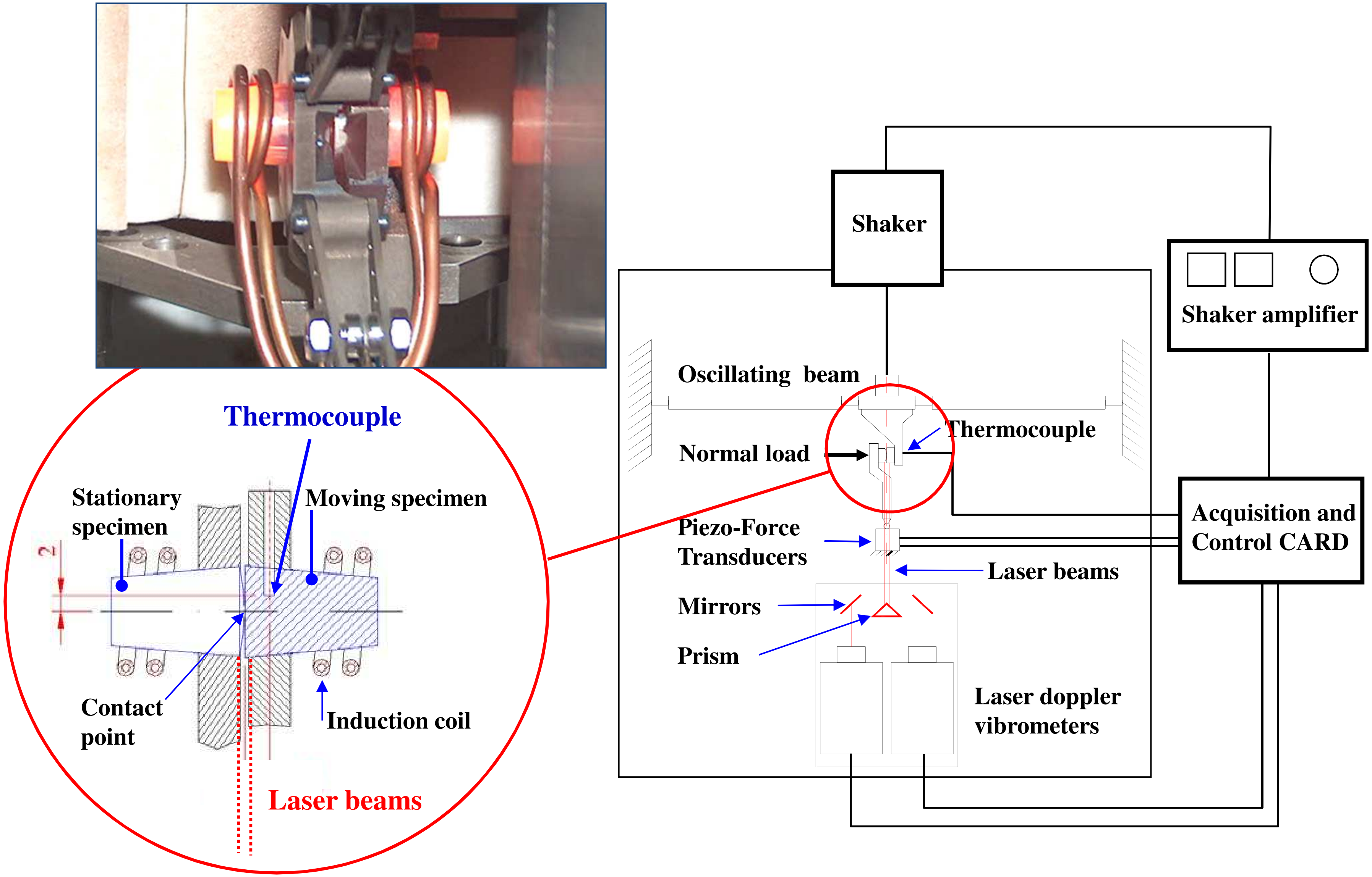

Thermocouple
Stationary specimen
Moving specimen
Contact point
Induction coil
Laser beams
Shaker
Shaker amplifier
Oscillating beam
Thermocouple
Normal load
Piezo-Force Transducers
Laser beams
Acquisition and Control CARD
Mirrors
Prism
Laser doppler vibrometers

Tilting mechanism

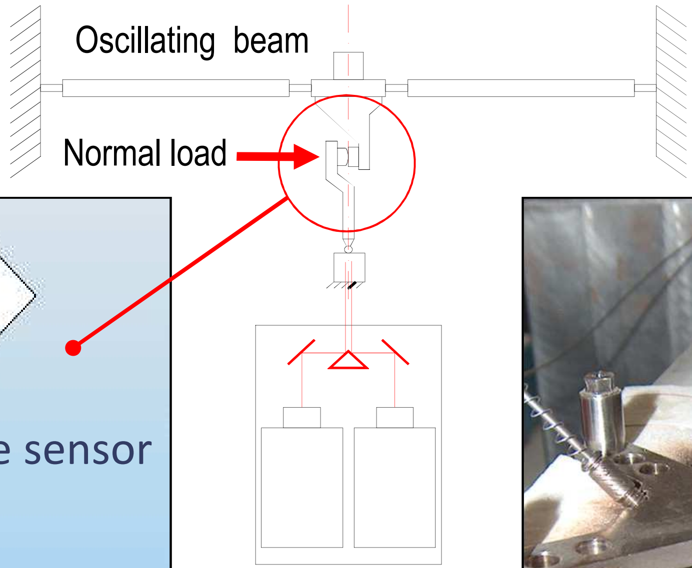

Normal load through dead weight and pulleys

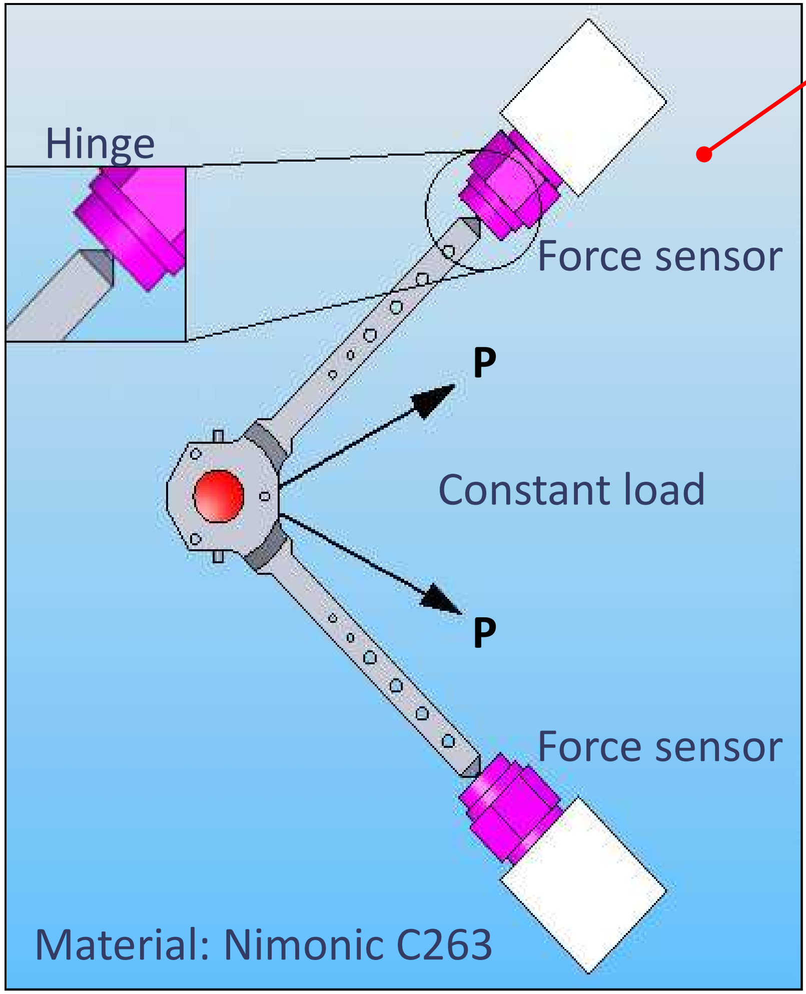

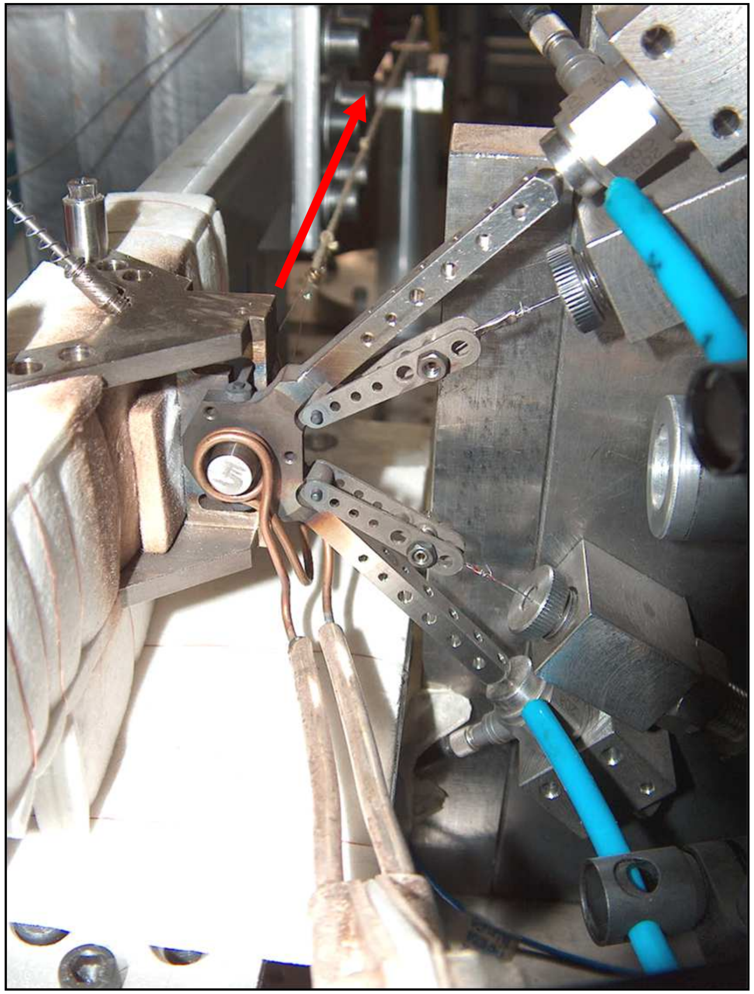

Overview

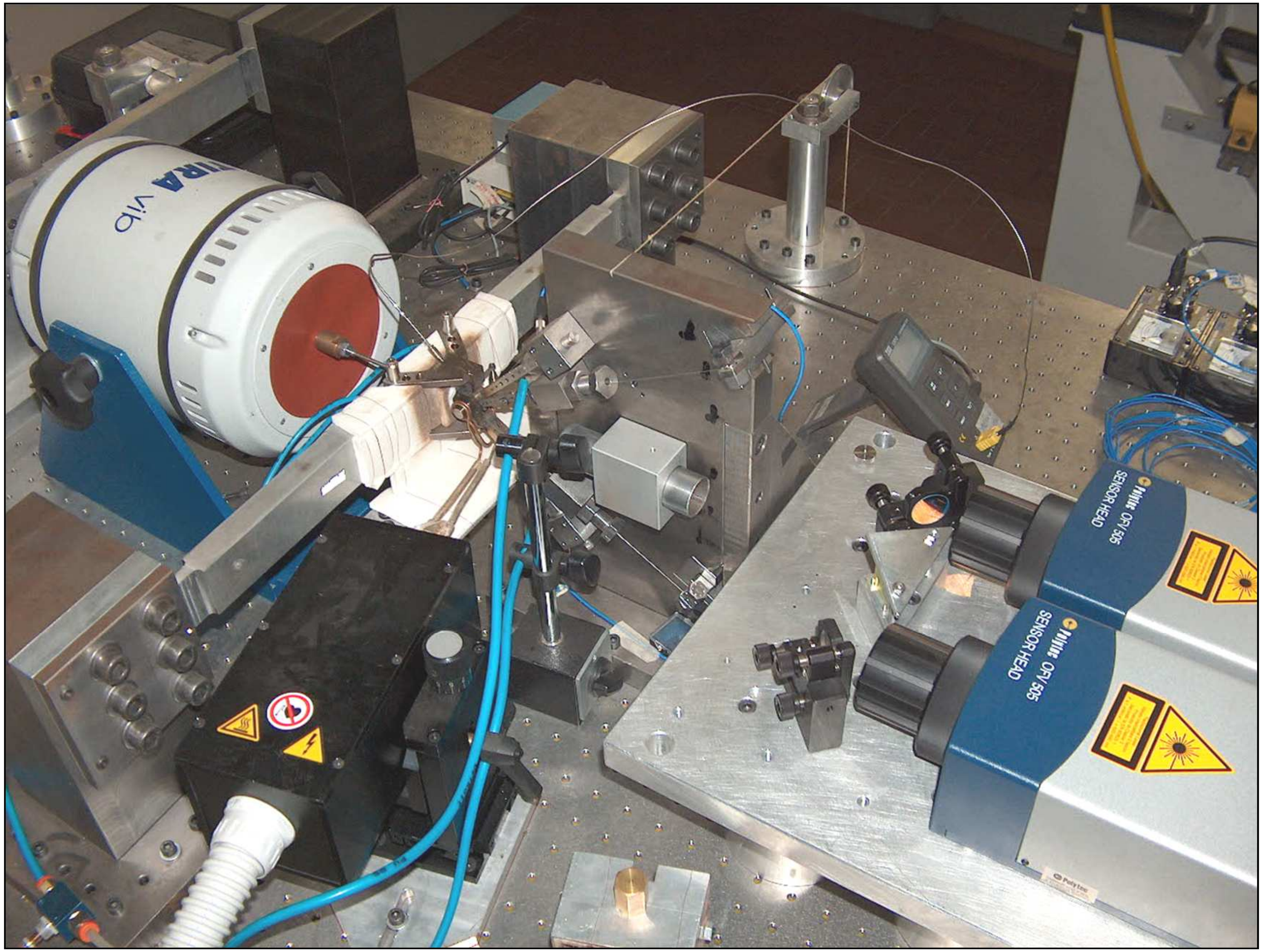

Test rig: flat-on-flat contact

Rigid approach

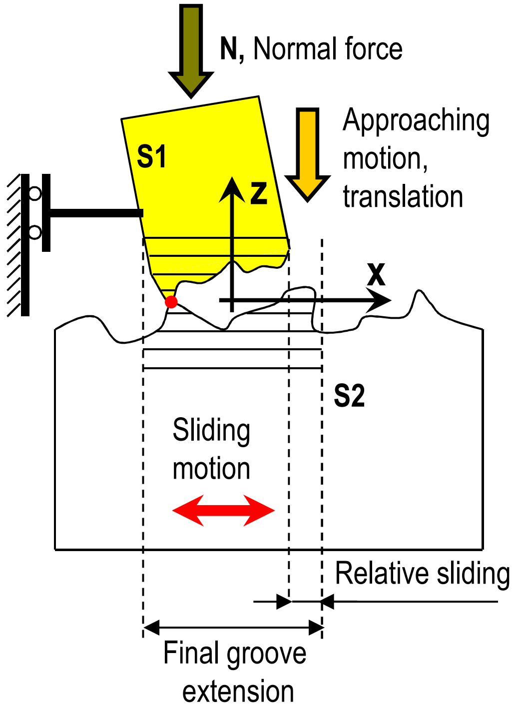

Rigid approach

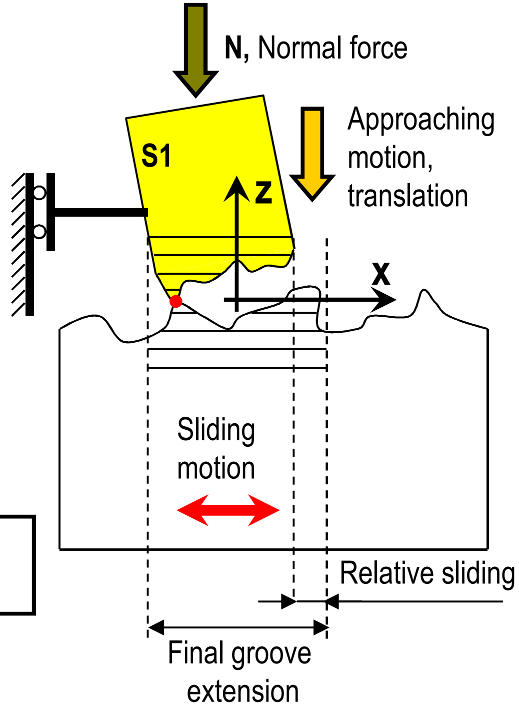

Floating approach

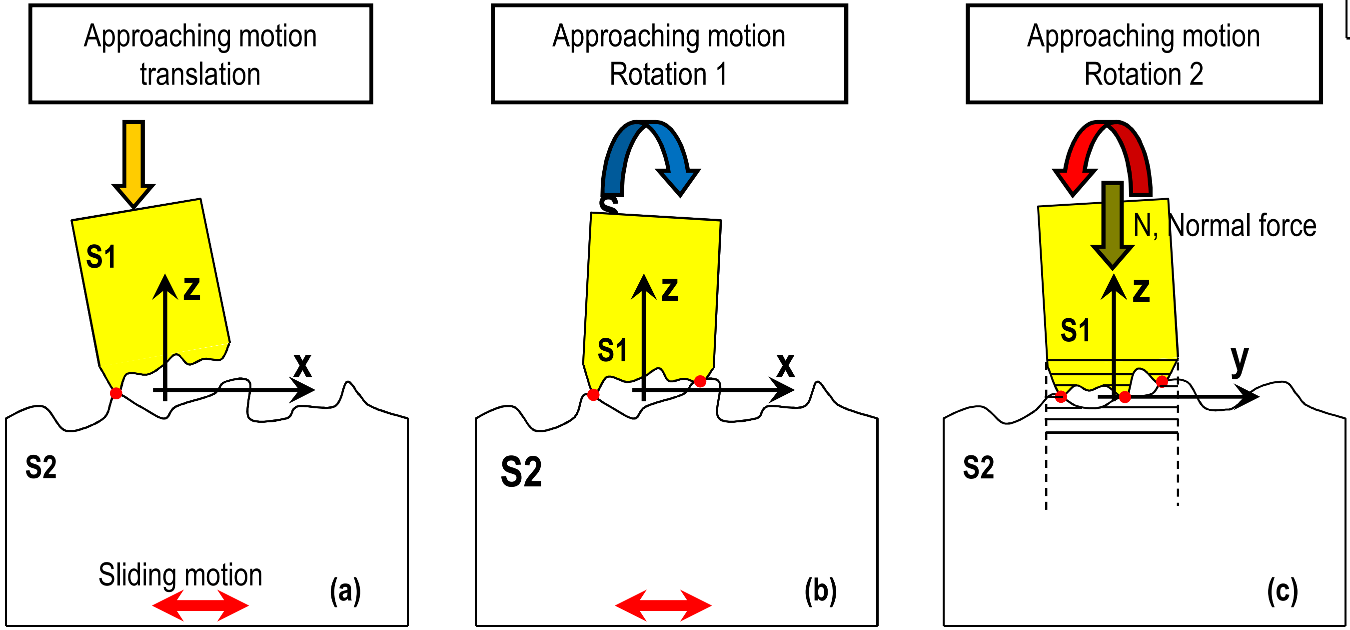

Test rig: specimens for flat-on-flat contact

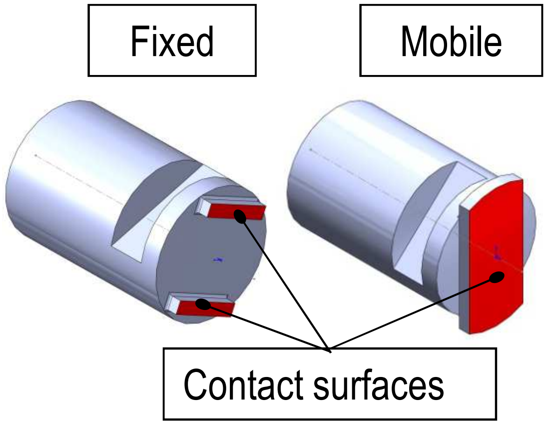

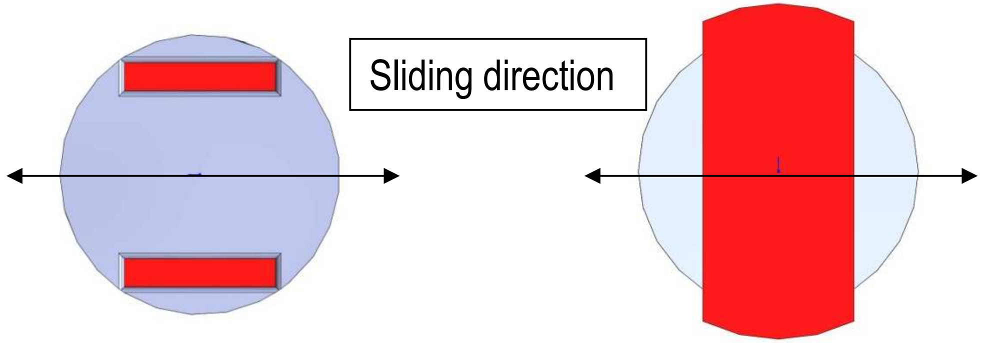

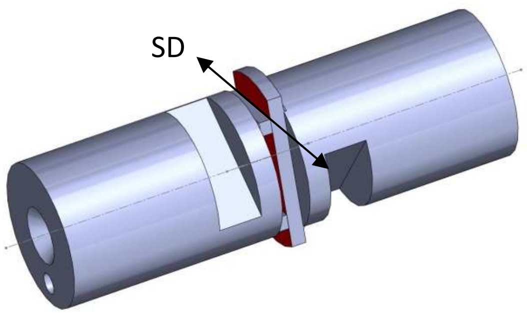

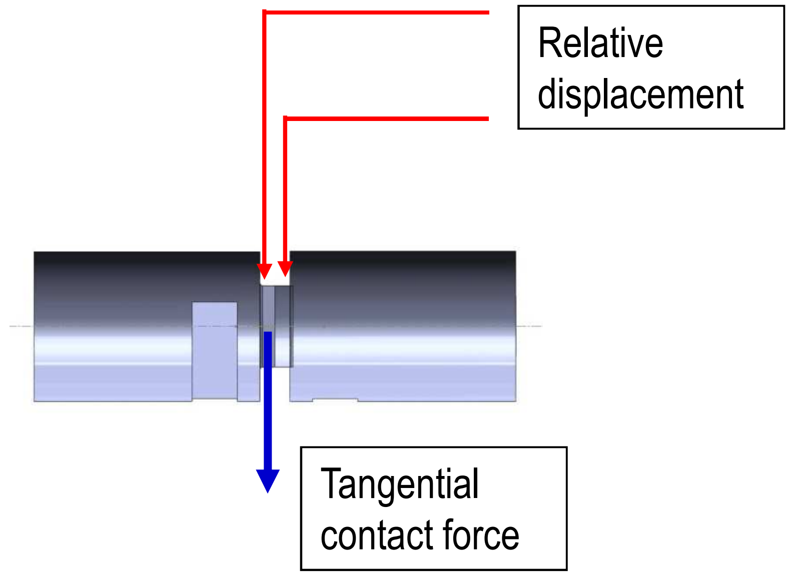

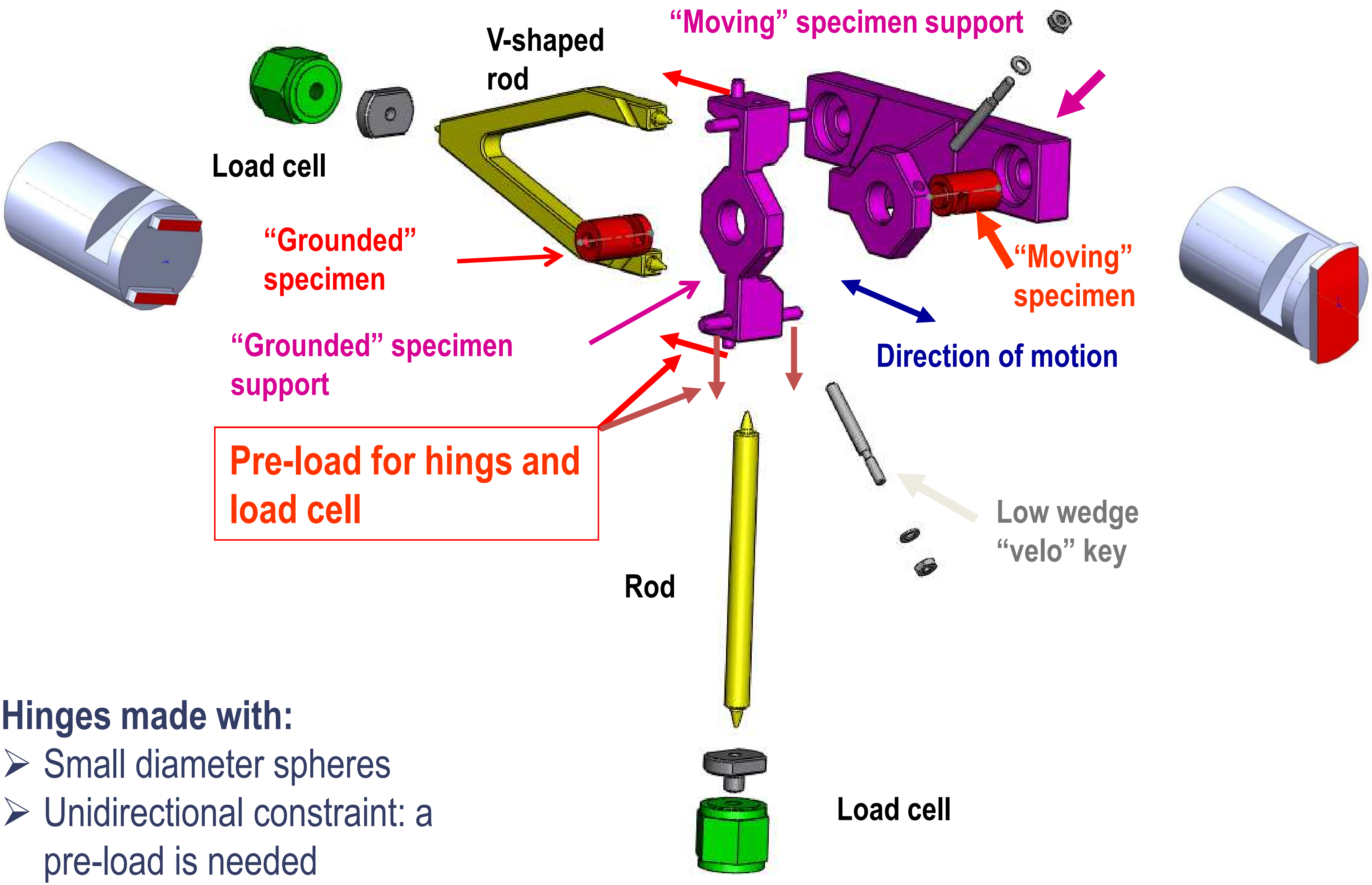

Hinges made with:

- Small diameter spheres
- Unidirectional constraint: a pre-load is needed

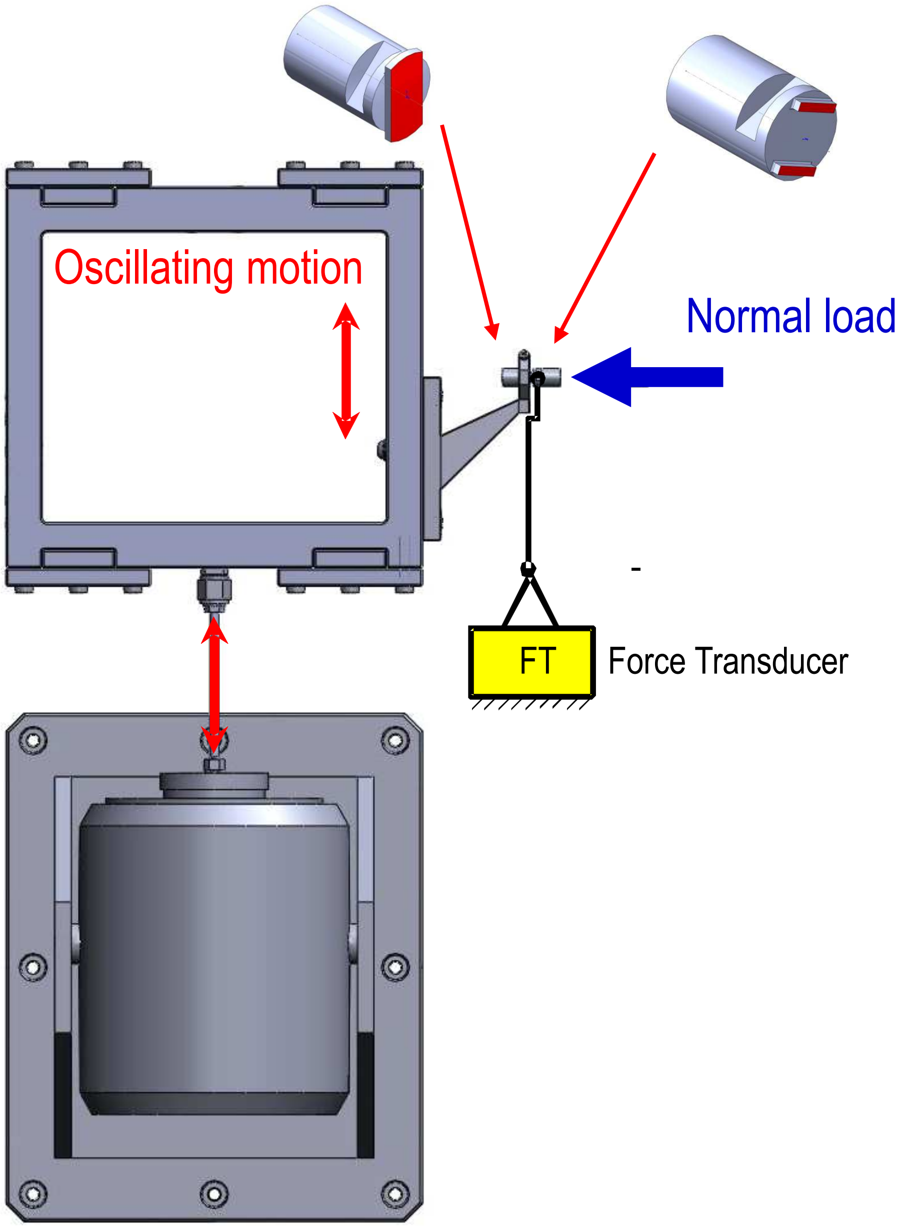
Oscillating motion
Normal load
FT
Force Transducer

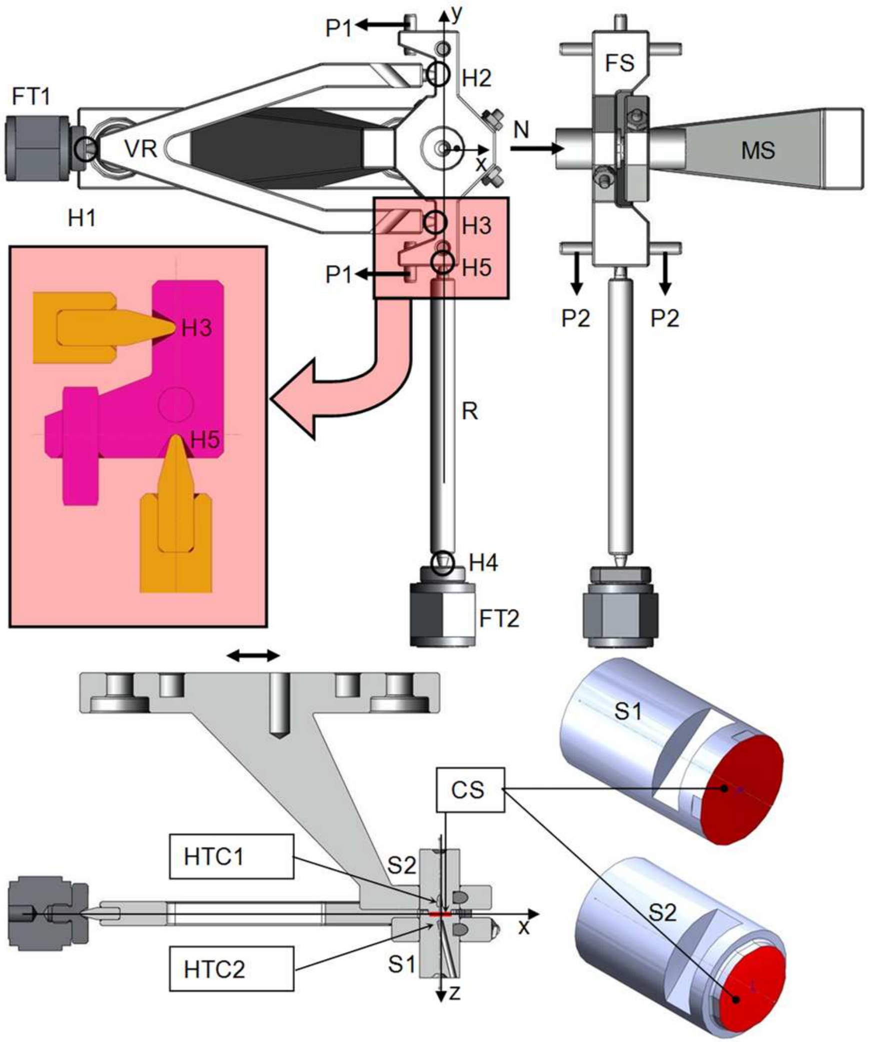
P1
y
H2
FT1
VR
N
x
FS
MS
H1
H3
H5
P1
P2
P2
H3
H5
R
H4
FT2
S1
CS
HTC1
S2
S2
x
HTC2
S1
z

(a) overall view,
(b) measurement apparatus
(c) exciting apparatus

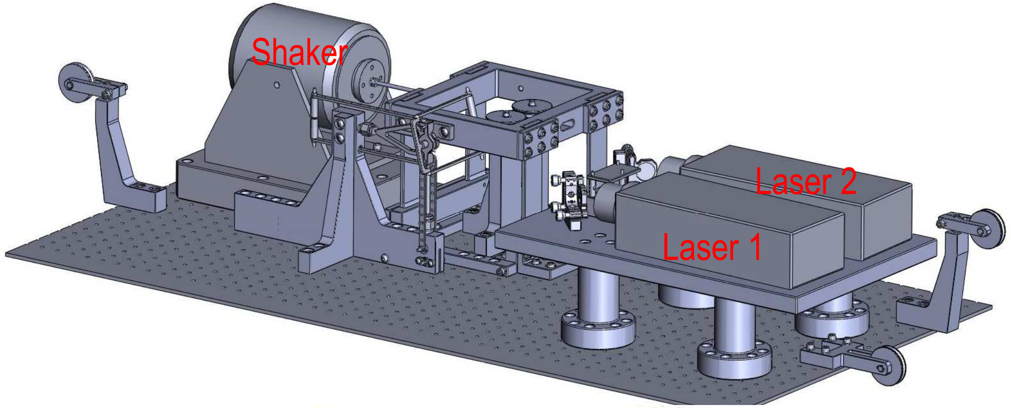

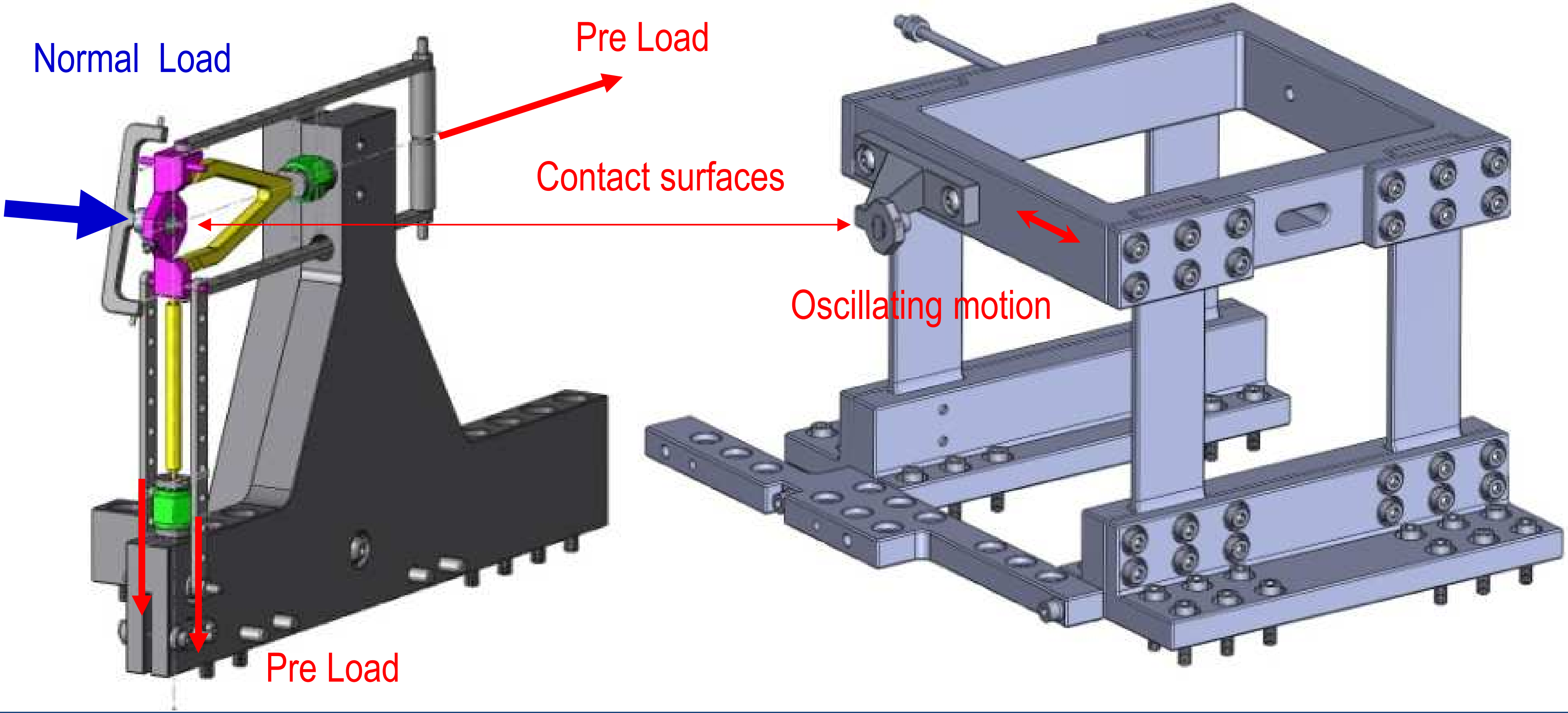

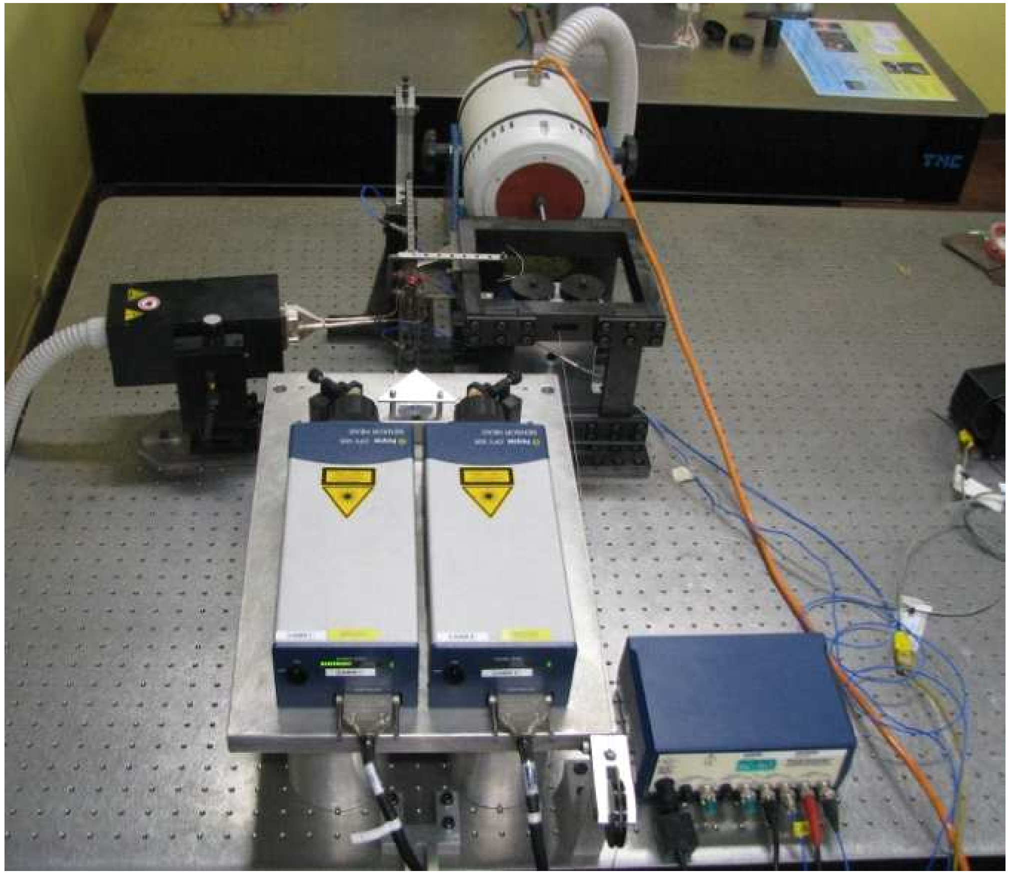

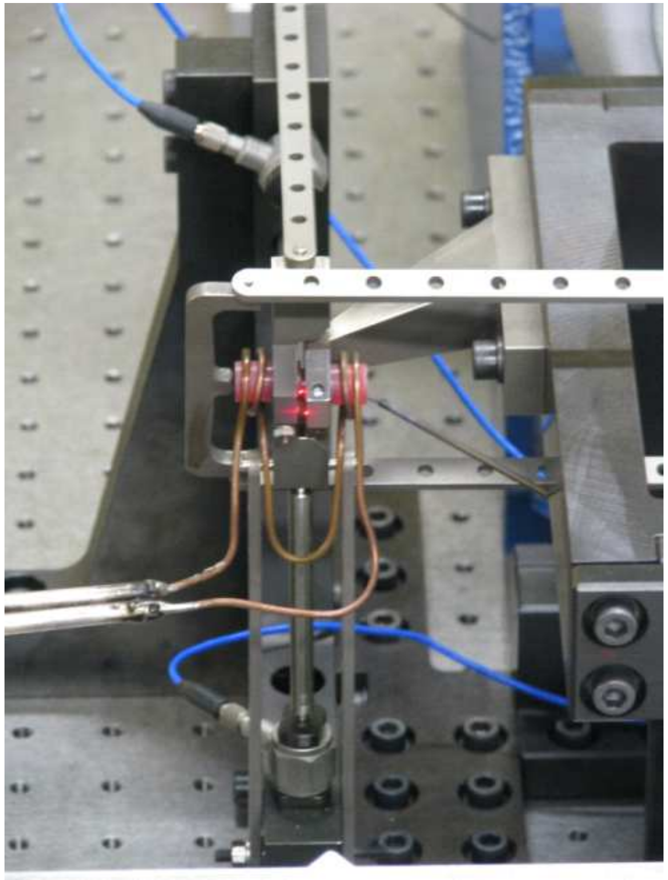

Test rig: data acquisition and control system 1/1

- Overall force measurement error : ~ 1%
- Overall displacement measurement error: < 1%
- Feedback control of the test conditions (temp. & displ.)

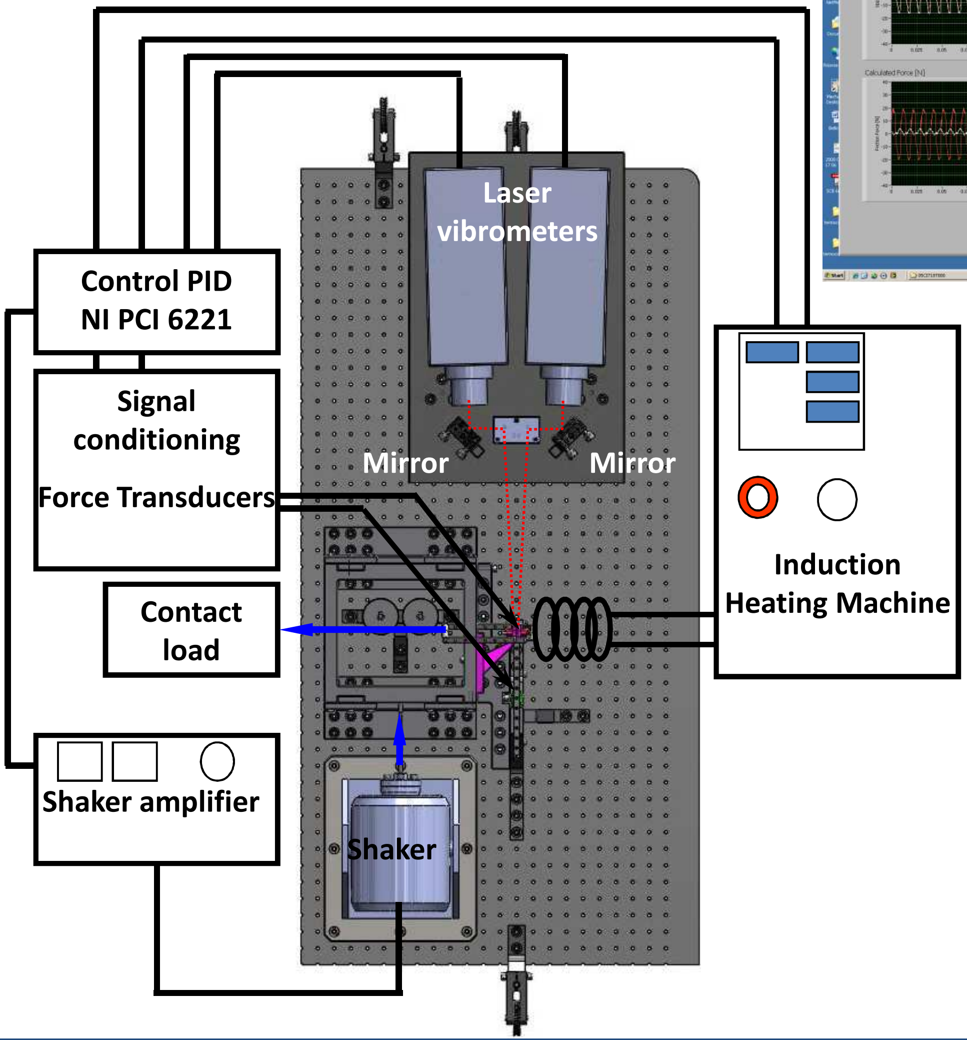

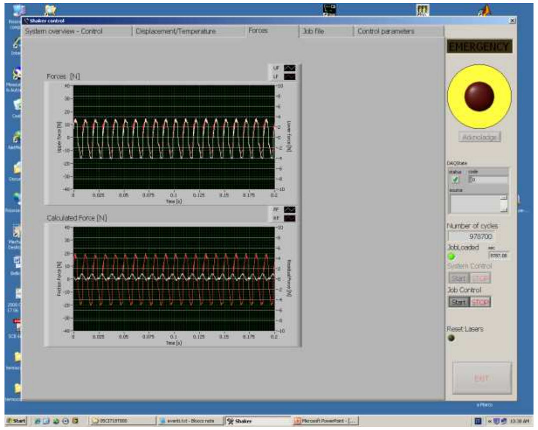

- Test Frequency: 2÷200 Hz;
- Normal Load: 15÷500N
- Contact pressure: ≤ 40 MPa
- Relative motion range 2÷100 μm
- Temperature up to 1000°C

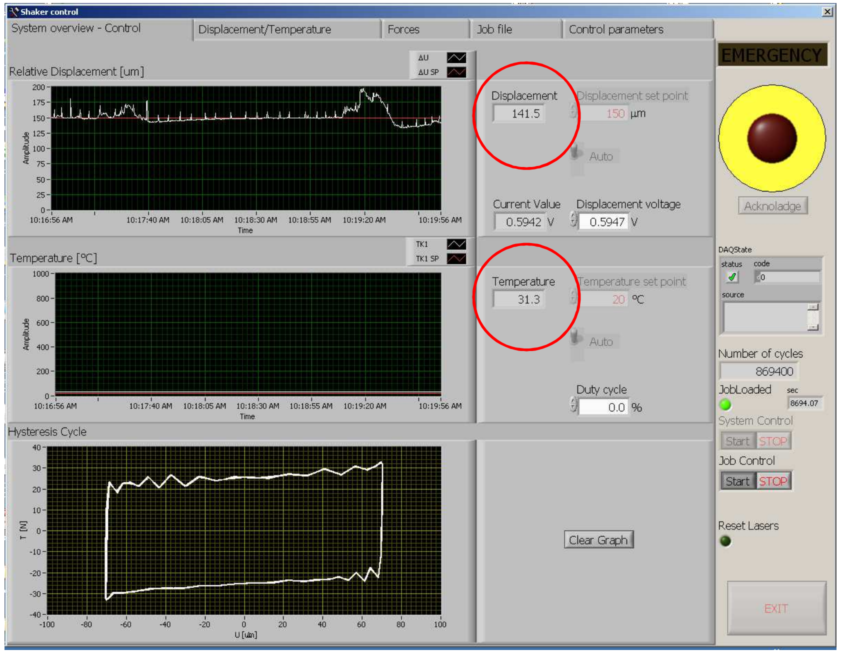

Underplatform dampers

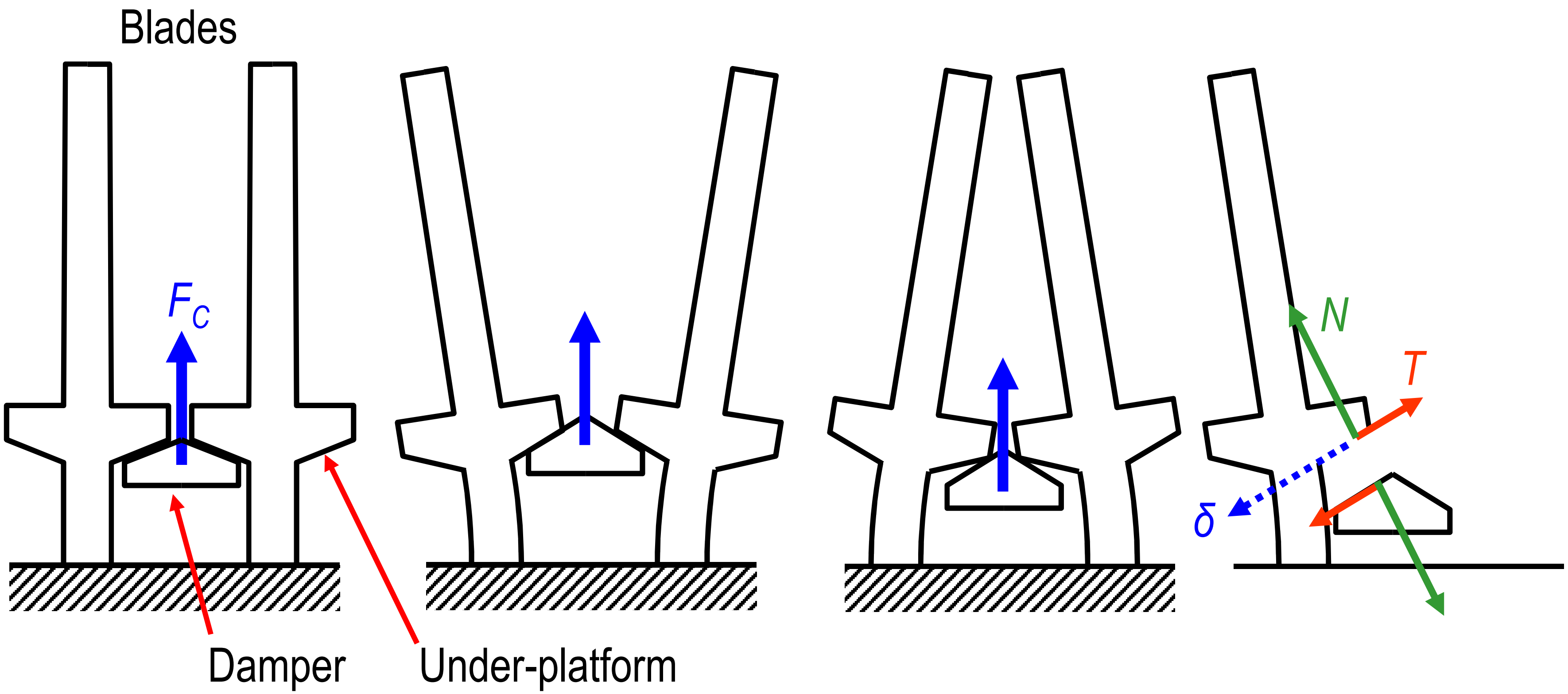

Constitutive parts

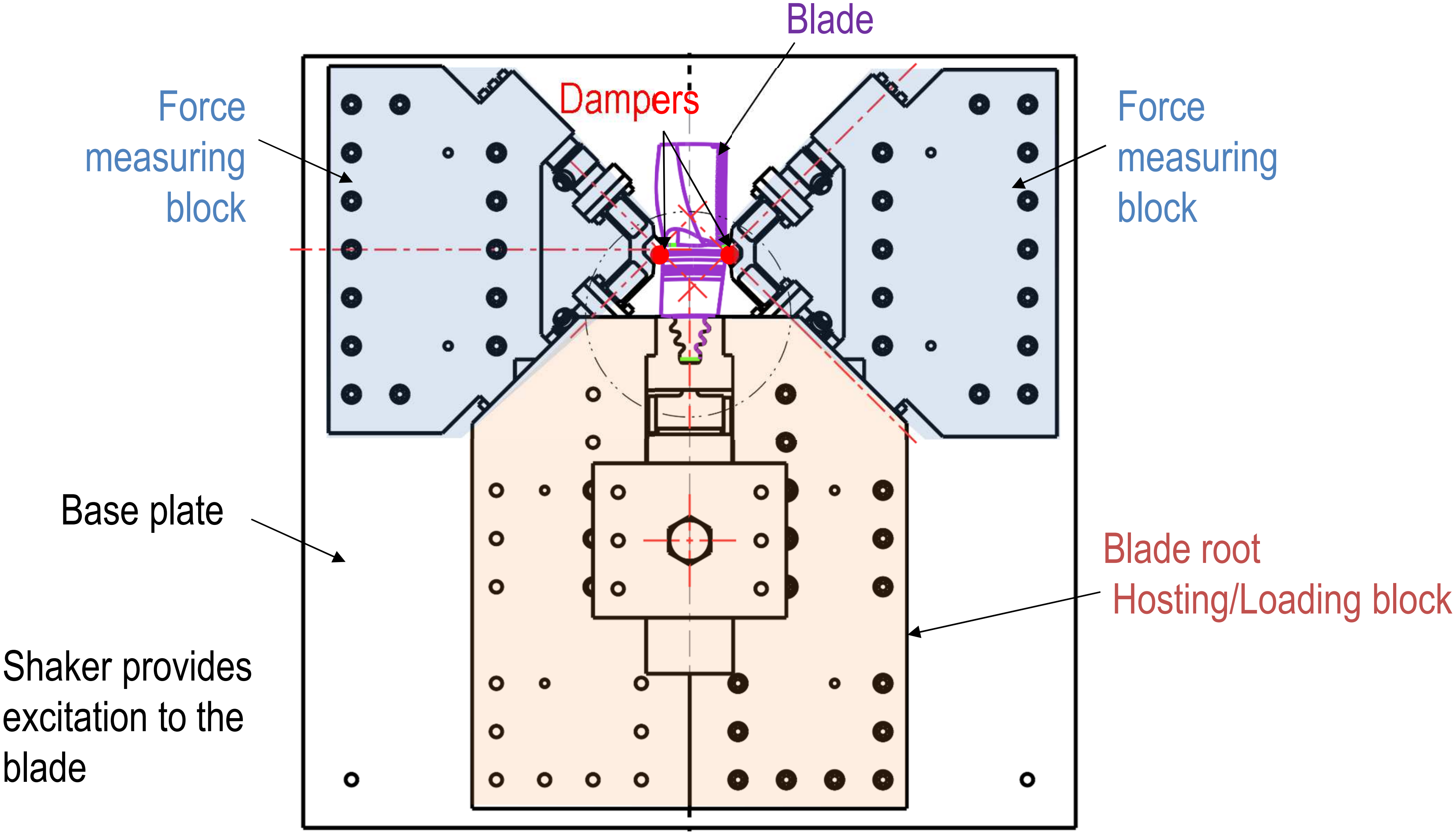

Constitutive parts

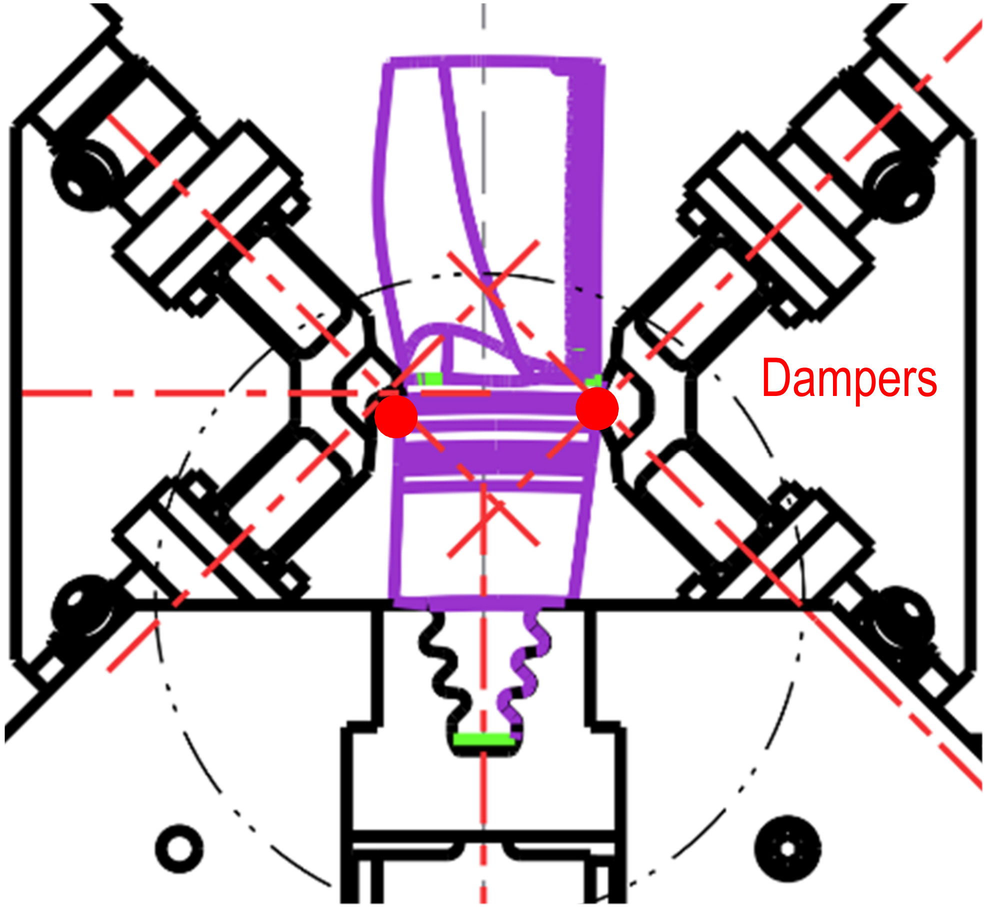

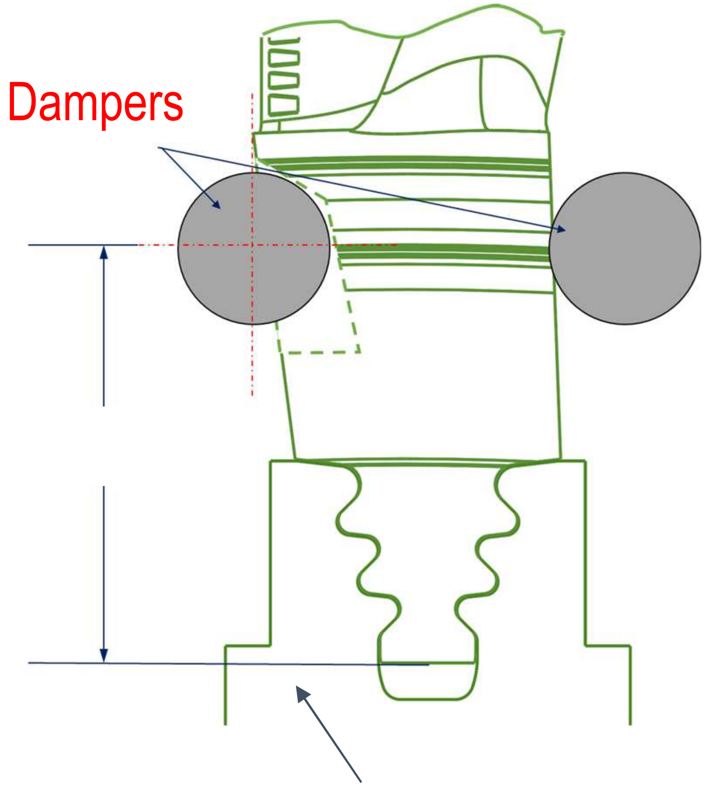

Removable fixture for different blades with different roots

A regulated and measurable clamping force is required to apply a force on the blade which simulates the effect of the actual centrifugal load while turbine runs.

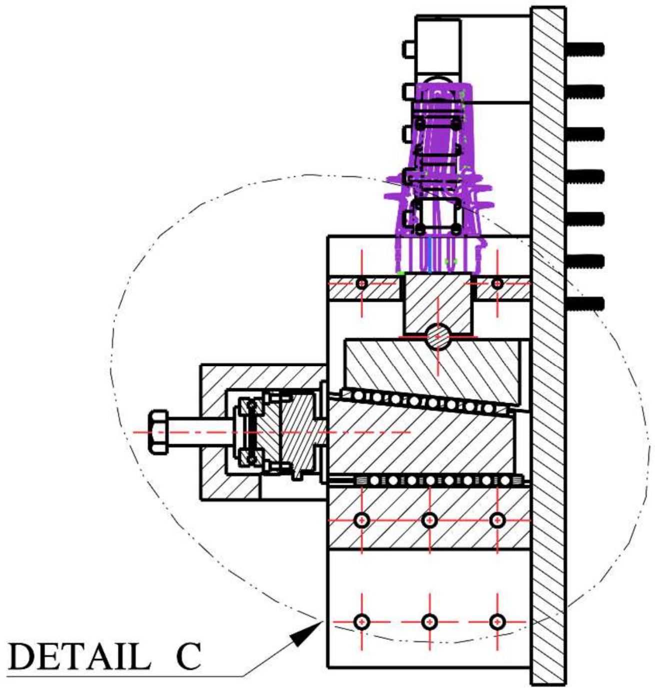

Section A-A

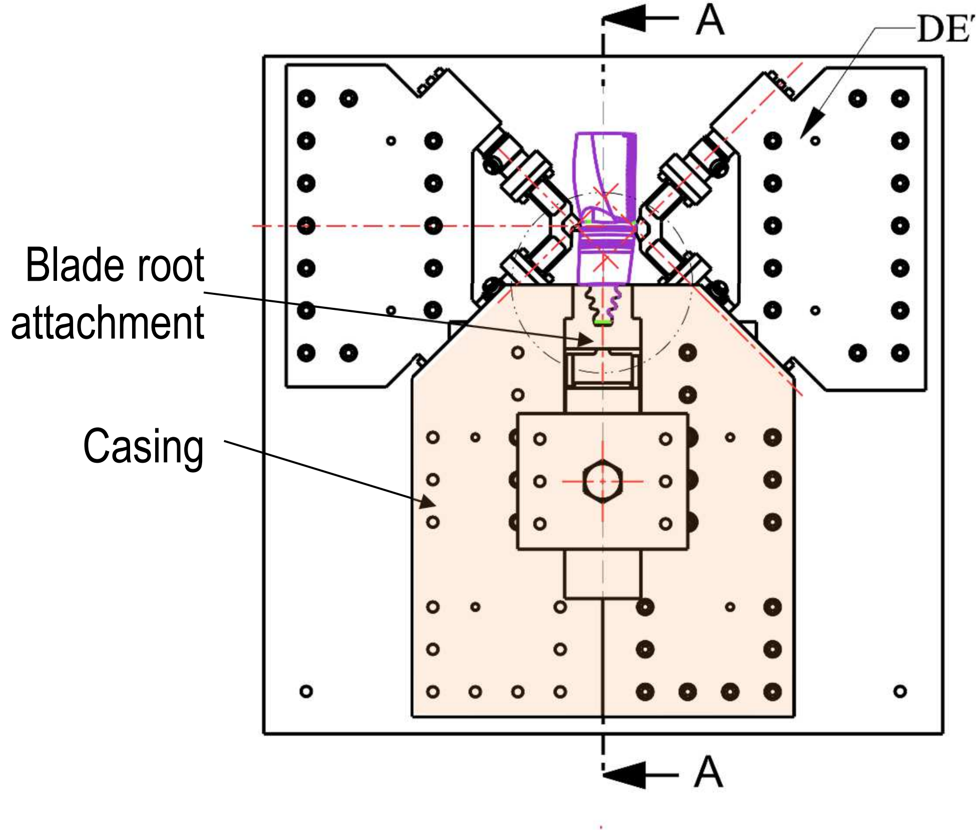

A regulated and measurable clamping force is required to apply a force on the blade which simulates the effect of the actual centrifugal load while turbine runs.

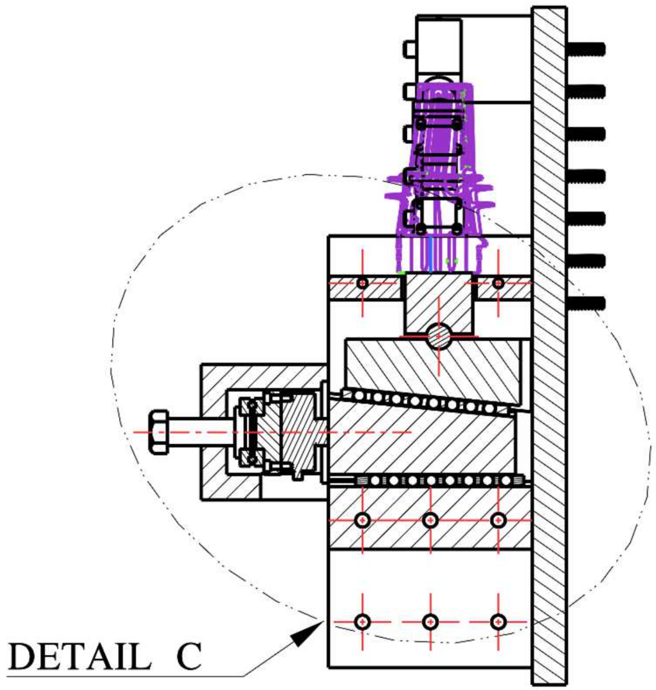

Section A-A

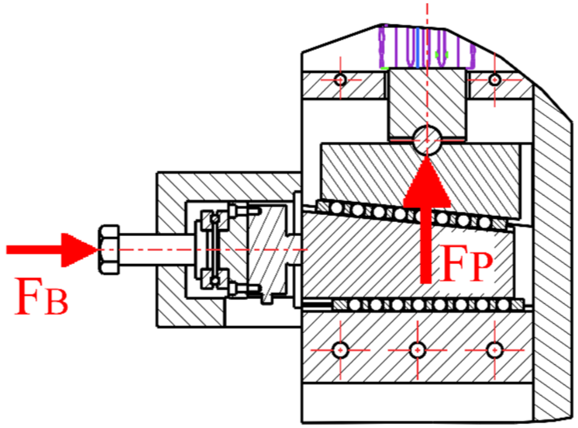

DETAIL C

Two wedge blocks (slope 1:10) convert the force F_B perpendicular to the blade axis into a pushing force F_P along the blade axis.
A load cell (strain gauge) cell measures the force F_B.

F_B up to 300 kN! (realistic range for investigated blades up to 100 kN)

The designed test bench must be capable of measuring the damper contact forces on the ground platforms.

The **DECOUPLER is purposely designed** to separate the contact force into two components acting along the limb axes. **The load cells experience only axial force**, i.e. negligible transverse force, and prevented crosstalk effect.

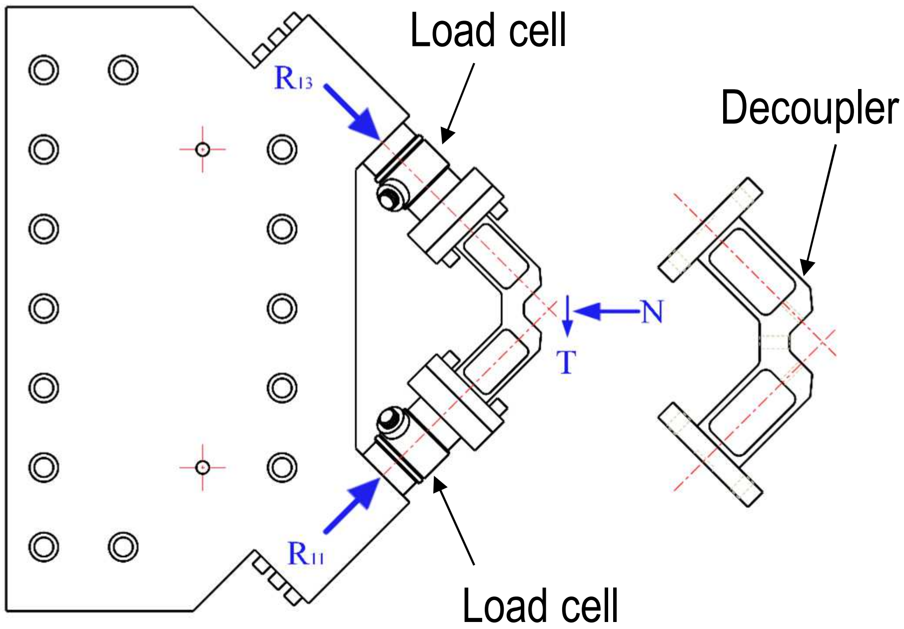

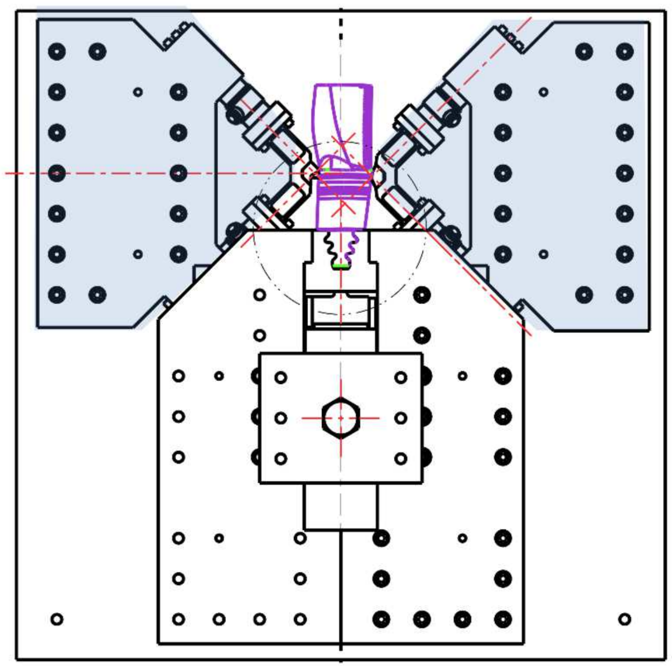

The designed test bench must be capable of measuring the damper contact forces on the ground platforms.

The DECOUPLER is A PSEUDO-STATICALLY DETERMINATE mechanism. Its efficiency is given by the “degree of separation”, R/F, here set at 99.4%.

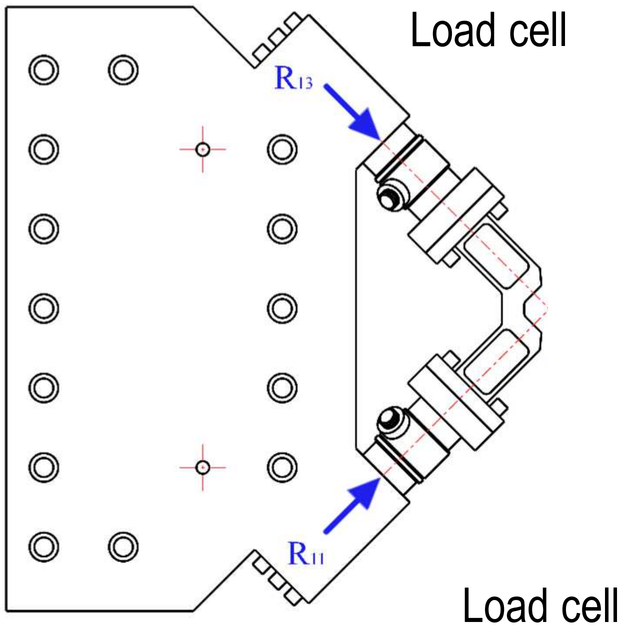

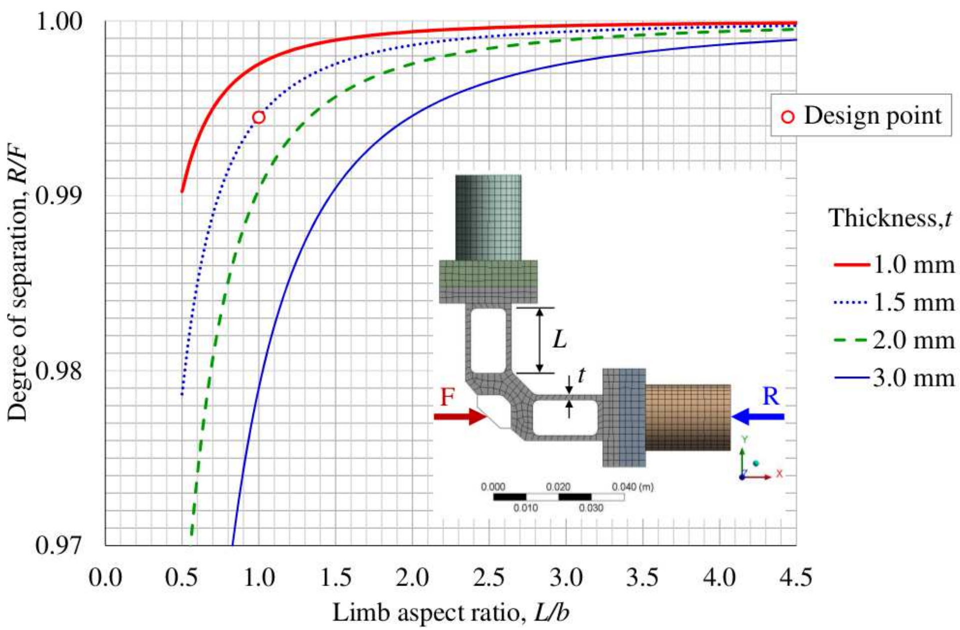

The designed test bench must be capable of measuring the damper contact forces on the ground platforms.

The selected load cells work with a charge amplifier with a low time-drift factor (< 5 mN/s). Both static and dynamic components of the contact forces are measured.

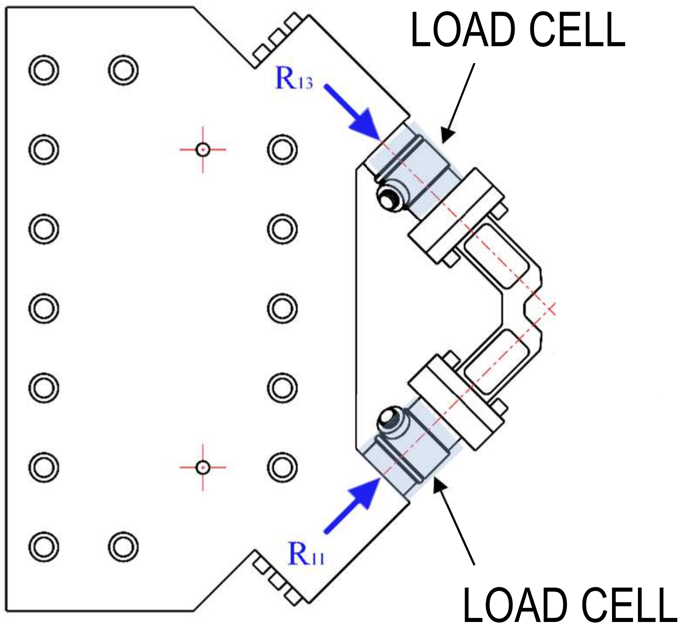

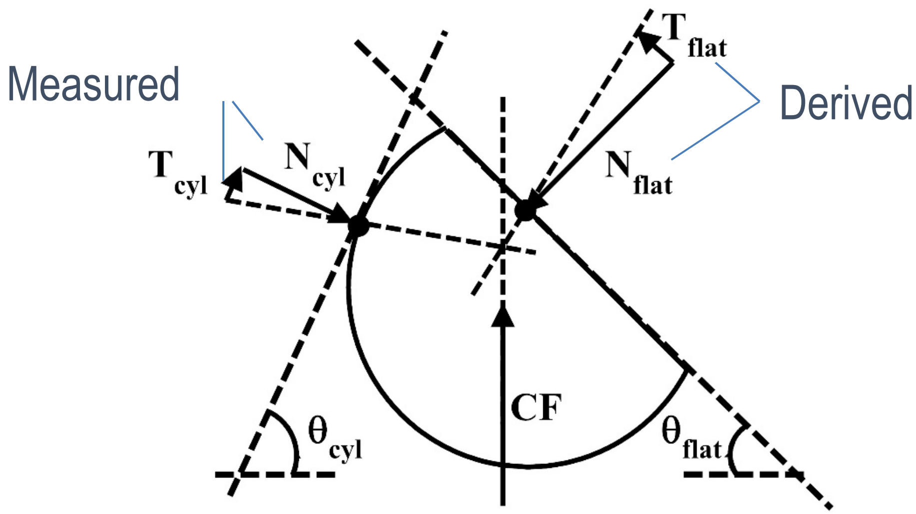

Experimental set-up

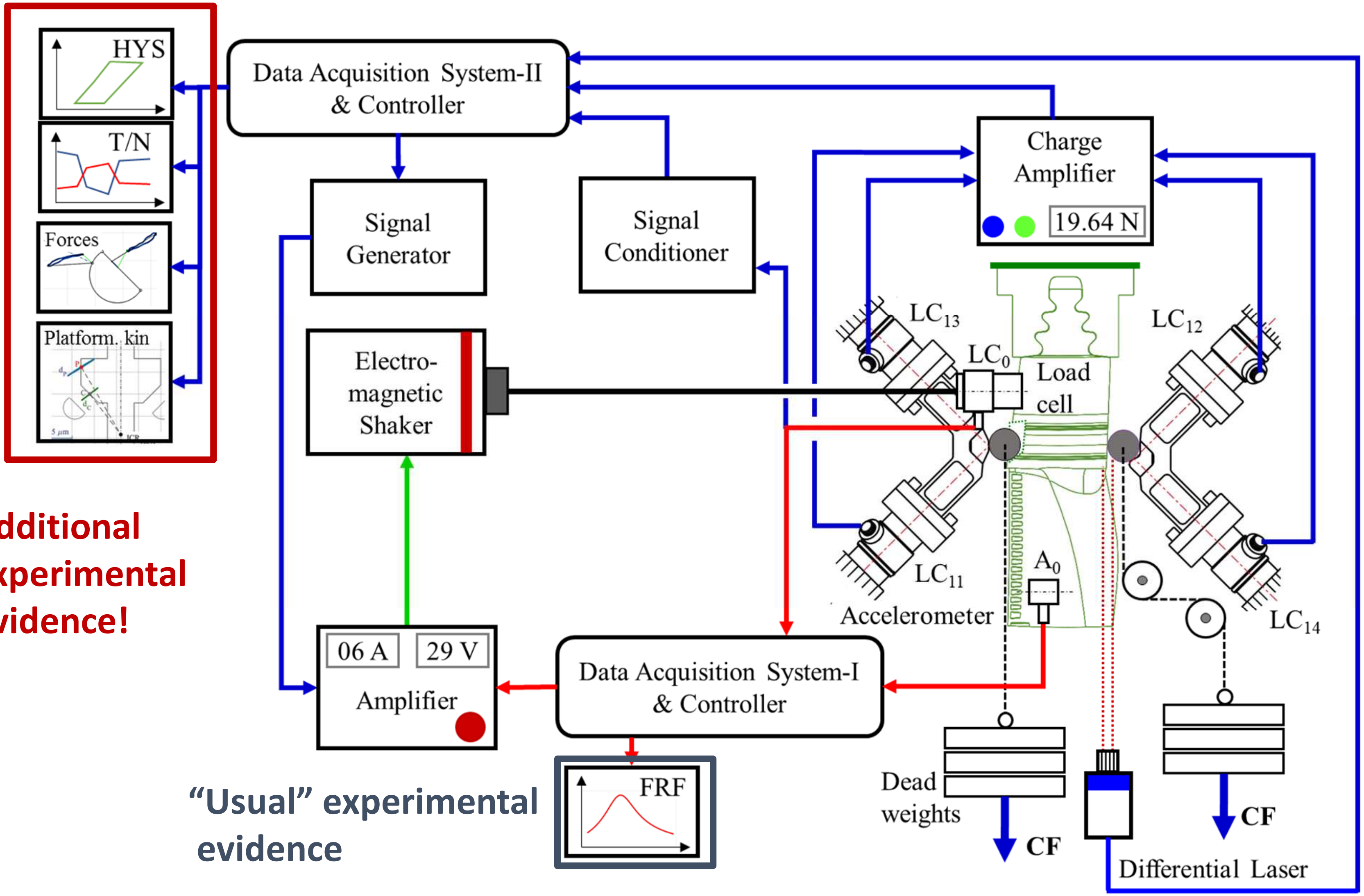

Additional experimental evidence!

"Usual" experimental evidence

Experimental set-up

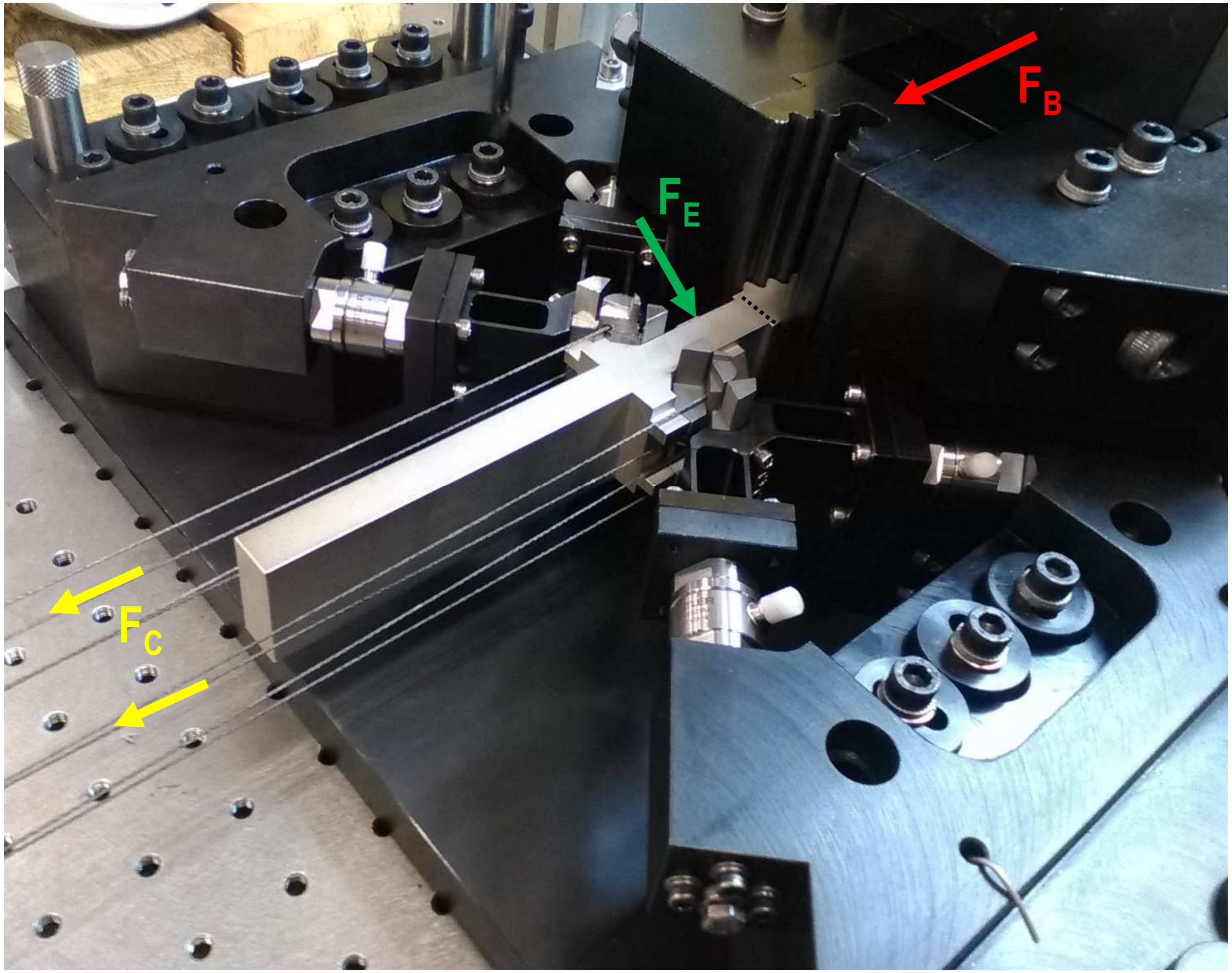

Experimental set-up

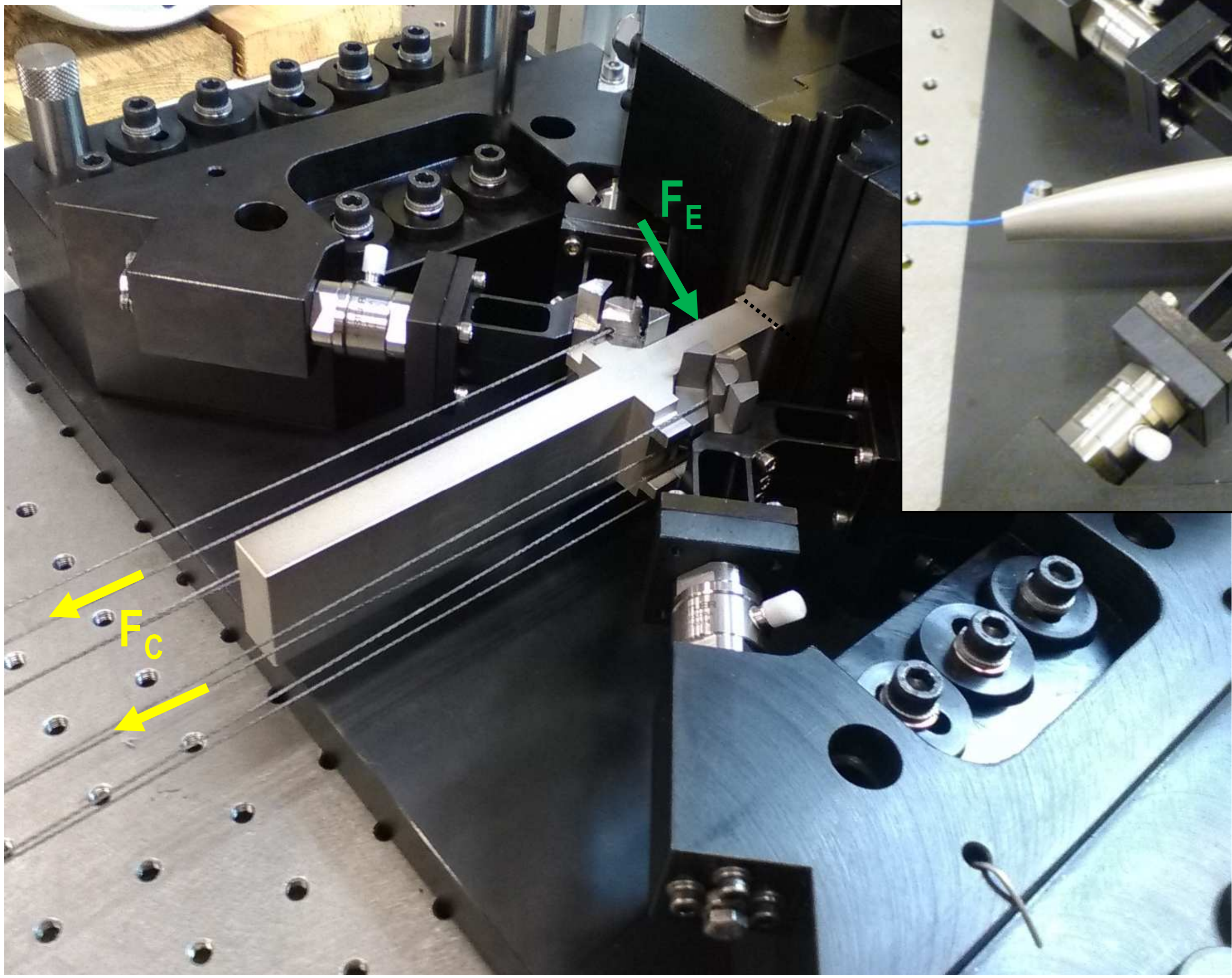

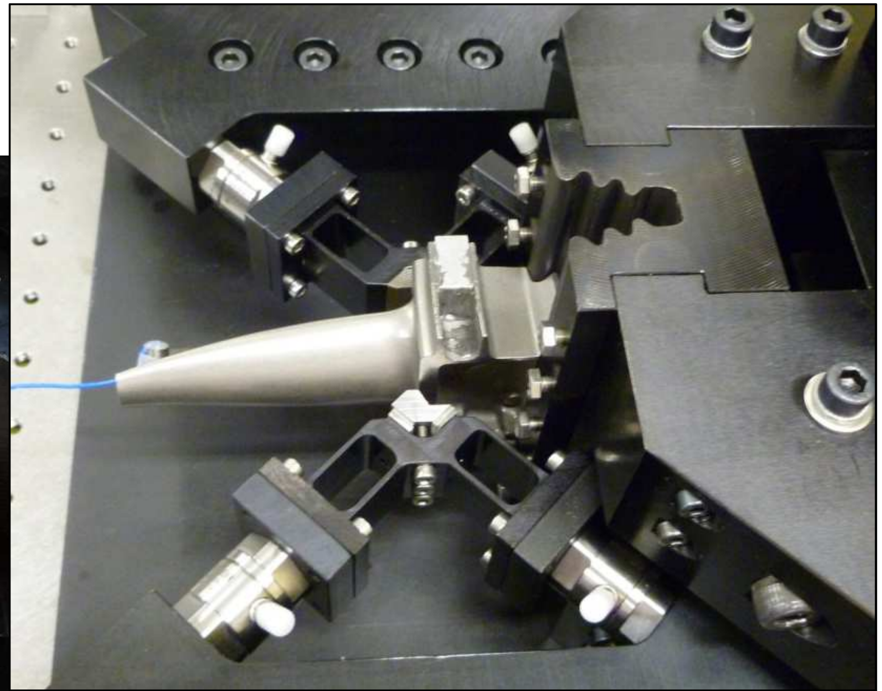

Experimental set-up

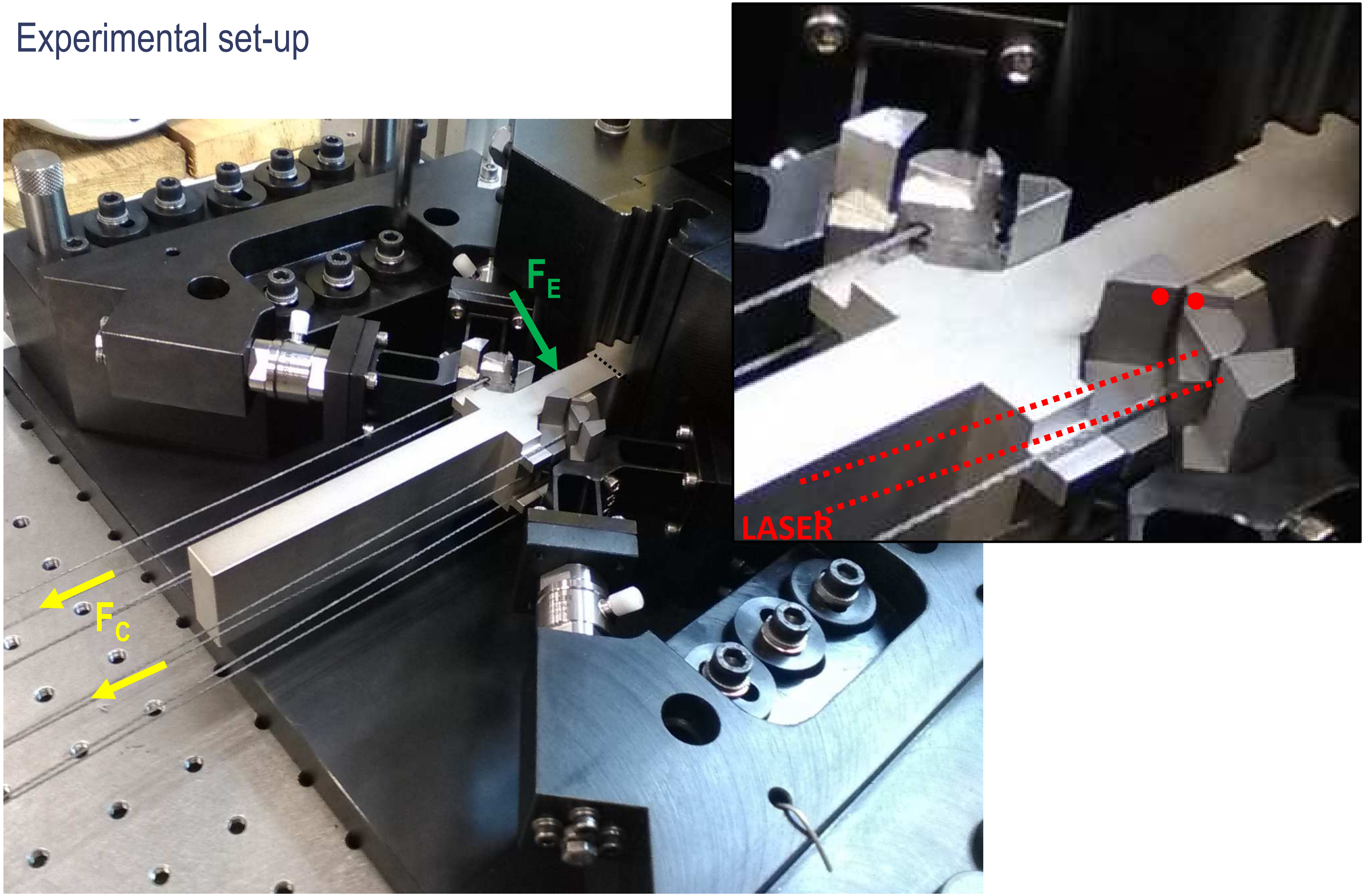

EXPERTISE

POLITECNICO DI TORINO
Department of Mechanical and Aerospace Engineering

Thank you for your kind attention!

Experiments for wear and underplatform damper mechanics

Stefano Zucca, Daniele Botto
Politecnico di Torino